Ita Junkar

PLASMA TREATMENT OF POLYMERS FOR BIOMEDICAL APPLICATIONS

Doctoral Dissertation

PLAZEMSKA OBDELAVA POLIMEROV ZA BIOMEDICINSKE APLIKACIJE

Doktorska disertacija

Supervisor: A/Prof. dr. Miran Mozetič

Co-Supervisor: A/Prof. dr. Uroš Cvelbar

Januar 2010

MEDNARODNA PODIPLOMSKA ŠOLA JOŽEFA STEFANA
JOŽEF STEFAN INTERNATIONAL POSTGRADUATE SCHOOL
Ljubljana, Slovenia

TABLE OF CONTENTS

List of abbreviations

XPS	=	x-ray photolelectron spectroscopy
AFM	=	atomic force microscopy
SEM	=	scanning electron microscopy
WCA	=	water contact angle
DSC	=	diferential scanning calorimetry
MTS	=	(3-(4,5-dimethylthiazol-2-yl)-5-(3-carboxymethoxyphenyl)-2-(4-sulfophenyl)-2H-tetrazolium)
OM	=	optical microscopy
PET	=	polyethyleneterephthalate
HMWK	=	high molecular weight kininogen
TF	=	tissue factor
RF	=	radio-frequency
HUVEC	=	human umbilical vein endothelial cells
PBS	=	phosphate-buffered saline
PFA	=	paraformaldehyde
PRP	=	platelet rich plasma
RPM	=	revolutions per minute

Abstract

Vascular grafts made of polyethyleneterephthalate (PET) polymers have successfully replaced large-diameter blood vessels, but the long-term performance of small-diameter (< 6 mm) vascular grafts is still disappointing. The main problem is insufficient biocompatibility of polymer surface with blood, which causes complications after implementation; such as thrombosis or restenosis. These complications immediately lead to an additional surgical procedure, which is expensive and unpleasant (or sometimes even fatal) for the patient. Many efforts have been done to improve surface biocompatibility of vascular grafts, mainly by coating the surface with bioactive substances such as gelatin, albumin, collagen and heparin. However, successful results have not yet been reported for small-diameter vascular grafts.

A promising way to modify surface properties of vascular grafts is by plasma treatment, as this method enables modification of surface properties in terms of surface roughness, surface chemistry, wettability and crystallinty, without changing the bulk attributes. Because these surface properties play a key role in biocompatibility of materials, the aim of the present work was to study effects of plasma treatment on polymer surfaces and correlate them with proliferation of endothelia cells and adhesion of platelets.

PET foils produced by different manufacturers and with different degree of crystalline fraction were exposed to radiofrequency (RF) oxygen and nitrogen plasma for different expouser times. By variation of discharge parameters (power, discharge frequency, type of gas) and plasma parameters (density of neutrals and ions, kinetic energy of electrons, gas temperature) it was possible to produce PET foils with different surface properties.

In the first part of the work, the influence of plasma treatment on surface parameters was conducted. It has been shown that already after short exposure time (3 s) wettability of the surface increased, as the water contact angle changes from 72 ° (untreated PET foil) to about 25 ° and 20 ° for nitrogen and oxygen plasma treated surface, respectively. Formation of nitrogen and oxygen functional groups was also achived shortly after plasma treatment and the concentration of newly formed oxygen functional groups was shown to increase with plasma treatment time. Plasma treatment also produces morphologycal changes of the surface, as the PET surface exhibited sphere like structures after expouser to nitrogen or oxygen plasma. The differences in morphology between nitrogen and oxygen plasma treated surfaces were also observed, as oxygen plasma treated surfaces exhibited more pronunced sphere like structures, which become elongated

after longer plasma treatment. Evidently the change in surface morphology also affects the change in surface roughness, which increased with longer plasma treatment time. However much higher surface roughness of PET foils treated in oxygen plasma was observed in comparison to nitrogen plasma treated surfaces. To some extent it was also possible to confirm that oxygen plasma treatment increases crystallinity, as a higher degree of crystalline fraction was observed on PET foil treated in oxygen plasma.

It has also been observed that PET foils with different initiall crystallinity may be treated in plasma differently. Much faster surface heating of amorphous polymers was observed during plasma treatment in comparison to semicrystalline polymers, which can be assigned to different interactions of neutral atoms with the surface of amorphous and semicrystalline polymers. Some changes in surface morphology between PET polymers of different manufacturers were also observed, though all plasma treated surfaces exhibited a similar sphere like formation. Similar morphology was also observed on PET fibres (used for vascular grafts) after oxygen plasma treatment.

In the second part of the work, the in vitro biological response of plasma treated surfaces was studied. It has been shown that the most significant changes in biological response were observed on oxygen plasma treated surfaces. These surfaces enabled improved proliferation of endothelia cells and reduced adhesion of platelets. This can mainly be attributed to newly formed oxygen functional groups, which seem to have remarkable influence on adhesion of platelets. It has also been shown that platelet adhesion is a function of polymer crystallinity, as much lower platelet adhesion was observed on untreated semicrystalline polymers in comparison to amorphous. Interestingly no correlation between platelet adhesion and surface wettability was observed during this study, as there were no significant differences in adhesion of platelets between highly hydrophobic or hydrophilic surfaces.

According to the in vitro studies done on plasma treated PET foils, it has been shown that oxygen plasma treatment is a promising technique to improve proliferation of endothelia cells and to reduce adhesion of platelets. Thus oxygen plasma could be a new method for improving hemocompatibile properties of vascular grafts made of PET polymers.

Povzetek

PET polimeri se že vrsto let uspešno uporabljajo kot žilni vsadki za žile večjih premerov, vendar pa njihova uporaba za žilne vsadke manjših premerov (manj od 6 mm) ni najbolj primerna. Glavni problem je nezadostna biokompatibilnost površine polimernega vsadka s krvjo, kjer pogosto prihaja do pooperativnih zapletov, kot so tromboza in restenoza. Posledice tovrstnih zapletov ponavadi pomenijo ponovne kirurške posege, ki so dragi in neprijetni (včasih celo smrtno nevarni) za bolnika. Narejenih je bilo mnogo poskusov s katerimi naj bi izboljšali biokompatibilnost umetnih žil, predvsem z uporabo različnih prevlek z bioaktivnimi substancami, kot so gelatin, albumin, kolagen in heparin. Kljub številnim poskusom pa umetne žile manjših premerov še vedno ne izkazujejo uspešnih rezultatov.

Zelo perspektivna tehnika za spremembo lastnosti površine umetnih žile je obdelava s plazmo, saj le ta omogoča spremembo površinskih lastnosti, kot so hrapavost, kemijska sestava, omočljivost in kristaliničnost pri tem pa ne vpliva na lastnosti celotnega materiala. Glavni namen tega dela je proučiti vplive plazemske obdelave na površini PET polimera in jih povezati s proliferacijskimi lastnostmi endotelijskih celic ter adhezijo trombocitov, saj te lastnosti površine igrajo pomembno vlogo pri biokompatibilnosti materialov.

S tem namenom so bile PET folije različnih proizvajalcev in z različno stopnjo kristaliničnosti izpostavljene termično neravnovesni radiofrekvenčni (RF) plazmi kisika in dušika pri različnih časih izpostave. S spreminjanjem razelektritvenih (moč, razelektritvena frekvenca, vrsta plina) in plazemskih parametrov (gostota nevtralnih delcev, ionov, kinetične energije elektronov, temperature plina) je bilo mogoče pripraviti PET polimere z različnimi lastnostmi površine.

V prvem delu naloge je bila opravljena analiza vpliva plazemske obdelave na lastnosti površine PET polimera. Izkazalo se je, da že po kratkem času izpostave polimera (3 s) kisikovi ali dušikovi plazmi dobimo bolj omočljive površine, saj se kontaktni kot iz začetnih 72° (neobdelan PET) zniža na 25° za dušikovo in na 20° za kisikovo plazmo. Takoj po obdelavi je na površini mogoče opaziti novonastale dušikove, oziroma kisikove funkcionalne skupine. Z daljšim časom obdelave pa se koncentracija kisikovih funkcionalnih skupin na površini še nekoliko poveča. Plazemska obdelava vplival tudi na spremembe v morfoloških lastnostih površine, tako je mogoče na plazemsko obdelanih površinah opaziti krožne strukture. Le te so nekoliko bolj opazne in večje na površinah obdelanih v kisikovi plazmi. Morfološke spremembe vplivajo tudi na spremembe v hrapavosti površine, ki se poveča s časom plazemske obdelave. Delno je mogoče tudi potrditi spremembe v

kristaliničnosti površine PET polimerov po obdelavi v kisikovi plazmi, saj smo po plazemski obdelavi opazili nekoliko večji delež kristalinične faze v polimeru.
Zanimiva je tudi ugotovitv, da se polimeri z različnim deležem kristalinične faze v plazmi obdelujejo različno. Amorfni polimeri se v plazmi segrevajo mnogo hitreje, kot semikristalinični polimeri, kar je mogoče pripisati različnim interakcijam nevtralnih atomov s površino amorfnega in semikristaliničnega polimera. Kljub temu, da so bile na neobdelanih PET polimerih različnih proizvajalcev opažene razlike v morfoloških lastnostih, je bilo po plazemski obdelavi na vseh vzorcih mogoče zaslediti značilno morfologijo. Podobne morfološke lastnosti je bilo mogoče opaziti tudi na vlaknih po obdelavi v kisikovi plazmi.
V drugem delu naloge so bili opravljeni *in vitro* testi biološkega odziva plazemsko obdelanih površin PET polimerov. Najbolj opazne spremembe v biološkem odzivu so opazne na PET polimerih obdelanih s kisikovo plazmo. Na teh površinah je proliferacija enodtelijskih celic povečana glede na neobdelane vzorce, predvsem pa je tovrstna obdelava vplivala na zmanjšanje adhezije trombocitov. Ugotovili smo, da tudi kristaliničnost polimerov pomembno vpliva na adhezijo trombocitov, saj je adhezija trombocitov mnogo manjša na neobdelanih semikristaliničnih PET polimerih v primerjavi z amorfnimi. Pri tem pa nismo našli povezave med omočljivostjo površine in adhezijo trombocitov, saj ni bilo bistvenih razlik v številu adheriranih trombocitov na izrazito hidrofobne ali hidrofilne površine.
Glede na rezultate *in vitro* študije lahko zaključimo, da je obdelava PET polimerov s kisikovo plazmo ena od obetavnih možnosti za izboljšanje proliferacije endotelijskih celic in zmanjšanje adhezije trombocitov na PET polimerih. S kisikovo plazmo lahko tako izboljšamo hemokompatibilne lastnosti umetnih žil izdelanih iz PET polimerov.

1. Introduction

Atherosclerotic cardiovascular disease is still the largest cause of mortality in Western society (Tu et al., 1997). In 2006 cardiovascular diseases cost the health care systems within the EU just under €110 billion. The cost of inpatient hospital care for people who have cardiovascular disease accounts for about 54% of these costs, while the cost of drugs accounts for about 28% (Allender et al., 2008).

Arterial damage produces localized reductions in the calibre of arteries (stenosis) which ultimately stops the flow of blood through the affected vessels (Mustard et al., 1975). The disease is treated surgically by bypassing the segment of affected vessels to restore blood flow (Chandy et al., 2000). Significant efforts have been made in recent years to develop novel vascular grafts, and some novel grafts have indeed been produced, among those are vascular grafts from avtogenous saphenous veins, homografts, autogenous arteries, PET (Dacron) prosthesis, PTFE grafts etc. (Dardik et al., 1991, Florian et al., 1976).

Wherever possible, an autograft is the best choice for a replacement vessel, in this procedure sections of the patient's healthy blood vessels (usually veins) are harvested and implanted into the required location. However many patients, especially those with pre-existing vascular diseases and patients who have already undertaken autograft procedures, do not have blood vessels healthy enough to adequately serve as replacements. In such cases, the most common form of treatment is by using synthetic polymeric materials, such as Dacron (PET - polyethylene terephthalate) or ePTFE (extended polytetra fluoroethylene), because they exhibit a unique through-pore microporous wall structure and because they also have highly flexible mechanical properties (Roald et al., 1994). These synthetic vascular grafts have been used successfully to replace large-diameter blood vessels, however the long-term patency for small-diameter vascular grafts is still unsatisfactory; this is primarily due to thrombus formations (Wissink et al., 2000). Post-surgical complications are observed in 10 % of patients most of such complications are due to inflammatory reactions, infections and aneurysm. In such cases the artificial blood vessel has to be removed and the new autologous material for vascular graft must be implanted. Such procedures more than double the costs of treatment (Allender et al., 2008).

Biological response to biomaterials is very complex and still not fully understood. As the surface of the biomaterial is responsible for initiating the primary interaction with body fluids it is of vital importance to ensure that the surface is suitably conditioned to ensure an appropriate biological response (biocompatibility). It was thought for many years that the surface of the biomaterial should be inert.

However, nowadays it has been found that the contact of biomaterials with blood enables integration with the body, prevents infections, inflammatory reactions, blood coagulation and other correlated reactions. It is of primary importance that the surfaces of hemocompatible materials exhibit anti-thrombogenic properties, as this prevents thrombosis. Thrombosis is initiated with the adsorption of blood plasma proteins on the surface of the biomaterial and is strongly influenced by its physical and chemical properties.

Surface properties of implants are usually described with wettability, chemistry, surface charge and texture (roughness). These factors all influence the sequence of protein adsorption and subsequent platelet adhesion/thrombus formation. Although the mechanism of occlusion and dysfunction of artificial prostheses is multifactorial, all the studies performed suggest that fibrinogen and platelet deposition play a predominant role (Joist and Pennington, 1987, Vroman and Bull 1988). It also seems that the outermost atomic layer of the surface of an alloplastic implant is a decisive factor for determining biocompatibility (Chandy et al., 2000).
One possible method to alter surface characteristics, such as wettability, chemistry, charge and morphology to improve biocompatibility of implant devices (Lee et al., 1998a) is by treatment of the surface with different gaseous plasma, like glow discharge created in different gases and by variation of discharge parameters (discharge power, pressure, etc.) (Chen et al., 2003), which in turn influence plasma parameters (density of atoms, energy of plasma particles, etc.). Plasma modification has been used recently to enhance biocompatibility of implant devices made from stainless steel, titanium and various polymers. The unique advantage of plasma modification of implant devices is that the surface can be modified without altering the bulk properties of the material (Terlingen et al., 1993). It is thus possible to obtain desired mechanical and physical properties of implant material and at the same time also improve its surface properties to accomplish biocompatibility.
The present work will focus on surface modification with plasma treatment of PET polymers, which are used for production of vascular grafts (Dacron grafts). Surface modification can be achieved by different plasma treatments and various working gases to produce desired characteristics of the material. In this thesis, it has been hypothesised that plasma treatment can enhance biocompatibility; this is because appropriate treatment could enable surface modification, which would promote the growth of endothelial cells and reduce platelet adhesion.

This thesis is structured into four chapters. The first chapter presents the state of the art in the filed of biomaterials and blood-connecting devices, the main focus is on reviewing the attempts that have been made for improving hemocompatible properties of surfaces. As will be shown below, many different approaches with disputable results have been proposed in a number of articles dealing with this issue. From this review it will become clear that so far no general rule for production of hemocmpatible surfaces exists. This chapter also includes a review of frequently used plasma treatment techniques and their effects on surface modification of polymers. In the second chapter the aims and hypothesis of this thesis are presented. In the third chapter the outlined experimental plan is presented and all the experimental details for each method used are also shown. The results of experimental methods and the discussion are presented in the fourth chapter. This chapter can be divided into two parts: the first part mostly deals with detailed material characterisation; characterisation of polymer chemical structures (XPS analysis), surface morphology (AFM, SEM analysis), wettability (water contact angle measurements) and thermodynamic properties (DSC analysis), and the second part deals with *in vitro* biological response, mostly the effects on proliferation of endothelia cells (MTS assay, OM) and platelet adhesion (SEM analysis). For clarity each method is presented in a separate sub-chapter and some discussion is included regarding the results of other methods. In the last sub-chapters the thesis also proposes some correlation between biological response and surface modifications. The last chapter (Chapter 6) presents the conclusions, which are made according to the results obtained from surface analysis and *in vitro* biological response.

1.1. Biomaterials

The biomedical field, as it is known today, does not have a long history; it was first introduced in the 1960s by a successful Clemson University symposium, which in 1975 led to the formation of the Society for Biomaterials. However, "biomaterials" were known even before, in fact 2000 years ago the Romans and Chinese already used gold in dentistry. Glass eyes and wooden teeth have also been in common use throughout history. With the turn of this century plastic materials become available and due to their beneficial properties quickly found their way into the biomedical filed. In 1937 the polymer, polymethyl methacrylate (PMMA) was introduced for use in dentistry. A cloth made out of polyvinyl chloride (Vinyon-N) was discovered by Voorhees after World War II and this was put to use for vascular prosthesis. In 1958 Rob issued a cardiovascular surgery text suggested that surgeons should visit their local draper's shop and purchase Dacron fabric, which could then be cut and fabricated for arterial prosthesis (Ratner et al., 2008).

Biomaterials are used for medical applications, for growing cells in culture, in apparatuses for handling proteins in a laboratory and also for various other applications (Ratner et al., 2008). Overall it could be said that these materials are used in contact with living tissue and biological fluids for prosthetic, therapeutic and storage applications (Bruck, 1977). The widely accepted definition of biomaterial is: "any natural or synthetic material, foreign to the body, which can be employed to substitute, totally or in part, any tissue, organ or body function" (Galletti and Boretus, 1983). It is also unquestionable that biocompatibility with tissue and body fluids is the essential requisite for a material to deserve the prefix "bio". However, there is no entirely satisfactory and comprehensive definition of biocompatibility. Usually biocompatibility is defined by ''the ability of a material to perform with an appropriate host response in a specific application'' (Williams, 1988).

Compatibility with blood is even harder to define, as there are no standard tests which might be preformed in order to assess compatibility with blood. Ratner's definition of blood compatibility is "the property of a material or device that permits it to function in contact with blood without inducing undesirable reactions". Unfortunately this definition gives little insight on what a blood-compatible material is. In some cases it is easier to view blood compatibility by considering a material that is not compatible with blood (thrombogenic material). Thus biocompatibility of blood contacting devices would be evaluated mainly by the thrombotic response

induced by the materials. Such materials would produce undesirable reactions when placed in contact with blood: formation of a clot or thrombus composed of various blood elements; shedding or nucleation of emboli (detached thrombus); the destruction of blood components; activation of the component system and other immunologic pathways (Ratner et al., 2008). Although no material has been found truly biocompatible, many cardiovascular devices function with low or acceptable risks of complications (Hanson, 1993).

This clearly shows the complexity of producing hemocompatible materials, which must provide satisfactory biological responses and at the same time must have appropriate bulk properties, especially physical and mechanical properties. As it is difficult to design biocompatible materials that satisfy both requirements, a common approach is to fabricate biomaterials with adequate bulk properties and then modify their surfaces in order to reach the desired biological response for the specific application (Kumar et al., 2007).

1.1.1. Cell attachment

To achieve a desired biological response, the attachment of cells to the surface of biomaterials is of primary importance. When a biomaterial is exposed to a living organism many extremely complex reactions may occur at the cell-biomaterial surface. These reactions include coagulation, healing, inflammation, mutagenicity, and carcinogenity and play an important role in the successful implementation of the implemented material or device (Shi, 2004, Ratner et al., 2008).
Immediately after contact of a biomaterial with body fluids, the layer of proteins is adsorbed onto its surface and this initiates the interaction between the material and the biological system (Lu and Sephia, 2001). Proteins are biological macromolecules, which consist of amino acids chains, linked together through the peptide bonds into one or several long chains. The sequence of amino acids, called the primary structure, is unique and specific for a given protein. The characteristics of hydrogen bonding on the backbone of the protein results in various secondary structures, such as α-helix and β-sheet. The α-helix is further folded into a more compact tertiary structure. The secondary and tertiary structures of proteins are of fundamental importance in determining the properties of the native proteins. Cells migrate to the surface covered by the protein film by diffusive and active processes. The cells can adhere to the surface and release active compounds, recruit other cells, or grow (Shi, 2004).

Figure 1 gives a schematic illustration of the interaction of the biomaterial surface with biological fluids. Surface parameters, such as wettability, surface chemistry, surface topography, surface roughness and, in case of polymers, the degree of crystalline fraction, influence protein adsorption, and the adsorbed protein layer further dictates subsequent cellular reactions. Thus, by carefully tailoring surface properties one could engineer the surface for a specific protein adsorption which would lead to a desired cellular response.

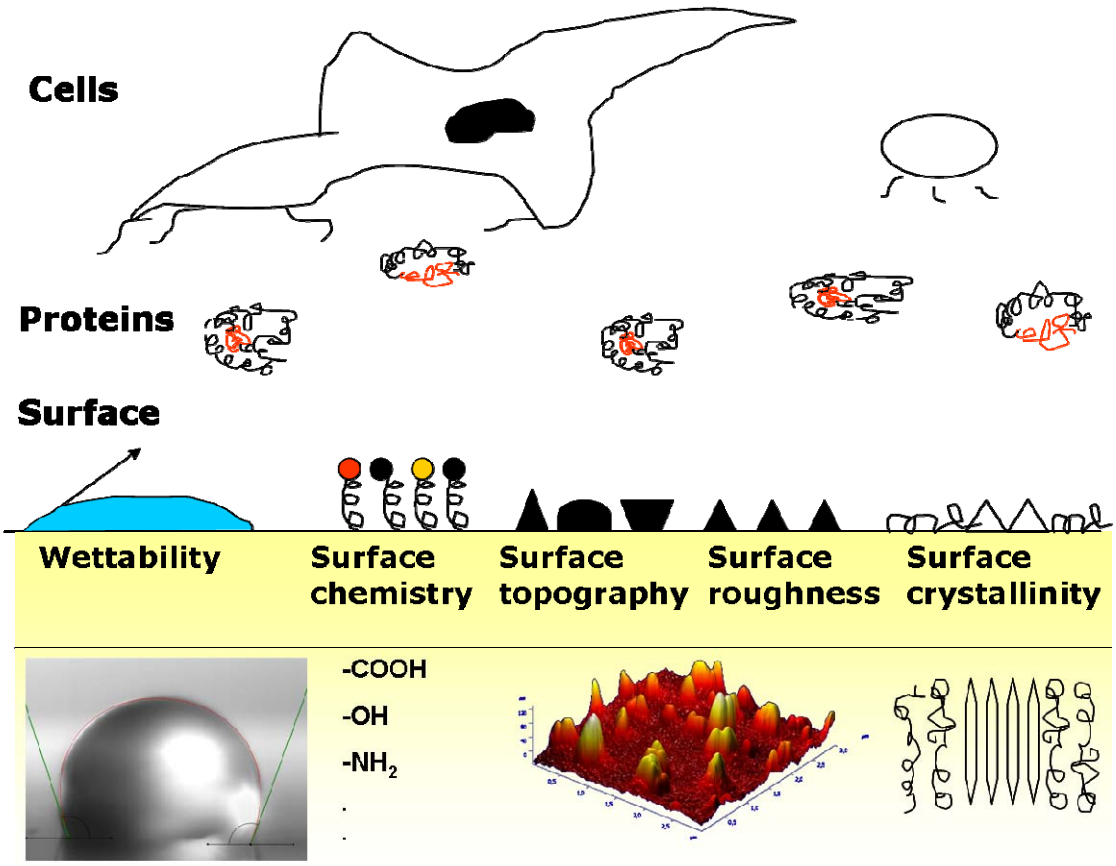

Figure 1 Shematic illustration of interactions between a biological system and polymer surface.

Once the protein film on the surface is formed adhesion of cells follows. Cells will adhere strongly to some surfaces while they will not adhere to others. This is mainly due to the special structure of individual cell membranes and the surface properties of materials. Different parts of a cell membrane correspond to different functions, such as adsorption, secretion, fluid transport, mechanical attachment, and communication with other cells. Three main adhesive sites on a cell membrane are responsible for cell-cell and cell-material surface interactions. These are adhering junctions (desmosomes), tight junctions and gap junctions (Shi, 2004).

Many mechanisms have been proposed for the adhesion of cells to the surface, the most common are the microscopic and atomic viewpoints. According to the microscopic viewpoint the adhesion of cells depends on the physiochemical properties of the surface. By contrast the atomic viewpoint considers that adhesion is driven by the receptor-ligand interactions. According to this theory the substrate is first bound by adhesive proteins, which generally have an RGD sequence (agenine, glycinine and aspartic acid). A number of integral proteins are embedded in the membrane which interact with the surface. These proteins enable cells to "recognize" and adhere to the surface by binding the RGD sequence to form cross-bridges which first induce the change in the cytoskeleton of cells and then the change in morphology of cells (Shi, 2004).

1.1.2. Blood – materials interactions

When polymer materials come into contact with blood they can cause various undesirable host responses such as thrombosis, inflammatory reactions, infections and various other responses. Such responses are minimised if the materials are be hemocompatible. In fact surface-induced thrombosis is one of the main problems associated with blood-contacting biomaterials.

Normal blood is a metastable state stabilized between two opposing driving forces coagulation and anticoagulation. Almost any external perturbation in the form of an artificial surface tends to trigger the coagulation system, i.e. blood clotting may occur (Kasemo, 2002). Once biomaterials are exposed to blood the adsorption of blood proteins immediately follows. The type, the amount and the conformational state of the adsorbed proteins determine whether platelets will adhere and become activated or not. The adsorption of fibrinogen (FNG), which is present in blood plasma, has been shown to be closely related to surface-induced thrombosis. The protein adsorption is an interfacial phenomenon and is strongly dependant on the physicochemical properties of the polymers, such as surface chemistry, surface energy, surface charge density, surface roughness, crystallinity of polymer and others. As thrombus formation begins with protein adsorption, the main efforts to improve hemocompatibility of materials have been directed towards controlling (mainly preventing) protein adsorption. Therefore, a modification of the material surface with protein-repulsive molecules has become a widely used approach for improving hemocompatibility of materials (Tzoneva-Velinova, 2003). The application on these grafts materials of a suitable protein coating may improve cell adhesion and proliferation. Commercially available collagen-, gelatin-, heparin- and albumin- coated vascular grafts have been developed to prevent the procedure of

clotting of the vascular graft before implantation. For collagen- or gelatin- coated vascular grafts, glutaraldehyde or formaldehyde are commonly used to crosslink the matrix (Weadock et al., 1993), in order to prevent rapid *in vivo* degradation. These cross linking agents, however, are incorporated into the graft material. Notably glutaraldehyde is known to evoke cytotoxic reactions by release of glutaraldehyde residues, during *in vitro* or *in vivo* degradation (Weadock et al., 1993, Huang-Lee et al., 1990). Heparin impregnation is also usually performed on these protein-immobilized systems (Kito and Matsuda, 1996, Gendler et al., 1984) to prevent coagulation. To enhance cell seeding on the vascular graft, surface modifications are made by immobilization of fibronectin, laminin, collagen and peptides (Kempezinski et al., 1985, Vohra et al., 1991). Another interesting method of surface modification of a vascular graft is by plasma treatment with the use of various gases, as it allows modification of its surface without dramatic changes in graft dynamics (Lin and Cooper, 1995). Plasma treatment is used together with various protein coatings as it improves protein adhesion and is widely used in the biomedical field to tailor surface properties and improve biocompatibility.

1.1.2.1. Blood coagulation

In order to understand the complexity of interaction of blood with the synthetic surface it is important to examine the mechanisms that lead to the undesirable activation of platelets and blood coagulation. Under normal conditions, blood contacts an endothelium which has anticoagulant and antithrombotic properties. When blood interacts with a cardiovascular device it represents a foreign surface and does not possess the same properties as the endothelium. Blood-material interactions trigger a complex series of events, including protein adsorption, platelet and leukocyte activation/adhesion, and the activation of complement and coagulation (Gorbet and Sefton, 2004). By contrast endothelia cells, that line the inner wall of the vascular system, are an ideal antithrombogenic material, which does not initiate any undesired reactions with platelets and blood coagulation factors. Any disruption of the cell lining, or replacement of the natural material with an artificial material (e.g. vascular grafts), triggers coagulation mechanism, which is essentially a "cascade" of reactions, by which normally inactive factors (e.g. factor XII) become enzymatically active following surface contact. As this sequence involves a series of steps, and because one enzyme molecule can activate many substrate molecules, the reactions are quickly amplified and significant amounts of thrombin are thus produced. This leads to platelet activation, fibrin formation and

finally to thrombus formation, which results in prevention of blood flow at the site at which the thrombus was first deposited (Ratner et al., 2008).

Initiation of clotting occurs either by surface-mediated reactions, or through tissue factor (TF) expression by cells. The two systems converge into a common pathway resulting in the formation of a fibrin clot due to action of thrombin on fibrinogen. At the final stage factor XIII, activated by thrombin, crosslinks and stabilizes the fibrin clot into an insoluble fibrin. Figure 2 shows a schematic presentation of mechanisms of coagulation, which are commonly divided into three parts: the intrinsic pathway or contact activation, the extrinsic pathway or activation by the tissue factor and the common pathway.

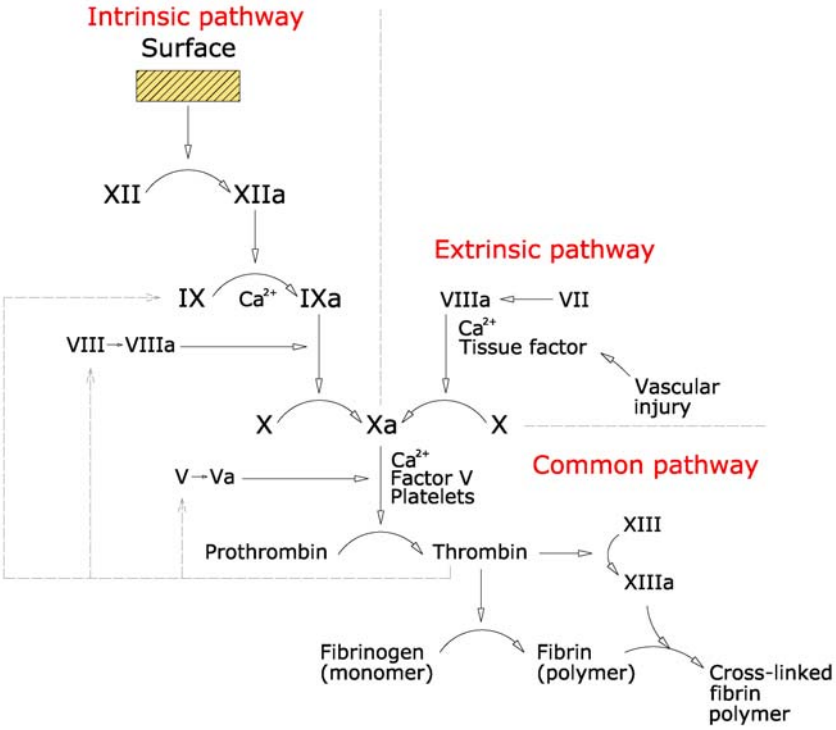

Figure 2. Simplified blood-coagulation cascade as presented in biomaterial textbooks (Hanson et al., 1996).

The intrinsic pathway is initiated by contact activation of high molecular weight kininogen (HMWK), prekallikrein and Factor XII; it is commonly said that these molecules require contact with (negatively charged) surfaces for zymogen activation *in vitro* (Schmaier, 1997). Contact activation depends on the conformational arrangement of factor XII after adsorption and the assembly of kallikrein and its cofactor HMWK. A middle phase of the intrinsic system begins with the first calcium dependent step, the activation of factor IX by factor IXa, which subsequently activates factor X. Factor VIII is an essential cofactor for the

intrinsic activation of factor X. In order to exert its cofactor activity, factor VIII must first be activated by a modification with an enzyme, such as thrombin. In the presence of calcium, factors IXa and VIIIa form a complex on phospholipide surface (as expressed on the surface of activated platelets) to activate factor X (Ratner et al., 2008). The significance of the intrinsic pathway to normal blood coagulation remains speculative, as the occurrence of negatively charged surfaces *in vivo* is limited. It is possible that the collagen present in the subendothelium after vessel injury could be the surface required for this reaction (Furie and Furie, 1988). Under physiologic conditions, the lack of relevance of the contact activation system is consistent with the fact that deficiencies of the contact proteins, HMWK, prekallikrein and Factor XII, have not been associated with abnormal bleeding (Rojkjaer and Schmaier 1999, Blajchman and Ozge-Anwar 1986).

The extrinsic system is initiated by activation of factor VII. This occurs when it interacts with the tissue factor, present in many body tissues. In the next step factor VIIa, an intracellular protein (thus not found in plasma), becomes an active enzyme for the extrinsic activation of factor X.

The common path begins when factor X is activated by either factor VIIa, tissue factor, or the factor IXa-VIIIa complex. The next step after formation of factor Xa, involves factor V, which has activity only after modification by another enzyme such as thrombin. In the presence of calcium and platelet phospholipids, factor Xa-Va then converts prothrombin (factor II) into thrombin (factor IIa). Like the conversion of factor X, prothrombin activation is effectively surface catalyzed. Thrombin, in addition to its ability to modify factor V and VII and activate platelets, acts also on the release of small peptides from fibrinogen. This causes the polymerization of fibrinogen monomers into fibrin polymer. Factor XIII is either trapped within the clot or provided by platelets, and is directly activated by thrombin. A strong, insoluble fibrin polymer is formed by the interaction of the fibrin polymer with factor XIIa (Ratner et al., 2008).

It should also be mentioned that hematology textbooks focus on the TF-dependent pathway. From their perspective the blood-coagulation cascade is not linear. Rather it consists of several feedback loops and begins with TF which is the physiological initiator of coagulation expressed on damaged cells at the site of vascular injury (Gorbet and Sefton, 2004). However, even from this perspective the extrinsic and intrinsic pathways are not independent of each other. When coagulation is initiated by a TF-dependent pathway, the intrinsic pathway remains important, since production of factor Xa by factor IXa–VIIIa complex has been shown to significantly contribute to thrombin generation. It appears that the extrinsic pathway TF–factor VIIa is responsible for the onset of coagulation, while the intrinsic pathway is the

major player in the propagation phase. The activation of FX by FIXa is all the more important because the tissue factor pathway inhibitor will reduce the production of FXa by TF-VIIa complex (Gorbet and Sefton, 2004).

1.1.2.2. Platelets

Platelets are non-nucleated, disk-shaped cells, with a diameter of 3-4 μm, produced in the bone marrow. They circulate at an average concentration of about $200 \cdot 10^6$ cells/ml and occupy approximately of 0,3 % of total blood volume and their life span is about 10 days (Gorbet and Sefton, 2004). Platelets are self sufficient as they contain all the necessary ingredients needed for adhesion, aggregation and formation of thrombi. In fresh blood platelets have spheroidal form, but have a tendency to extrude hair-like filaments from their membranes and can adhere to each other (Shi, 2004). Their function is to arrest bleeding through the formation of platelet plugs and to stabilise platelet plugs by catalyzing coagulation reactions which lead to the formation of fibrin, as described above.
The basis for understanding platelet function is their structure. In an un-stimulated state platelets have a discoid shape, which is maintained by a cytoskeleton of microtubules. The external surface coat of platelets contains membrane-bound receptors (glycoproteins Ib and IIb/IIIa) that mediate contact reactions of adhesion (platelet – surface) and aggregation (platelet – platelet). The membrane also provides a phospholipid surface, which accelerates the coagulation cascade and forms a spongy, canal-like open network that represents an expanded reactive surface to which plasma factors are selectively adsorbed (Ratner et al., 2008).
A possible way to asses the activation degree of adherent platelets is to study their shape and the number of adherent platelets. According to Goodman (Goodman et al.; 2006), their shape can be categorised on a scale from lower to higher level of activation as: round or discoidic (R); dendritic or early pseudopodial (D); spread-dendritic or intermediate pseudopodial (SD); spreading or late pseudopodial (S) and fully spread (FS). Figure 3 presents different degrees of platelet activation measured by SEM (Rodrigues et al., 2006).

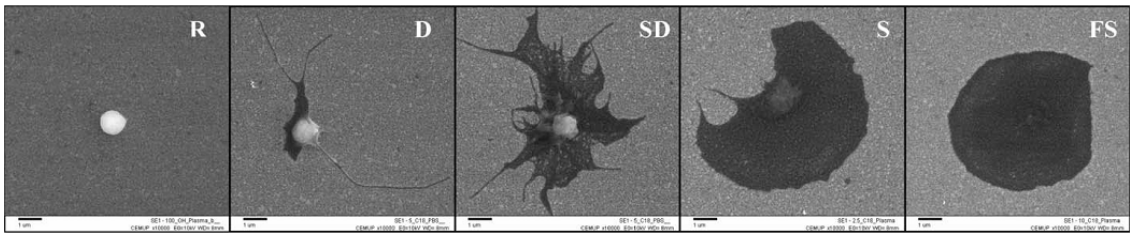

Figure 3. Different platelet activation measured by SEM. (R) round or discoid; (D) dendritic or early pseudopodial; (SD) spread-dendritic or intermediate pseudopodial; (S) spreading or late pseudopodial and (FS) fully spread. Marker bars represent 1 micrometer (Rodrigues et al., 2006).

1.1.2.3. Blood vessels

In order to produce vascular grafts with adequate mechanical, physical and surface properties it is important to provide a better insight into the processes taking place in blood vessels, which requires an understanding of how natural blood vessels are build. Large and medium sized arteries have distinct structural features; they are categorised as the intima, media and adventitia, although these are less obvious in small arteriols and do not exist in capillaries. The intima forms the layer closest to the blood flow; it consists of a lining of endothelial cells attached to a connective tissue bed of basement membrane and matrix molecules. Mechanical properties critical to blood vessel function include tensile stiffness, elasticity, compressibility and viscoelasticity. Collagens provide tensile stiffness, elastin provides elastic properties, while proteoglycans contribute to compressibility, and when combined with collagen and elastin they are responsible for the viscoelastic properties. This complex mixture of molecules and the way in which they are organised provides blood vessels with their properties and enables them to function throughout life (Hoffman and Weyand, 2002.)

The make-up of a natural blood vessel wall is intriguingly sophisticated; as mentioned above its structure consists of three layers:

1. The blood-contacting intima, a monolayer of endothelial cells on a basement membrane.
2. The media composed of smooth muscle cells embedded in an extracellular matrix of collagen, elastin and mucopolysaccharides.
3. The adventitia, consisting of fibroblast cells, surrounded by an extracellular matrix comprising mainly of collagen.

This description of the arterial wall also explains why there are so many difficulties in developing functional artificial prostheses for blood vessels.

1.1.2.4. Vascular grafts

Prosthetic grafts are made of yarn, Dacron (PET) or an extruded polymer (ePTFE and polyurethane). These grafts have to undergo special preparation before they can be utilized in humans. Instead biological grafts can be used; these grafts can be obtained from a human source (allografts) or from a non-human source (heterografts).

Polyethylene terephthalate (PET- Dacron grafts) and polytetrafluoroethylene (PTFE) are the two most common prosthetic materials available today for vascular grafts. Figure 4 shows their surface morphology, as obtained from SEM images.

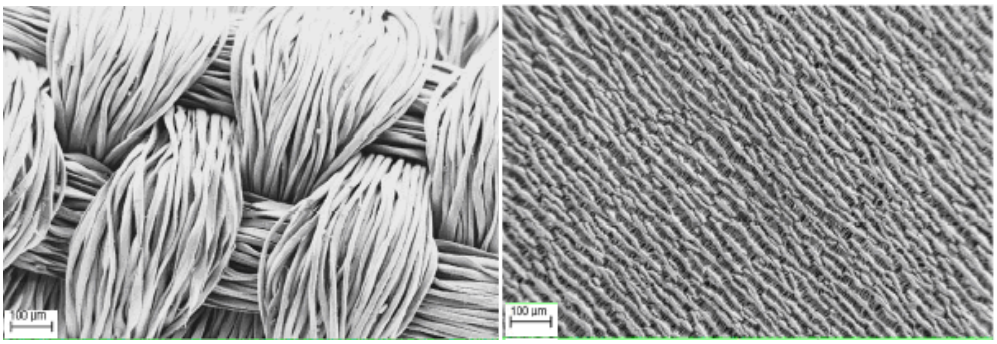

Figure 4. Scanning electron microscopy pictures of PET (left) and ePTFE (right) vascular grafts.

Brittle handling, complex suturing qualities, and high thrombogenicity of Dacron (Björck et al., 1994) prompted its replacement by knitted Dacron (Guidoin et al., 1984), which required intraoperative preclotting because of its high permeability (Quinones-Baldrich et al., 1986). Currently, knitted Dacron is impregnated with gelatin (Drury et al., 1987), albumin (Domurado et al., 1975) or collagen (Humphries et al., 1981) to reduce its permeability and to obviate the need for preclotting (Barraet al., 1995, Guidoin et al., 1984). The coated vascular graft surface of Dacron or ePTFE was improved by chemical crosslinking with glutaraldehyde, formaldehyde or diepoxided poly(ethylene glycol) and heparin impregnation of these protein immobilized systems (Kito et al., 1996, Drury et al., 1987). However, successful results have not yet been reported for small-calibre vascular grafts. ePTFE and Dacron vascular grafts possess many of the properties of ideal vascular prostheses, but they are highly hydrophobic surfaces and thus limit endothelial surface adhesion (Callow, 1988). Modifications of the surfaces to stimulate endothelialization could reduce thrombosis, eliminate platelet deposition, resist bacterial infection and extend graft patency (Callow, 1988, Kempezinski, 1985).

- Dacron vascular implants

Dacron yarn is a multifilament polyester yarn consisting of small continuous filaments which make the graft soft, elastic and easy to handle. The yarn can be fashioned into a prosthetic graft by weaving or knitting (see Figure 5). In woven grafts, fabric threads are interlaced into a simple over and under pattern both in lengthwise and circumferential directions. Woven fabric grafts have little or no stretch in any direction. The grafts are tightly constructed and have low porosity; they are relatively strong and relatively stiff. The small interstices reduce bleeding and their relative strength decreases the likelihood of elongation and dilatation. However, the graft has less desirable handling characteristics. Because of their low porosity, woven grafts have reduced perigraft healing. In a knit structure, the yarn is orientated in a predominantly longitudinal (warp knitted) or circumferential (weft knitted) direction. Since warp knitted grafts are more stable they are most commonly manufactured. In the manufacturing process the spacing of the yarn, and hence the pore dimensions, can be varied. The result is that knitted grafts generally have higher porosity, with theoretically enhanced healing, improved compliance, and superior handling characteristics and also have a lesser tendency to fray, compared to woven grafts. On the downside, it is necessary to preclot the graft, which reduces graft strength and can lead to long term dilatation (Nunn and Freeman, 1979).

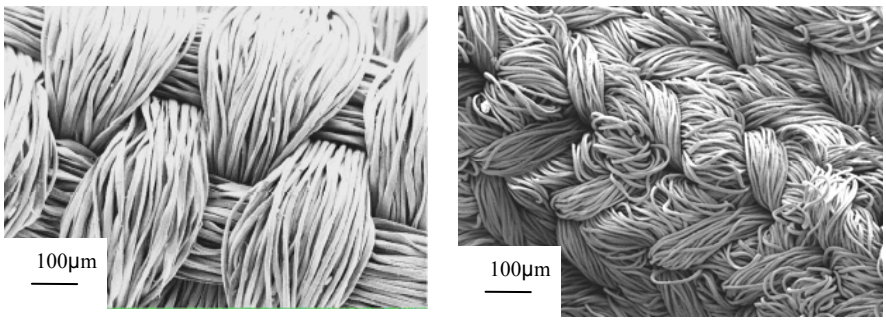

Figure 5. SEM image of woven and knitted Dacron vascular grafts.

Graft impregnation with substances such as collagen, albumin or gelatin, are increasingly being used in the manufacture process of Dacron grafts. The addition of these biological substances renders the graft leak proof without destroying favourable handling characteristics of the underlying porous material. Upon implantation the sealant is completely digested, thereby allowing normal healing of the underlying porous material. Some evidence suggests that such graft coatings may reduce early thrombogenicity of the graft surface with an expected improvement in graft patency (Chakfe et al., 1996). A more significant advantage

may be their ability to bond with antibiotics. At present all coated grafts are significantly more expensive than standard textile grafts.

- Chemical structure and properties of PET

Polyethylene terephthalate (PET) is a linear, aromatic polyester which was first manufactured by Dupont in the late 1940s. Depending on its processing and thermal history, it may exist both as an amorphous (transparent) and as a semi-crystalline (opaque and white) material with glass temperature from 60 °C to 75 °C and melting point between 253 °C and 260 °C. The PET polymer contains about 0.4-0.6 % of TiO_2, however the content of TiO_2 in polymer can be as high as 2.5 % or as low as 0.05 %. It is manufactured under trade names Arnite, Impet, Rynite, Ertalyte, Melinex and Mylar films, and Dacron, Terylene & Trevira fibers. Dacron is commonly used for vascular implants (Cook, 2009). The chemical structure of PET is shown in Figure 6.

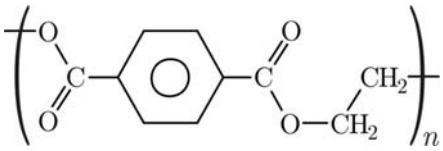

Figure 6. Chemical structure of PET polymer (Cook, 2009).

1.2. Biological response

Surface properties of biomaterials play a major role in determining biocompatibility; they have a significant influence on biological response and also determine the long term performance *in vivo*. The main goal in designing biomaterials is therefore to ensure that they exhibit appropriate surface properties as well as desired physical and mechanical characteristics, which would enable them to function properly in the biological environment. It is hard to satisfy all of these characteristics; this is why surface treatment techniques are commonly employed in order to improve surface properties. It is still a highly challenging task to modify surface properties in order to produce hemocompatible surfaces, and many controversial results are reported in the literature. This chapter will present some of the most important surface properties and review their biological response.

1.2.1. Wettability

Surface wettability is believed to be one of the most important parameters which affect biological response to a biomaterial. It is established that protein adsorption is the first event that takes place on the surface of a biomaterial with biological fluids (Horbett, 1993, Montdargent and Lettourneur, 2000, Roach et al., 2005), and that the biological response is controlled by the nature and confirmation of the proteins adsorbed to the surface. Thus, wettability is believed to play an important role in the amount and conformational changes of adsorbed proteins (Vroman, 1988) platelet adhesion/activation, blood coagulation (Lee and Lee, 1998b) and adhesion of cells (Choe et al., 2004, Faucheux et al., 2004).

Generally hydrophobic surfaces are considered to be more protein-adsorbent than hydrophilic surfaces, due to strong hydrophobic interactions occurring at these surfaces (Dee et al., 2002, Kongde et al., 2005, Xu et al., 2007). It has been shown by the study of Xu et al. that a stark transition between protein adherent and protein non-adherent materials was in the range of water contact angles 60–65 degrees. Statistical analysis of the adhesion force measurements done on differently wettable surface of LDPE and protein coated AFM tips demonstrated that proteins were more strongly adherent onto poorly wettable (hydrophobic) surfaces than to wettable surfaces.

The adhesion of proteins to the surface is a time-dependent process, which involves relatively high energy scales together with conformational and

reorientational changes following contact with the surface (Tan and Martic, 1990). Therefore wettability and surface chemistry greatly influence time dependent conformational changes in adsorbed proteins and mediate adsorption kinetics, the strength of binding (Fang et al., 2005, Xu et al., 2007) and subsequent protein activity (Hylton et al., 2005).

Figure 7 shows the sequence of events taking place on the hydrophilic and hydrophobic surface of biomaterial. The first molecules to reach the surface (time scale of order ns) are water molecules. Water is known to interact and bind differently depending on surface properties. The properties of the surface water ''shell'' are an important factor and influence proteins and other molecules, which arrive a little later. Wettability of the surface may determine whether proteins denature or not, it may also determine their orientation, coverage, strength of interaction etc. In cases where different proteins are presented in a biological fluid, such as in blood plasma, the competition between these proteins to the surface takes place on the order of time scale. The strength of protein interactions, which first reach the surface, further influence the exchange reactions between different proteins and some exchanges may not even take place (Hylton et al., 2005). When cells arrive to the surface they respond to a protein-covered surface; the protein layer has properties that were initially determined by the preformed water shells. Thus, cell–surface interactions are ultimately interactions between cells and surface bound proteins (or other biomolecules) (Sipehia, 1993, Lu and Sipehia, 2001). Generally, more wettable surfaces, as opposed to low wettable surfaces, were also reported to promote cell adhesion.

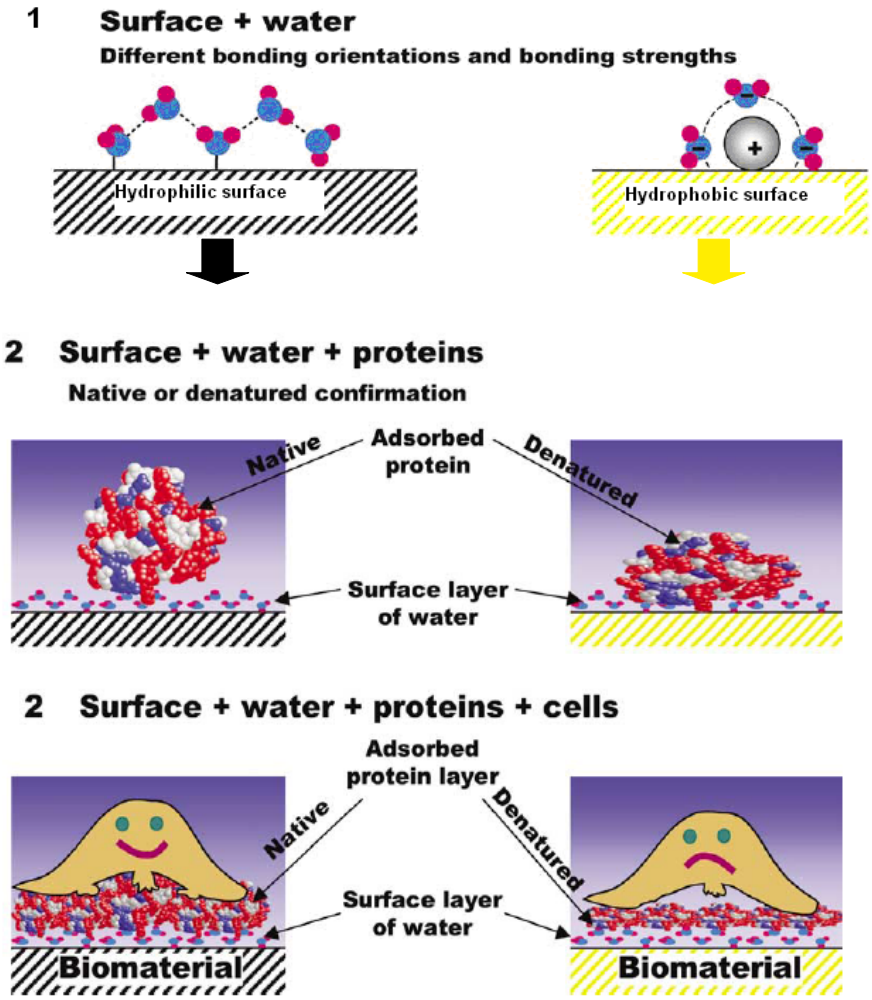

Figure 7 Schematic illustration of the successive events following implantation of a medical implant (Lu and Sipehia, 2001).

Many theories have been proposed regarding platelet adhesion and surface wettability. According to the Lampert rule, blood coagulation is proportional to the capacity of the surface to repel water (hydrophobic surface). Donovan and Zimmerman attributed longer clotting time (lower thrombogenicity) of polyethylene to low surface wettability (Donovan and Zimmerman, 1949). Vogler et. al. showed that coagulation is the step function of surface wettability, with very low activation for poorly wettable surfaces and high activation for fully wettable surfaces (Vogler et al., 1995). Contrary to this it was shown by C. Sperling et al. that surfaces with more hydrophobic characteristics (contact angle 72 degrees -112 degrees) greatly enhance platelet adhesion (Sperling et al., 2005). Similar observations were also reported in the study by Rodrigues et al., where the most hydrophobic surfaces showed the highest number of adherent platelets in a highly activated state. In contrast to more hydrophilic surfaces (-OH terminated self assembled monolayers),

where only a small amount of adherent and activated platelets was observed (Rodrigues et al., 2006).

Although surface wettability probably plays an important role in hemocompatibility of materials no straight correlation between surface wettability and blood compatibility has so far been acknowledged, as the results of different studies are still controversial. This is probably due to the high degree of complexity of the reaction paths in the blood, it is also important to take into consideration other important surface parameters (such as surface chemistry, surface charge, morphology etc.).

1.2.2. Chemical composition

The chemical nature of the surface in contact with blood is closely linked to its biological response. One of the strategies to improve hemocompatibility of the surface is to introduce new functional groups, such as hydroxyl (-OH), amine (-NH_x), methyl (-CH_3) sulphate (-SO_4) or carboxylic (-COOH) (Tzoneva et al., 2008, Sperling et al., 2005, Seifert et al., 2002). This is either employed to tailor the biological response (improve cell proliferation, reduce platelet adhesion etc.) or to enable immobilisation of biomolecules (enzymes, proteins etc.). The effects of functional groups on hemocomaptibilility have been extensively studied, but again results are not always consistent. It has been generally observed that increased surface hydroxyl concentration causes increased complement activation (Sefton et al., 2001), whereas increased methylation results in reduced complement activation (Tengvall, et al., 1992). Yet, increased oxygen concentration has been shown to reduce coagulation activation (Grunkemeier et al., 1998, Tyan et al., 2002), while increasing the negative charge of the surface has generally increased surface activation (Tankersley and Finlayson, 1984). Interestingly, the study by Wilson et. al. has shown that treatment of polymer (polyethyetherurethane- PEU) surface with RF ammonia and nitrogen plasma (incorporation of nitrogen groups) significantly reduces contact activation. However, no changes in thrombogenicity, as compared to the untreated surface, were observed after oxygen and argon plasma (incorporation of oxygen groups). Similar results were obtained for RF plasma treatment of polydimethylsiloxane (PDMS) by Williams (Williams et al., 2001).

1.2.3. Surface morphology

Numerous studies have dealt with cell behaviour on different nanosurfaces; this is because nanomorphology of material may significantly influence protein and cell adhesion. Cells can sense the chemistry and topography of the surface to which they adhere. Focal adhesions interacting with the surface are established by cell filopodia (which are 0.25-0.5 μm wide and 2-10 μm long) (Burridge and Chrzanowska-Wodnicka, 1996). Filopodia can interact with the surface due to surface features which are either arranged randomly or in some geometrical order, and have dimensions from the micro to the nanometer range (Dalboy et al., 2003). Beyond micrometers, it has been shown that nanometric (1-500 nm) features can elicit specific cell response (Curtis and Wilkinson, 2001, Dalby et al., 2002). In addition, it is known that the recognition of topography by cells also depends on cell type and origin (Schröder et al., 2003).
Surface morphology is also important in protein adsorption and subsequent cell response (Kam e tal., 2001). Thus, Reidel and colleagues showed that adsorption of albumin dramatically increased due to presence of nanoislands (Reidel et al., 2001). While Vertegel et. al. showed that the adsorption of lysozyme to silica nanoparticles decreased with decreasing nanoparticle size (Vertegel et al., 2004). They proposed that the increase in the radius of curvature of small nanoparticles, (which are thus almost the same size as proteins), results in less protein denaturation on these surfaces, preserving native protein conformation. According to the literature proteins adhere to nanostructures, but it is difficult to develop broad generalisations regarding the strength of adhesion and whether the proteins would be denaturised on these surfaces.

Surface topography plays an important role in providing three-dimensionality of cells (Dalby et al., 2002). For instance the topography of the collagen fibres, with repeated 66 nm binding, has shown to affect cell shape (Curtis and Wilkinson, 1999). Techniques based on micropatterning of biologically important proteins (e.g., laminin and fibronectin) are of a particular interest because these proteins could provide cell guidance (Tai and Buettner, 1998). The formation of large clusters of immobilized peptides on glass surfaces have been shown to affect the cell-substratum adhesiveness of endothelia cells (Kouvroukoglou et al., 2000). Thus, by properly adjusting surface topography on a micro and nanometer scale it might be possible to obtain a specific biological response from cells. This would be a very attractive way to design biomaterial surfaces for specific applications.

1.3. Plasma – the fourth state of matter

In this section the term plasma will refer to ionised gas, or forth state of matter. It has nothing to do with blood plasma, which was introduced in the previous chapters. However, it is interesting to note that the term plasma actually got its name from blood plasma, as Irvin Langmuir first introduced this name in 1982. Ionised gas is usually called plasma when it is electrically neutral (i.e., electron density is balanced by that of positive ions) and contains a significant number of electrically charged particles, which is sufficient to affect its electrical properties and behaviour (Fridman, 2008). Therefore plasma is composed of highly excited atomic, molecular, ionic, and other native radical species. It is typically obtained when gases are excited into energetic states by radio-frequency (RF), microwave, or electrons from a hot filament discharge (Ferencz et al., 2004). To produce plasma, electron separation from atoms or molecules in gas state, or ionization is required. When an atom or a molecule gains enough energy from an outside excitation source or via interaction (collisions) with one another, ionization occurs (Venugopalan, 1971).

Plasma states can be divided into two main categories: thermal near-equilibrium plasmas and thermodynamically non-equilibrium plasmas or cold plasmas. Thermal near-equilibrium plasmas are characterized by very high temperatures of heavy particles (often about 10000K). Non-equilibrium plasmas are composed of low temperature heavy particles (charged and neutral molecular and atomic species) and very high temperature electrons (often about 50000K). Most plasmas of practical importance have electron temperatures of 1-20 eV with electron densities in the range of 10^{6}-10^{18} cm^{-3}. (i.e. 1 eV approximately equals 11600K).

However, not all particles in plasma need to be ionised; a common condition in plasma chemistry is for the gases to be only partially ionized. The ionization degree (i.e. the ratio of density of major charged species to that of neutral gas) in conventional plasma-chemical systems is in the range between 10^{-7}-10^{-4}. Where ionization is close to unity, such plasma is referred to as completely ionized plasma (usually in thermonuclear systems: tokomaks, stellarators, plasma pinches, etc.). Plasmas with low ionization degree are referred to as weakly ionised plasma (Fridman, 2008) and this is the plasma that was employed in the present work.

Plasma can also be divided into man made and natural plasma. Natural plasma refers to sun, stars, lightening etc., and it is estimated that more than 99% of the known universe is in the plasma state (Venugopalan, 1971). On the other hand plasma can be produced in the laboratory by raising the energy content of matter regardless of the nature of the energy source. Thus plasmas can be generated by

mechanical (close to adiabatic compression), thermal (electrically heated furnaces) chemical (exothermic reactions, e.g. flames), radiant (high energy electromagnetic and particle radiations, e.g. electron beams), nuclear (controlled nuclear reactions), and electrical (arcs, coronas, direct-current (DC) and radio-frequency (RF) discharges and by a combination of them. An example is the combination of mechanical and thermal energies (e.g. explosions) (Nasser, 1971).

Non-equilibrium cold plasmas are further divided into high and low pressure plasma. Low-pressure non-equilibrium discharges (Nasser, 1971) are initiated and sustained by DC, RF, or microwave (MW) discharge. These plasma sources operate at low-pressure because the breakdown electric field is smaller and the current is more controllable and so it can generate large area uniform plasma with a well controlled electron density (Venugopalan, 1971). Non-equilibrium atmospheric pressure discharges (Boeuf and Pitchford, 1996) are often recognized as Partial Discharges (PD). They can operate in a wide range of temperature and pressure conditions. PDs are localized or confined electrical discharges, and often exhibit a non-stationary character (an unpredictable transition between different plasma modes). These discharges are very complex and manifest themselves in different modes (patterns). Accordingly, Dielectric- Barrier Discharges (DBD,) Corona Discharges (CD), Constricted Glows (CG), Electron Avalanches (EA), Localized Townsend Discharges (LTD), and Streamers (ST), are considered as distinctive PDs.

The present work deals with RF plasma treatment of polymers and the interactions of such plasma with polymers are presented in the following chapters. The details of plasma treatment, together with discharge and plasma parameters, are described in Chapter 4.2.2.

1.3.1. Plasma treatment of polymers

Polymers have been successfully applied in a wide range of applications such as biomaterials, composites, microelectronic devices, thin film technology etc. Although polymers usually have excellent bulk physical and chemical properties, are inexpensive and easy to process, their surface properties are usually inappropriate for certain applications. In order to implement polymers for required applications they must possesses special surface features regarding their chemical composition, hydrophylicity, roughness, crystallinity, conductivity, lubrictivity (Chan et al., 1996). Therefore, surface modification techniques, which enable appropriate surface modification, have become valuable for the polymer industry.

Especially valuable are techniques which enable surface modification without altering the bulk attributes of the polymer. One such technique is plasma treatment, whereby the surface can be modified to:

- produce new functional groups at the surface;
- increase surface energy;
- increase hydrophylicity or hydrophobicity;
- change its morphology and roughness;
- increase or decrease crystallinity;
- remove weak bound layers or contaminants.

This is why plasma techniques have become important industrial processes for modifying polymer surfaces. The reactions that take place between plasma and polymers can be classified as follows:

- Surface reactions or plasma modification

  Reactions between gas-phase species and surface species and reactions between surface species produce functional groups and crosslinking at the surface. These reactions include plasma treatment by oxygen, nitrogen, nitrogen dioxide.

- Plasma polymerization

  The formation of a thin film on the surface of a polymer via polymerization of an organic monomer such as CH_4, C_2H_6, C_2F_4, and C_3F_6 in plasma. It involves reactions between gas-phase species, reactions between gas-phase species and surface species, and reactions between surface species.

- Plasma cleaning and etching

  Materials are removed from a polymer surface by chemical reactions and physical etching at the surface to form volatile products. Oxygen-containing plasmas are used to remove organic contaminants from polymer surfaces, e.g., oligomers, anti-oxidants, anti-block agents or mold-release agents. Etching differs from cleaning only in the amounts of materials that are removed from the surface. Oxygen plasmas and oxygen- and fluorine-containing plasmas are frequently used for the etching of polymers (Yasuda et al., 1990, d'Agostino et al., 1990).

1.3.1.1. Chemical reactions on the polymer surface

The major chemical products that are created during non-thermal plasma treatment are stimulated by plasma components, especially by electrons, ions, excited particles, atoms, radicals and UV radiation. These products are mainly free radicals, non-saturated organic compounds, cross-links between polymer macromolecules, products of destruction of the polymer chains, and gas phase products (mostly molecular hydrogen). Processes that form radicals on the polymer surface are influence by breaking the R-H and C-C bonds by electron impact and UV radiation in plasma. These can be described by the following reactions (Fridman, 2008):

$$RH \rightarrow R^{\bullet} + H, \qquad RH \rightarrow R_1^{\bullet} + R_2^{\bullet} \qquad (1)$$

The direct formation of non-saturated organic compounds with double bonds on the polymer surface can be described by:

$$RH \rightarrow R_1\text{-}CH{=}CH\text{-}R_2 \qquad (2)$$

While secondary reactions of the atomic hydrogen usually lead to the formation of molecular hydrogen through different mechanisms, including recombination and hydrogen transfer with the polymeric molecule:

$$H + H \rightarrow H_2, \qquad H + RH \rightarrow R^{\bullet} + H_2 \qquad (3)$$

The secondary reaction of atomic hydrogen with organic radical R can result not only in recombination but also in simultaneous formation of molecular hydrogen – a double bond in the organic macromolecule, which can be illustrated as:

$$H + R^{\bullet} \rightarrow R_1\text{-}CH{=}CH\text{-}R_2 \qquad (4)$$

When plasma gas contains oxygen, the free organic radical R, generated by non-thermal plasma treatment of polymer surface (1), effectively attaches molecular oxygen from the gas phase, thus forming active peroxide radicals:

$$R^{\bullet} + O_2 \rightarrow R\text{-}O\text{-}O\text{-} \qquad (5)$$

The RO_2 peroxide radicals, which are formed on the polymer surface by treatment in non-thermal plasma systems, are able to initiate different important chemical processes. The simplest process known by the RO_2 radicals relate to the formation of hydro-organic peroxide and other peroxide compounds on the surface of polymers:

$$R\text{-}O\text{-}O\text{-} + RH \rightarrow R\text{-}O\text{-}O\text{-}H + R^{\bullet} \quad (6)$$

$$R\text{-}O\text{-}O\text{-} + RH \rightarrow R\text{-}O\text{-}O\text{-}R_1 + R_2^{\bullet} \quad (7)$$

The reactions (6) and (7) together with attachment process (5) create a chain reaction for formation of hydro-organic peroxide and other peroxide compounds on the polymer surface under treatment by oxygen-containing plasma. These compounds are formed on the relatively thin surface layers of polymers, due to low energies of plasma electrons and ions and high coefficients of excitation of UV radiation in polymers (Fridman, 2008).

The incorporation of nitrogen functionalities can be reached by using nitrogen containing plasma. In such cases the free radicals react with the reactive atomic and molecular species, which are created in such plasmas (d'Agostino et al., 1990).

$$R^{\bullet} + N_2 \rightarrow R\text{-}NH_2 \text{ or } R\text{-}NH\text{-}R_1 \quad (8)$$

1.3.1.2. Etching of polymers

Etching of polymers in plasma is another effect that must be considered. Treatment of polymers by non-thermal plasma causes etching by two mechanisms: physical sputtering and chemical etching. Physical sputtering occurs due to ion bombardment, while chemical etching occurs due to surface reactions and gasification of polymers, particularly provided by atomic oxygen, fluorine, ozone and electronically excited oxygen molecules O_2 (Fridman, 2008) Therefore etching effects and plasma modifications can never be separated, as both processes take place during plasma treatment. However, it is possible to tailor the balance between the reactions by altering discharge and plasma parameters. Some studies have been conducted in order to study etching effects on polymers treated by different gases. For example Inagaki et al. showed that a difference in etching rates on PET polymers can occur by employing different gasses for plasma treatment (oxygen, nitrogen, ammonia, nitrogen and argon) (Inagaki et al., 2004). The treatment was done by RF plasma at different powers ranging from 25, 50 and 100 W, at the frequency of 13,56 MHz. The etching rate seemed to be linear with magnitude of RF power, with the highest etching occurring after treatment in oxygen plasma. This complies with the theory described above, according to which etching is mainly caused by atomic oxygen. It is also important to note that differences in etching rates are also observed between different polymers due to their chemical structure and degree of crystallinity. For example fluorocarbon polymers are known by their low etching rates in plasma, while the etching of hydrocarbons is much faster. The polymers least resistive to etching are the ones with heteroatoms especially those containing oxygen groups (Fridman, 2008).

1.3.1.3. Ageing effects on polymers

Long term stability of the plasma modified surface is crucial for applications where the material is not immediately used. It has been observed by many researchers that with time the modified polymer surfaces tend to recover to its untreated state (Morra et al., 1991, Griesser et al., 1991); this process is also known as ageing. This phenomenon could be the result of four major mechanisms (see Figure 8) (Fridman, 2008):

- re-orientation and shift of the polar groups formed on the polymer surface inside the polymer material due to thermodynamic relaxation;

- diffusion of the low-molecular-weight admixtures and oligomers from the bulk of the polymer material to the surface;
- diffusion to the polymer surface of the low-molecular-weight products formed during plasma treatment in the relatively thick surface layer;
- post-plasma treatment reactions of free radicals and other plasma-generated active species and groups between themselves and with the environment.

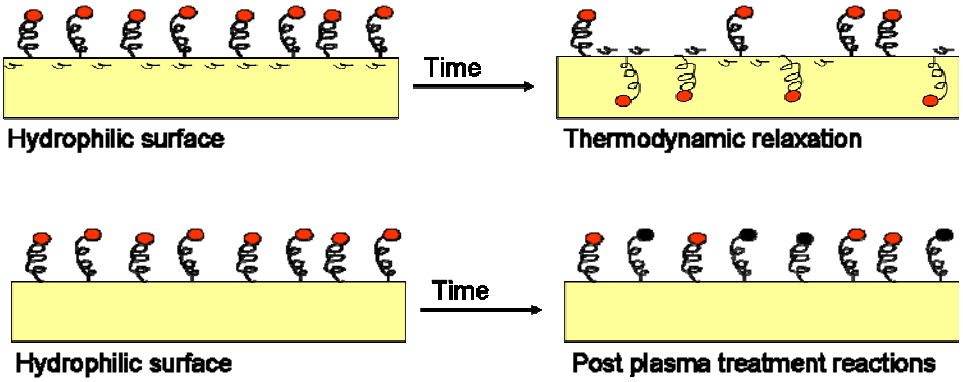

Figure 8 Different mechanisms involved in ageing of plasma treated polymers in air.

2. Aims and hypothesis

There have been many attempts to correlate biomaterial properties to biological performance, but with no obvious success, as either subtle or large differences gave rise to unremarkable changes in biocompatibility. Due to complexity of blood–material interactions, finding a solution to thrombotic complications associated with cardiovascular devices is still a major challenge in biomaterial science. The currently used vascular grafts have successfully replaced large-diameter blood vessels, but the long-term performance of small-diameter (< 6 mm) vascular grafts is still disappointing.

Therefore the aim of this work is to present possible surface modification of commercial vascular grafts (made from PET polymer) by oxygen and nitrogen plasma treatment. As plasma treatment is known to affect surface parameters such as wettability, chemistry, surface charge, morphology and crystallinity, which are thought to play a crucial role in biological response, the main hypothesis is that by optimising plasma treatment a desired biological response could be achieved. Thus plasma treatment would be prospective surface modification technique. This is because modification is obtained without having to introduce additives or chemical groups, which would leach out of, or migrate to the surface in an uncontrolled manner, which is often the case in adhesion of bioactive coatings. Another advantage of plasma treatment is that it modifies only the surface of biomaterial and does not affect its bulk attributes.

Gas plasma treatment is one of the strategies for enhancing surface properties by enriching the surface with new functional groups known to enhance cell proliferation – such as oxygen or nitrogen (Kim et al., 2000, Chi-lan et al., 2006, Coen et al., 2003). Some studies have already shown that reduced activation of coagulation can be achieved on polyetherurethane (PEU) and polydimethylsiloxane (PDMS) with nitrogen and ammonia plasma treatment. Therefore, it may be hypothesised that it is possible to tailor blood-contact interactions by plasma treatment. This hypothesis has been tested in the present work.

The hypotheses of this work are:

- Different surface modification of PET polymers can be achieved by optimising oxygen and nitrogen plasma treatment. This means that different concentrations, as well as different functional groups can be formed on the

surface. Moreover, desired surface morphology and wettability could also be achieved by variation of plasma parameters.

- Plasma treatment enables modification of surface morphology on the nano-scale. Figure 9 presents the size distribution of cells and plasma proteins together with the size distribution of features on vascular grafts. Modification of the surface on the nanometer scale is achieved with plasma treatment therefore this modification is in the range of plasma proteins, which are thought to play an important role in cell attachment. Thus, it is hypothesised that by tailoring surface morphology on the nano-scale it is possible to obtain a desired biological response.

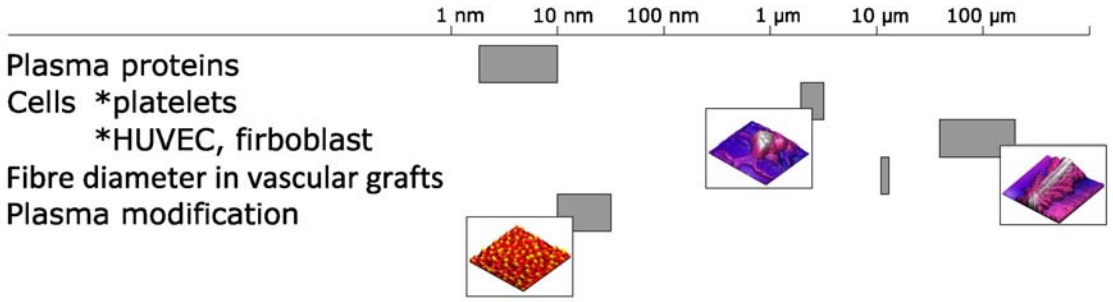

Figure 9 Size distribution of cells and plasma proteins together with the size distribution of features on PET vascular grafts.

- The degree of crystalline fraction in polymers influences the interaction of plasma species with the surface. Thus, the surface modification of polymers with different crystalline fraction may vary due to different etching effects; this would mainly result in different surface morphology.

- Different gases employed for surface modification of PET polymers would influence the biological response, mainly due to introduction of different functional groups onto the surface.

- With optimisation of plasma parameters also other surface parameters could be altered, such as wettability, surface morphology and crystallinity, which could influence platelet adhesion.

The first objective of this work was to characterize surface changes on PET polymers induced by oxygen and nitrogen plasma treatment. As working directly on vascular grafts is hard, due to problems associated with analysing techniques, most of the work was done on PET foils. It has been hypothesised that effects of plasma treatment could differ on chemically identical polymers due to the difference in their crystalline fraction. As fibres from vascular grafts have higher crystalline fraction, the effects of plasma treatment on PET polymers with different degree of crystallinity were also studied. In this work much emphasis was also put on the characterisation of the surface, as these parameters may be correlated to biological response.

The second objective was to investigate the biological response of untreated and plasma treated surfaces under *in vitro* conditions. As endothelia cells are thought to be an ideal natural antithrombogenic material the proliferation of endothelia cells on untreated and plasma treated surfaces was studied. Hemocompatibility of materials is closely linked to platelet adhesion and their activation, thus interactions between platelets and the surface were studied as well.
The final goal of the work was to optimise plasma treatment of PET surfaces in order to obtain surface properties, which would enable good proliferation of endothelia cells and would also reduce platelet adhesion on PET foils and PET vascular grafts.

3. Materials and methods

The PET polymer was modified in weakly ionized, highly dissociated, low-pressure radio frequency (RF) oxygen and nitrogen plasma. Plasma treatment was done on PET polymers with different degree of crystallinity. Various surface analysing techniques were employed to study the effects of oxygen and nitrogen plasma treatment on PET polymers: chemical composition was characterized by x-ray photoelectron spectroscopy (XPS); morphology was characterised by atomic force spectroscopy (AFM) and scanning electron spectroscopy (SEM); and wettability by measuring the water contact angle (WCA). The etching rate of polymers with different degrees of crystallinity was determined by gravimetry, while the degree of crystallinity was determined from DSC measurements. The effects of plasma treatment on biological response were also studied in order to determine biocompatibility and hemocompatibility of the plasma modified polymers. Fibroblast cells and endothelia cells (HUVEC) were employed in order to assay the biocompatibility of plasma modified surfaces. Hemocompatibility was assessed from studying the adhesion and activation of platelets to variously plasma modified surfaces. The biological response of plasma treated surfaces was analysed by cell attachment assay as well as by counting the cells from images taken by optical microscopy (OM), scanning electron microscopy (SEM) and atomic force microscopy (AFM). The detailed plan of the experimental work is shown in Figure 10.

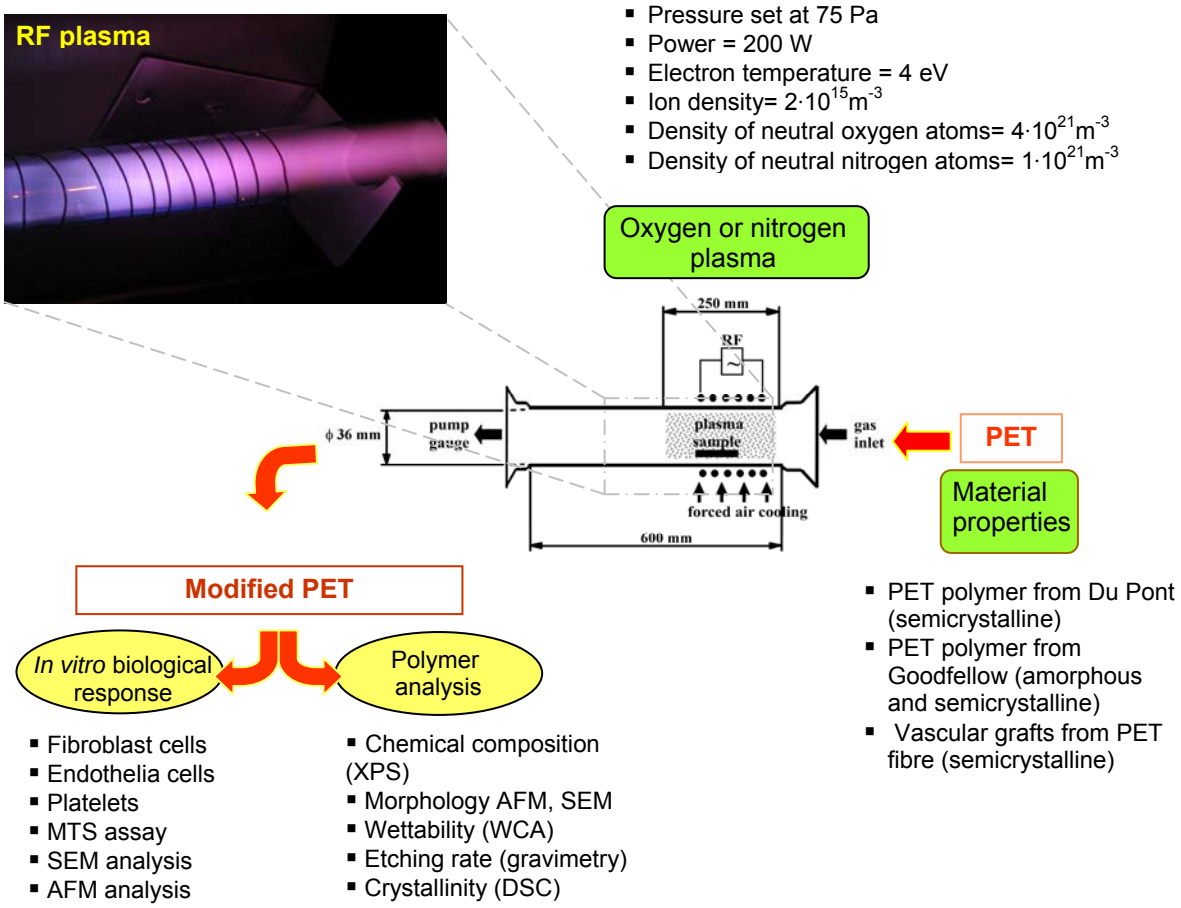

Figure 10 Outlined plan of the experimental work.

The experimental work also focused on studying the effects of plasma treatment on PET polymers emanating from different producers and with different crystalline fractions. Although vascular grafts are made from PET fibres, most of the experimental work was done on PET foils as these provide a much easier analysis. However, some final analyses were also done on PET fibres from vascular grafts. As PET polymers emanating from different manufacturers vary in degree of crystalline fraction, the effects of crystalline fraction on plasma treatment were also studied. Amorphous and semicrystalline PET foils from Goodfellow and semicrystalline foils from Du Pont were used. Effects of plasma treatment on semicrystalline vascular grafts made from PET fibres (Dacron vascular grafts, Inter Vascular^{TM}) were also studied. The plan of the experimental work is shown in the table below (Table 1), while the detailed description of the materials and methods used is presented in the following chapters.

Material	Methods			
	Cleaning procedure	Plasma treatment	Polymer analysis	*In vitro* biological response
PET foil semicrystalline (Goodfellow)	washed ultrasonically in EtOH, air dried	• oxygen • nitrogen treatment time (3s-180s)	• AFM • SEM • XPS • WCA • DSC • gravimetry	platelets • SEM • AFM
PET foil amorphous (Goodfellow)	washed ultrasonically in EtOH, air dried	• oxygen • nitrogen treatment time (3s-60s)	• AFM • SEM • XPS • WCA • DSC • gravimetry	platelets • SEM • AFM
PET foil Semicrysatlline (Du Pont)	washed ultrasonically in EtOH, air dried	• oxygen • nitrogen treatment time (3s-300s)	• AFM • SEM • XPS • WCA • DSC • gravimetry	HUVEC cells • OM • MTS assay Fibroblast cells • MTS assay platelets • SEM • AFM • MTS assay
PET vascular graft	/	• oxygen • nitrogen treatment time (3s-30s pulsed)	• AFM • SEM • XPS	platelets • SEM • MTS assay

Table 1 Outlined plan of the experimental work.

3.1. Materials

3.1.1. PET foils

The materials used for plasma treatment were PET foils emanating from Goodfellow and Du Pont. Two foils with different degrees of crystalline fraction were bought from Goodfellow, one was amorphous (fraction of crystalline part measured by DSC was less than 4.4 %) and the other was semicrystalline (fraction of crystalline part measured by DSC was 30.6 %). Both were 250 μm thick and the semicrystalline PET foil (biaxially oriented) also had silica additives embedded in the polymer matrix. Three PET foils with different thickness (8 μm, 125 μm and 250 μm) have been bought from Du Pont (PET type Maylar A). The crystalline fraction measured from DSC for Du Pont foils was 36.5 % for 125 μm thick and 33 % for 8 μm thick foil. PET foil with the thickness of 8 μm was used for measuring the difference in crystalline fraction before and after plasma treatment. Table 2 shows which foils have been used for plasma modification and the methods employed for their analysis.

Producer of PET polymer	Thickness	Crystalline fraction	Methods used
Goodfellow – amorphous	250 μm thick	4.4 %	all described methods
Goodfellow - semicrystalline	250 μm thick	30.6 %	all described methods
Du Pont – semicrystalline	125 μm thick	36.5 %	all described methods
Du Pont – semicrystalline	8 μm thick	33 %	only DSC analysis

Table 2 Methods used for characterisation of PET foils.

3.1.2. Vascular grafts

Uncoated knitted PET vascular grafts (Inter Vascular^{TM}, La Ciotat, France) with 6 mm in diameter were used to study the effects of plasma modification on vascular grafts. The measured degree of crystalline fraction from DSC was 40.4 %.

3.2. Methods

3.2.1. Preparation of PET polymers

PET foils were cut into squares of 2x2 cm^2 or 1x1 cm^2 and into disks measuring 10 or 13 mm in diameter, depending on the analysing method. Prior to plasma treatment the samples were ultrasonically cleaned for 5 min with 99,9 % ethanol and subsequently air dried.

Foils cut to squares were used for measuring:

- water contact angle (WCA);
- chemical composition by XPS;
- morphology by AFM or SEM;
- calorimetric properties by DSC; and
- etching rate by gravimetry.

While foils cut to disks were used for measuring:

- cell attachment by optical microscopy;
- cell proliferation by MTS assay;
- platelet attachment by SEM; and
- platelet attachment by MTS assay.

Vascular grafts made from PET were cut into squares measuring 1x1 cm^2 and treated in plasma on the inner side of the graft. As the received vascular grafts were sterile the cleaning procedure of PET vascular grafts prior to plasma treatment was not required.

3.2.2. Plasma treatment

Plasma treatment of PET foils was conducted by RF oxygen or nitrogen plasma. The samples were treated in the experimental system shown in Figure 11. The system was evacuated with a two-stage oil rotary pump, with a pumping speed of $4.4x10^{-3}$ m^3/s. The discharge chamber was a Pyrex cylinder measuring 0.6 m in length and with an inner diameter of 0.036 m. The plasma was created with an inductively coupled RF generator, operating at a frequency of 27.12 MHz and an output power of about 200 W. The plasma parameters were measured with a double Langmuir probe and a catalytic probe (Babic et al., 2001, Poberaj et al., 2002, Mozetic et al., 2005, Mozetic et al., 2006). Commercially available nitrogen or oxygen was leaked

into the discharge chamber. The pressure was measured by an absolute vacuum gauge. The pressure was adjusted during continuous pumping by a precise leak valve. In our experiments, the pressure was fixed at 75 Pa, as at this pressure the highest degree of dissociation of molecules, as measured by the catalytic probes, was obtained. At these discharge parameters, plasma with an ion density of about $2 \cdot 10^{15}$ m^{-3}, an electron temperature of 4 eV, and neutral atoms density of about $4 \cdot 10^{21}$ m^{-3} for oxygen plasma and about $1 \cdot 10^{21}$ m^{-3} for nitrogen plasma was obtained. The samples were placed into the discharge chamber as shown in Figure 11.

The samples of PET foil were treated in nitrogen or oxygen plasma at various times ranging from 3 to 240 s. Vascular grafts were treated in plasma in pulses from 3 s to a maximum of 30 s in order to prevent overheating and degradation.

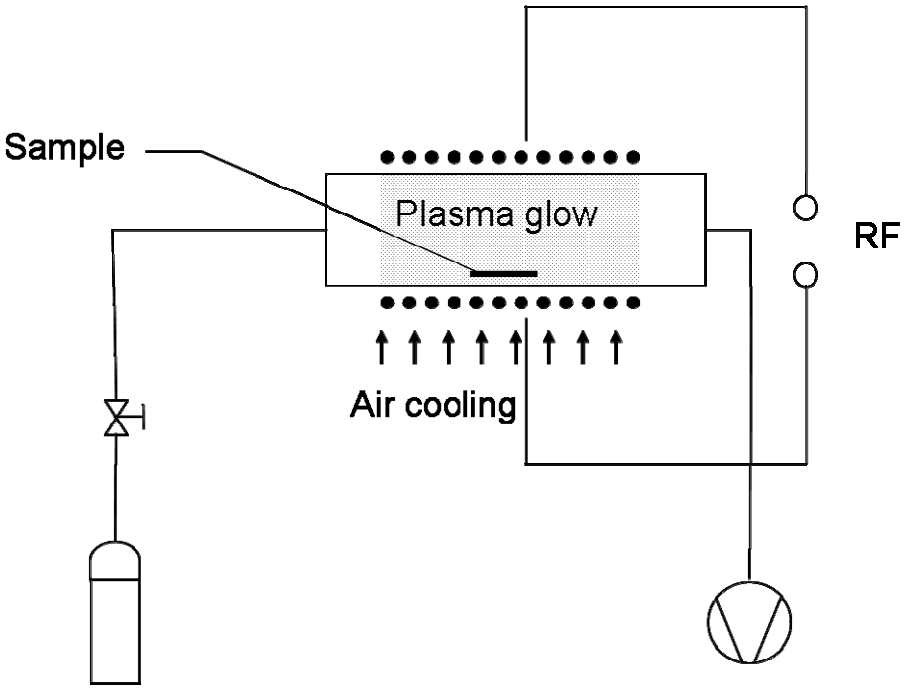

Figure 11 The RF plasma reactor chamber with the sample in position.

3.2.3. Polymer analysis

As complex methods must be employed to analyse PET fibres from vascular grafts, in this work PET foils were used. The chemical composition of the polymer surface was analysed by XPS, while surface wettability of PET polymers was determined by water contact angle measurements (WCA). The morphological properties of the surface were analysed with atomic force microscopy (AFM) and scanning electron microscopy (SEM). The comparison of PET polymers in form of fibres and in foils emanating from different producers was carried out with differential scanning calorimetry (DSC) in order to determine glass temperature (Tg), melting temperature (Tm), crystallisation temperature (Tg) and crystallinity. Due to differences in polymer crystallinity and the different gases employed for plasma treatment the etching rate was determined by measuring the difference in weight of PET foils before and after plasma treatment. All of these methods are described in detail in the following chapters.

3.2.3.1. Chemical composition by XPS

The surface of the sample was analyzed with an XPS instrument TFA XPS Physical Electronics. The base pressure in the XPS analysis chamber was about 6×10^{-8} Pa. The samples were excited with X-rays over a 400-µm spot area with a monochromatic Al $K_{\alpha1,2}$ radiation at 1486.6 eV. The photoelectrons were detected with a hemispherical analyzer positioned at an angle of 45° with respect to the normal to the sample surface. The energy resolution was about 0.5 eV. Survey-scan spectra were made at a pass energy of 187.85 eV, while for C 1s, O 1s and N 1s individual high-resolution spectra were taken at a pass energy of 23.5 eV and a 0.1 eV energy step. Since the samples are insulators, we used an additional electron gun to provide surface neutralization during the measurements. All spectra were referenced against the main C 1s peak of the carbon atoms, which was given a value of 284.8 eV. The XPS spectra were measured for the untreated sample and for samples treated for different treatment times ranging from 3 s to 90 s by nitrogen or oxygen plasma. The concentration of different chemical states of carbon in the C 1s peak was determined by fitting the curves with symmetrical Gauss-Lorentz functions. The spectra were fitted using MultiPak v7.3.1 software from Physical Electronics, supplied with the spectrometer. A Shirley-type background subtraction was used.

3.2.3.2. Water contact angle measurements

Wettability was examined immediately after plasma treatment by measuring the water contact angle with a demineralised water droplet of volume 3 µl. Each determination was obtained by averaging results of 10 measurements. The relative humidity (45%) and the room temperature (25°C) were monitored continuously and were found not to vary much during the contact angle measurements. Ageing effects of plasma-treated surfaces were observed with the same procedures as were used for contact angle measurements. In this case the measurements were done on PET foil after different time intervals have elapsed from plasma treatment; during these time intervals the samples were stored in air at room temperature (25°C) and at constant humidity (45%). The measurement error of wettability angle was less than 3 degrees.

3.2.3.3. Surface morphology

Surface morphology was observed by atomic force microscopy (AFM) and scanning electron microscopy (SEM). Topographic changes of PET foil after plasma treatment were monitored with AFM (Solver PRO, NT-MDT, Russia) in the tapping mode in air. The samples were scanned with standard Si cantilever with a force constant of 10 N/m and at a resonance frequency of 170 kHz. All the measurements were done in air, a day after plasma treatment, on areas of 10x10 μm^2, 5x5 μm^2 and 3x3 μm^2. The average surface roughness (Ra) was calculated from images made of areas measuring 3x3 μm^2 (corresponds to the average value of height of the surface). To obtain representative results average surface roughness was obtained from 5 different areas.

Scanning electron micrographs were obtained using a field emission microscope Carl Zeiss Supra 35 VP at accelerating voltage of 1-keV. Before analysis the PET foils were coated with gold to prevent charging of samples during SEM analysis.

Surface roughness was measured on 2x2 μm^2 AFM images, as this size of the area was the most representative for roughness measurements of our samples. The surface roughness was expressed in terms of average roughness (Ra) and corresponded to the average height of the features at the surface.

3.2.3.4. Thermal analysis

Differential scanning calorimetry (DSC) was used to investigate melting and crystallization behaviour of semicrystalline and amorphous PET foils as well as PET fibres. The samples were investigated using Mettler-Toledo DSC821^e at heating and cooling rates of 10°Cmin^{-1} between 20°C and 300°C. The samples were purged with nitrogen at a flow rate of 50 ml/min. Melting enthalpy was obtained from the melting peak area, while the polymer crystalline fraction was calculated by dividing the melting enthalpy by fusion energy of 100% crystalline PET (H°=140 J/g (Kong and Hay, 2002)). The amorphous polymer DSC scans exhibited two cold crystallization peaks, corresponding to crystallization of amorphous regions. The crystalline fraction of this sample was calculated by subtracting the heat of cold crystallization (cold crystallization peaks' area) from the melting enthalpy and then dividing it by the fusion energy of 100% crystalline PET polymer (Kong and Hay, 2002).

To investigate the increase in temperature of PET surface during plasma treatment a pyrometer (ε = 0.95) was used to measure temperature at different time intervals during plasma treatment. Temperature effects were also studied from AFM and SEM analysis, as the change in morphology could be correlated to temperature effects.

3.2.3.5. Etching rates

The etching rates of the PET samples during exposure to oxygen and nitrogen plasma were determined gravimetrically. The samples were cut to squares of equal size (2x2 cm^2) and were weighed before and after the plasma treatment. To assure that the deposited degradation products were removed from the surface before weighing they were washed with ethanol and air dried until obtaining constant mass. The change in weight was calculated as an average of 5 independent measurements. The etching rates were calculated taking into account the PET density of 1.39 g/cm^3.

3.2.4. *In vitro* biological response

The biological response of untreated and plasma treated PET surfaces was analysed. Proliferation and viability of fibroblast and endothelia cells on PET surfaces was analysed by the use of MTS assay, while the number of cells attached to the surface was determined by optical microscopy. Hemocompatibility of the surface was analysed by counting the number and morphology of adhered platelets on PET surface from SEM images. The adherence of platelets was also analysed by an MTS assay.

3.2.4.1. Fibroblast cells

A normal adult human skin sample was obtained from reductive surgery. The skin was cut to small pieces, which were incubated overnight at 37 °C in a collagen solution (200 U/ml) (Gibco BRL, Invitrogen). Subsequently, the epidermis was discarded and dermal cells were isolated from the dermal layer of the skin after another overnight digestion with collagenase. Dermal cells were subcultured in a complete fibroblast medium supplement with insulin, bFGF, FBS, gentamicin (50μg/ml) and amphotericin B (2 μg/ml) (FGM-2, Cambrex) at 37 °C in a humidified CO_2 incubator. Incubation of the PET surface (13 mm in diameter) with fibroblast cells ($3 \cdot 10^3$ cells per sample in each well) was done 2 h after plasma treatment. The surfaces of PET foils were incubated with fibroblast cells in 24 well plates for different incubation times (20 min and 40min) in a fibroblast growth medium (FMK-2, Clonetics). The unattached cells were removed from the surface together with the growth media and then the surfaces were incubated for 2 min with PBS. Afterwards the PBS was removed and the growth medium was added. The number of attached cells was counted from images taken by optical microscopy. After 9 days of incubation at 37 °C in a humidified CO_2 incubator the proliferation and viability of fibroblast cells was assessed by an MTS assay (Sigma-Aldrich Chemie).

3.2.4.2. HUVEC cells

Human umbilical vein endothelial cells (HUVEC-c, PromoCell GmbH, Heidelberg, Germany) were cultured in endothelial cell growth medium (ECGM) containing endothelial cell growth supplements (PromoCell, Heidelberg, Germany). All HUVEC used in this study were no more than passage three. HUVECs were grown to 70% confluence and were then incubated with PET surfaces in 24 wells plate for 15 min

at 37 °C in a humidified CO_2 incubator. Incubation of PET surface (13 mm in diameter) with HUVEC (10^4 cells per sample in each well) was done 2 h after plasma treatment. The number of attached cells was counted from images taken by optical microscopy. After 3 days of incubation at 37 °C in a humidified CO_2 incubator the proliferation and viability of HUVEC was quantified by an MTS assay (Sigma- Aldrich Chemie).

3.2.4.3. Whole blood

The PET foils were incubated for 1 hour with whole blood or with platelet rich plasma (PRP). Whole blood was drawn from healthy volunteers via vein puncture. The blood was drawn into 9 ml tubes with tri sodium citrate anticoagulant (Sigma), and the number of platelets in whole blood was counted (Cell-DYN 3200, Abbott). Afterwards the fresh blood was incubated with PET surfaces in 24 well plates for 1 hour at room temperature and at gentle shaking at 300 RPM. Each sample (measuring 13 mm in diameter) was incubated with 1 ml of whole blood. After 1 h of incubation, 1 ml of PBS was added to the whole blood. The blood with PBS (phosphate-buffered saline) was then removed and the PET surface was rinsed 5 times with 2 ml PBS in order to remove weakly adherent platelets. Further preparation of the surface was conducted according to the analysing methods used for characterisation of platelets adhesion (SEM, AFM, MTS assay).

3.2.4.4. Platelet rich plasma

The PRP was drawn from healthy volunteers by aphaeresis. The number of platelets was counted (Cell-DYN 3200, Abbott) and the PRP was diluted prior to incubation with 0,9 % NaCl solution (PRP : 0,9 % NaCl = 1 : 4). The PET surfaces were then incubated with 1 ml of diluted PRP per well for 1 hour at room temperature. 1 ml of PBS was added to the whole blood. The blood with PBS was then removed and the PET surface was rinsed 5 times with 2 ml of PBS in order to remove weakly adherent platelets. Depending on further analysis the adherent platelets were either prepared for SEM analysis, AFM analysis or for an MTS assay.

3.2.4.5. MTS assay

After incubation, the cell proliferation or attached cells were measured with an MTS assay (Celltiter 96 Aqueous One Solution Cell Proliferation Assay,

Promega). This is a colorimetric assay, which is based on bioreduction of MTS tetrazolium compound (Owenís reagent) by metabolically active cells to coloured formazan product that is soluble in tissue culture medium. This conversion is presumably accomplished by NADPH or NADH produced by dehydrogenase enzymes in metabolically active cells (Berridge, 1993). The quantity of formazan product as measured by the absorbance at 490 nm is directly proportional to the number of living cells in culture. Cultures were incubated for 2 hours in a culture medium with 20% of MTS reagent and absorbance was measured at 490 nm on a microtiter plate reader. Each measurement was done in three replicates.

3.2.4.6. Surface analysis by SEM, OM and AFM

The surface of PET foils with platelets was prepared for SEM analysis in the following manner. After incubation of cells with PET surface, the weakly adherent cells were removed from the surface by rising with PBS. Adherent cells were subsequently fixed with 400 µl of 1 % PFA (paraformaldehyde) solution for 15 min at room temperature. Afterwards the surfaces were rinsed with PBS and then dehydrated using a graded ethanol series (50, 70, 80, 90, 100 and again 100 vol.% ethanol) for 5 min and in the last stage in the series (100 vol.% ethanol) for 15 min. Afterwards the samples were placed in a Critical Point Dryer, where the solvent is exchanged with liquid carbon dioxide. By raising the temperature in the drier the liquid carbon dioxide passes the critical point, at which the density of the liquid equals the density of the vapour phase. This drying process preserves the natural structure of the sample and avoids surface tension which could be caused by normal drying. The dried samples were subsequently coated with gold and examined by means of SEM (Carl Zeiss Supra 35 VP) at accelerating voltage of 1-keV.

The number of attached fibroblast or endothelia cells was determined from images taken with optical microscopy. The morphology of the fibroblast and platelets was analysed with an AFM (Solver PRO, NT-MDT, Russia) in the tapping mode in air. For this purpose the cells, which have been incubated with PET surface, were fixed with 1 % PFA for 15 min at room temperature. After fixation the samples were air dried and scanned with standard Si cantilever with a force constant of 10 N/m and at a resonance frequency of 170 kHz.

4. Results and discussion

4.1. Chemical composition by XPS

The chemical composition of the surface of untreated and plasma treated PET polymers was obtained with XPS analysis. The analysis was done on Du Pont PET foils, which have a thickness of 125 μm, and on amorphous and semicrystalline PET foils from Goodfellow with a thickness of 250 μm. XPS spectra were also recorded for untreated and plasma treated vascular grafts from PET fibres.

4.1.1. PET foils from Du Pont

Treatment of PET foils (Du Pont) in oxygen plasma resulted in a remarkable increase in oxygen concentration already after 3 s of treatment. After this treatment time the oxygen concentration increases from initial 21 at.% to 39 at.%. Even with a prolonged exposure to oxygen plasma the concentration slowly increased, and at 90 s it reached 44 at.% (Table 3).

Treatment time	C	O	O/C
0 s	79.2	20.8	0.26
3 s	60.8	39.2	0.65
10 s	59.8	40.2	0.67
30 s	58.3	41.7	0.72
60 s	57.5	42.5	0.74
90 s	55.8	44.2	0.79

Table 3 Variation of the surface composition of the PET foil treated in oxygen plasma versus the exposure time.

On nitrogen plasma treated samples nitrogen concentration increased from 0 at.% to 12 at.% after 3 s of treatment time, and after 90 s of treatment it reached about 14 at.% (Table 4). During nitrogen plasma treatment a small increase in oxygen concentration was also observed.

Treatment time	C	O	N	O/C	N/C
0 s	79.2	20.8	0	0.26	0
3 s	63.5	24.3	12.2	0.38	0.19
10 s	62.5	25.0	12.5	0.40	0.20
30 s	60.2	26.1	13.7	0.43	0.23
60 s	61.8	23.3	14.9	0.38	0.24
90 s	59.7	26.0	14.3	0.44	0.24

Table 4 Variation of the surface composition of the PET foil treated nitrogen plasma versus the exposure times.

These results indicate that the first few seconds of nitrogen plasma treatment are most important for chemical changes of the surface, as only slight changes in the chemical composition are observed after longer treatment times. However, with oxygen plasma treatment, the saturation with newly formed oxygen functional groups could be observed after 60 s of treatment.

The formation of new functional groups on the surface was determined from high resolution C 1s spectra. Figure 12 shows C 1s spectra of the samples treated in nitrogen plasma for different treatment times, while Figure 13 shows the C 1s spectra for oxygen plasma treatment.

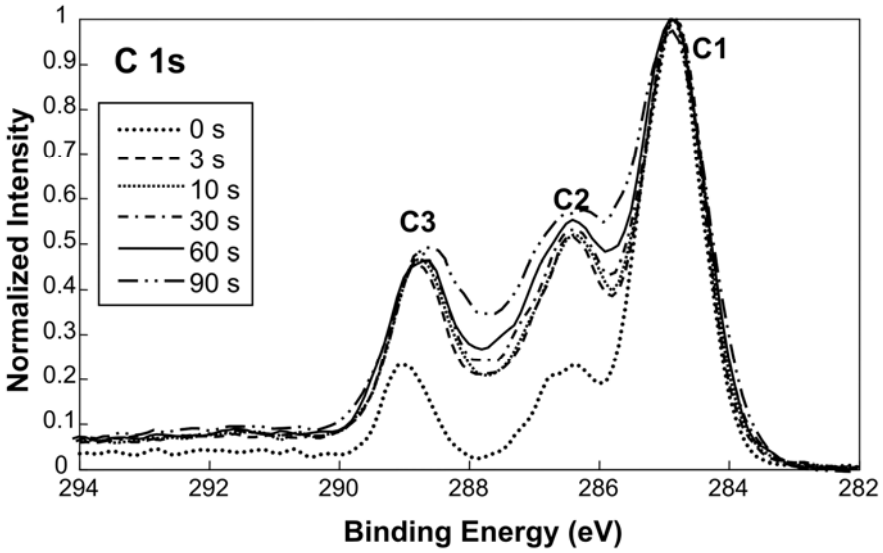

Figure 12 Comparison of high-resolution C 1s peaks of the untreated PET and PET treated in nitrogen plasma.

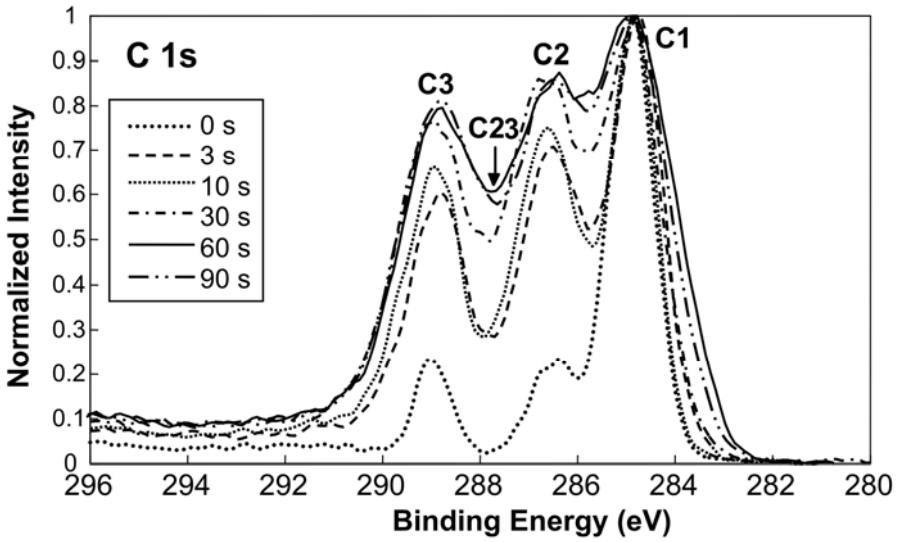

Figure 13 Comparison of high-resolution C 1s peaks of the untreated PET and PET treated in oxygen plasma.

The C 1s peak of the untreated PET sample consists of three peaks: a peak (C1) at a binding energy of 284.8 eV corresponding to C-C and C-H bonds in the phenyl ring (Figure 10); a peak (C2) at a binding energy of 286.6 eV corresponding to C-O bond; and a peak (C3) at a binding energy of 288.9 eV corresponding to O=C-O bond. In all cases the peaks (C2) and (C3) have increased after the treatment due to incorporation of oxygen or nitrogen into the surface of the samples. This leads to the formation of new functional groups; their concentration is shown in Table 5 and 6.

Treatment time	C1 C-C	C2 C-O	C23 C=O	C3 O=C-O
0 s	75.8	13.0	0	11.2
3 s	34.0	30.4	3.9	31.7
10 s	35.6	29.1	4.6	30.7
30 s	33.4	29.4	4.8	32.4
60 s	36.1	25.3	10.6	28.0
90 s	35.7	25.1	11.5	27.7

Table 5 Concentration of different functional groups on the PET surface treated in oxygen plasma for different exposure times.

Treatment time	C1 C-C	C2 C-O,C-N	C3 O=C-O, O=C-N
0 s	75.8	13.0	11.2
3 s	47.3	30.5	22.3
10 s	47.2	31.2	21.7
30 s	44.7	34.5	20.7
60 s	42.3	36.8	20.9
90 s	38.4	40.9	20.7

Table 6 Concentration of different functional groups on the PET surface treated in nitrogen plasma for different exposure times.

After oxygen plasma treatment for 90 s the peak C1 decreased from 76% to 36%, while peaks C2 and C3 increased from 13% to 25% and from 11% to 28% respectively. Moreover, a new peak C23 appeared at a binding energy of 287.5 eV, which corresponds to C=O bond. At 90 s of treatment its concentration was 11%. After nitrogen plasma treatment, for the same time period, the increase of the peak C2 was more pronounced. In this case the peak C1 decreased from 76% to 38%, the peak C2 increased from 13% to 41% and the peak C3 increased from 11 to 21%. A strong decrease of the C1 peak indicates that both plasmas attack mostly phenyl rings rather than the ester groups. With oxygen plasma treatments the increase of peaks C2 and C3 is mostly due to formation of C-O and O=C-O groups, while with nitrogen plasma treatments C-N and O=C-N groups are probably formed. It is difficult to determine the exact type and concentration of nitrogen functional groups, since there is a problem with strong overlapping of oxygen- and nitrogen-containing functionalities, because they appear at similar binding energies (Beamson and Briggs, 1992). Moreover, relevant literature reports different data for binding energies of different nitrogen peaks which are positioned quite close together: C-N (285.5 eV – 286.3 eV), C=N (285.5 eV – 286.6 eV), C≡N (286.7 eV – 287.0 eV) (Larrieu et al., 2005a, Charpentier et al., 2006, Deslandes et al., 1998, Wilson et al., 2001, Wang et al., 2005, Grace et al., 2003) and this makes the interpretation of XPS spectra very difficult. Also the N1s peak cannot give a decisive answer about the nitrogen containing functionalities (Morent et al., 2008). The examination of the N1s spectra shows that the N1s peak is composed of a relatively broad symmetric peak centred at a binding energy of 399.7 eV that could correspond to different nitrogen states. According to the literature we can find several carbon-nitrogen species (like amines, amides, imides, nitriles, etc.) in the range between 399.1 eV and 400.2 eV (Morent et al., 2008, Beamson and Briggs, 1992). As reported by Morent at al, it is very difficult to incorporate nitrogen into polymer surfaces (Morent et al., 2008). Therefore, it can be assumed that only nitrogen singly-bonded to carbon exists on the surface. Amide groups (N-

C=O) can be also present at the surface, while the presence of the groups where nitrogen is bound to oxygen (nitro, oxime and nitrate groups) can be definitively excluded, since they should appear at energies 406-408 eV (Morent et al., 2008, Beamson and Briggs, 1992). Therefore, the enrichment of the peak C2 after nitrogen plasma treatment can be attributed to amine groups, while the enrichment of the C3 peak can be attributed to amide groups.

A comparison of Figures 12 and 13 shows that longer exposure to oxygen plasma treatment produces an increase of the C2 and C3 peaks (Figure 13) as well as the C23 peak (Table 5); whereas, with nitrogen plasma treatment (Figure 12) the changes are not as pronounced. Although it seems that the surface is more or less saturated after few seconds of treatment in N_2-plasma, Table 6 shows that the concentration of the peak C2 actually still increases with treatment time. The observed difference in time-dependence of the concentration of functional groups for oxygen and nitrogen plasma treatment (as seen in Figures 12 and 13) is probably due to various numbers of sites that are available for incorporation of oxygen or nitrogen functionalities. The density of O-atoms is about $4 \cdot 10^{21}$ m^{-3} and the density of N-atoms is about $1 \cdot 10^{21}$ m^{-3} as was measured by the catalytic probe. The resultant flux of neutral atoms is $j = 1/4 \cdot n \cdot v$, where v is the mean thermal velocity of O-atoms (v = 630 m/s) and N-atoms (v = 673 m/s). The flux is therefore $6.3 \cdot 10^{23}$ $m^{-2}s^{-1}$ for O-atoms and $1.7 \cdot 10^{23}$ $m^{-2}s^{-1}$ for N-atoms. Taking into account that the surface atom density is in the order of 10^{19} m^{-2}, it is clear that the surface should become saturated with new functionalities in less than 1 ms of treatment time in both plasmas, assuming that the probability for incorporation is 1. This assumption for sticking probability of 1 is very high, since it is known that sticking probability on polymer materials is much lower than on metals. It is difficult to find useful values of sticking probability on polymer materials. According to the literature the values reported are in the range between 10^{-2} – 10^{-4} (Schwarzenbach et al., 2001, Meier et al., 2003). Taking into account these more realistic values the surface is still saturated with adsorbed atoms in less than 1 s, which is less than the treatment time used for the experiments, as the minimum treatment time, was 3 s. Nevertheless, the observed difference in time-dependence of the concentration of functional groups between oxygen and nitrogen plasma treatment may be explained with the differences in probabilities of oxygen and nitrogen incorporating into the surface. It should also be noted that we actually have a combination of two effects: sticking of neutral atoms at the surface and etching by ions, which limits the build-up of polar functionalities. The competition between functionalization by atoms and degradation by ion etching balances sooner or later. Moreover, the increased surface area with treatment time causes an increase of the

area available for chemical interactions of atoms (Strobel et al., 1994). In the present case the density of ions ($n_i = 10^{15}$ m^{-3}) and their flux $j_i = 10^{17}$ m^{-2}s^{-1} is a few orders smaller than the flux of neutral atoms to the surface and can thus easily be neglected in the calculation above.

- Ageing of the plasma treated surface

Functional groups formed on the plasma treated surface are not stable with time, as the surface tends to recover to its untreated state. Thus, the surface is loosing its hydrophilic character and becomes hydrophobic. In order to determine the rate of ageing of the PET surface treated in nitrogen and oxygen plasma, XPS and contact angle measurements (Chapters 3.2.3.1 and 3.2.3.2) were carried out continuously for several days. In the meantime the PET samples were stored in a dry plastic box at constant room temperature of 25 °C and constant humidity of 45 %.

The surface composition of the PET foil, which was treated for 3 s in nitrogen plasma, is shown in Table 7 as a function of ageing time. The ageing of the sample obtained from this analysis shows that nitrogen functional groups are fairly stable with time, as their concentration does not change much after plasma treatment. Thus, immediately after nitrogen plasma treatment the nitrogen concentration on the surface is 12 at.% and after 35 days it decreases to 9.7 at.%.

Ageing time (days)	C	O	N	O/C	N/C
0	63.5	24.3	12.2	0.38	0.19
1	64.2	24.4	11.3	0.38	0.18
2	65.8	23.7	10.5	0.36	0.16
5	65.1	24.7	10.2	0.37	0.16
7	65.9	24.0	10.1	0.36	0.15
35	66.5	23.8	9.7	0.36	0.15

Table 7 Variation of the surface composition of a PET foil treated in nitrogen plasma for 3 s versus ageing time.

The C1s peaks are shown in Figure 14 and the concentration of different functional groups is shown in Table 8. These results demonstrate that newly formed functional groups are fairly stable with time. Thus, the change in peaks is almost unnoticeable (Figure 14), and the concentration of the functional groups (Table 8) is practically unaffected by ageing time.

Ageing time (days)	C1	C2	C3
0	47.3	30.5	22.3
1	48.2	31.4	20.4
2	48.5	31.0	20.5
5	50.0	30.2	19.7
7	51.2	29.9	18.9
Untreated	75.8	13.0	11.2

Table 8 Concentration of different functional groups on the PET surface treated in nitrogen plasma for 3 s versus ageing time.

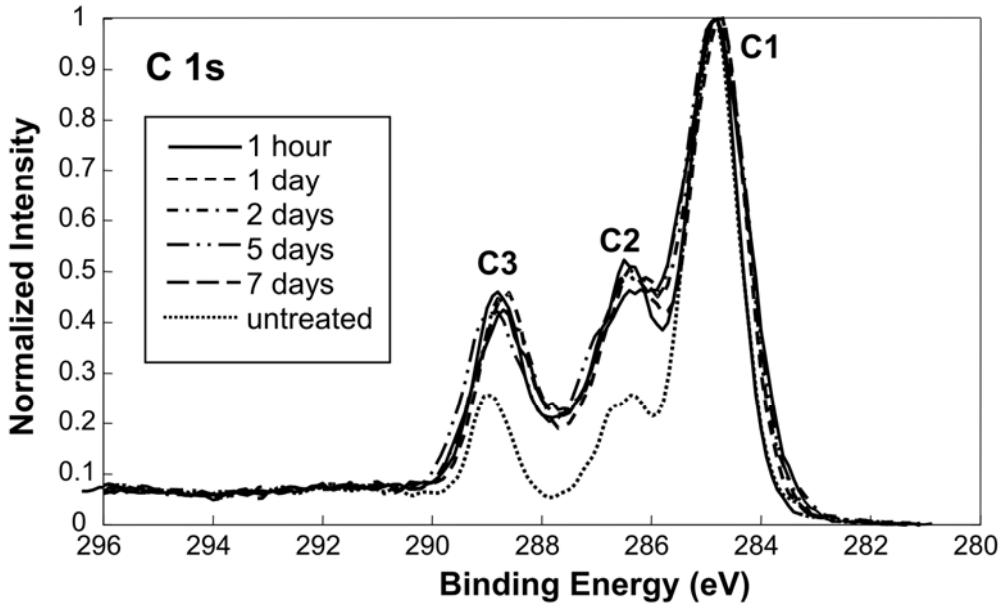

Figure 14 Ageing of the C 1s peak of the PET foil treated in nitrogen plasma for 3 s.

The XPS results for oxygen plasma treatment show a high rate of surface ageing. As seen from Table 9, the concentration of oxygen on the surface decreases with time and after one week about 10 at.% of oxygen is lost from the surface.

Ageing time (days)	C	O	O/C
0	60.8	39.2	0.65
1	61.6	38.9	0.63
2	64.1	35.9	0.56
5	69.2	30.8	0.45
7	70.0	30.0	0.43

Table 9 Variation of the surface composition of a PET foil treated in oxygen plasma for 3 s versus the ageing time.

The decrease in O-concentration is also reflected by the decreasing intensity of the C1s-subpeaks belonging to the oxygen functional groups as shown in Figure 15 and Table 10. After 1 week the concentration of the peak C1 increased from 34% to 58%, while the peak C2 decreased from 30% to 21%, the peak C3 decreased from 32% to 18% and the concentration of the new peak C23 decreased from 4% to 2%. These values are still significantly different from the untreated ones: 76% for C1, 13% for C2 and 11% for C3.

Ageing time (days)	C1	C2	C23	C3
0	34.0	30.4	3.9	31.7
1	45.7	27.6	3.1	23.5
2	48.6	26.4	2.8	22.1
5	57.9	22.0	2.5	17.6
7	58.3	21.3	2.1	18.3
untreated	75.8	13.0	0	11.2

Table 10 Concentration of different functional groups on the PET surface treated in oxygen plasma for 3 s versus ageing time.

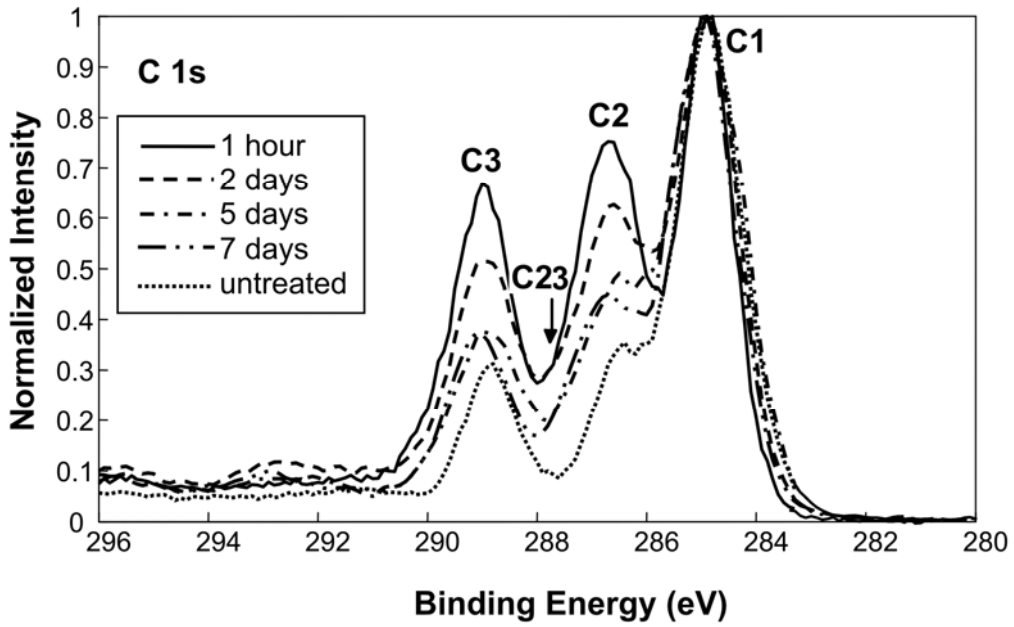

Figure 15 Ageing of the C 1s peak of the PET foil treated in oxygen plasma for 3 s.

4.1.2. PET foil from Goodfellow

The difference in surface functional groups between amorphous and semicrystalline polymer subjected to oxygen plasma were studied by XPS. As shown in Table 11, there are only slight variations in the surface composition of pristine amorphous and semicrystalline PET. After 3 s of plasma treatment, oxygen concentration increased from initial 28.9 at.% and 26.6 at.% to 39.7 at% and 40.7 at% for amorphous and semicrystalline polymer, respectively. With further increasing treatment time the oxygen concentration was still slowly increasing for semicrystalline polymer and it reached about 42 at.% after 30 s of treatment; while the amorphous polymer showed saturation in oxygen concentration already after 3 s of treatment (Table 11). After 30 s of treatment, the oxygen concentration on the surface of the amorphous polymer even decreased because of polymer degradation due to melting, which confirms that amorphous polymers can only be treated in plasma for shorter times (less than 30 s) compared to semicrystalline polymers.

Treatment time (s)	Amorphous polymer				Semicrystalline polymer			
	C	O	Si	O/C	C	O	Si	O/C
0	71.1	28.9	0	0.41	72.1	26.6	1.3	0.37
3	59.8	39.7	0.5	0.66	57.3	40.8	2.0	0.71
15	59.2	40.3	0.5	0.68	55.9	42.6	1.5	0.76
30	60.7	38.9	0.4	0.64	56.7	41.9	1.4	0.74

Table 11 Surface composition of amorphous and semicrystalline PET foil versus treatment time in oxygen plasma.

High resolution spectra were recorded in order to enable a more detailed analysis. Figures 16a and 16b show the comparison between C 1s spectra of the samples treated in oxygen plasma. C 1s peak of the untreated amorphous (A) and semicrystalline (S) samples consists of three peaks: peak (C1) corresponding to C-C and C-H bond at 285.0 eV, peak (C2) corresponding to C-O bond at 286.5 eV and peak (C3) corresponding to O=C-O bond at 289 eV. After treatment, the peaks (C2) and (C3) increased for both polymers, due to incorporation of oxygen into the surface and formation of new functional groups. The increase of peaks (C2) and (C3) is due to surface enrichment with C-O and O=C-O groups as well with C=O groups. The concentrations of functional groups versus treatment time for both polymers are shown in Table 12. For the semicrystalline polymer the concentration of oxygen functional groups generally increases with treatment time; while for amorphous polymer a decrease of oxygen functional groups at 30 s of treatment can be observed. This can be explained by the loss of functional groups due to a rise in surface temperature and degradation of the amorphous polymer after 30 s of plasma treatment (Figure 16b).

Treatment time (s)	Amorphous polymer				Semicrystalline polymer			
	C-C	C-O	C=O	O-C=O	C-C	C-O	C=O	O-C=O
0	61.9	22.2		15.8	66.4	20.8		12.8
3	37.1	32.6	3.1	27.1	36.7	33.5	1.5	28.3
15	35.6	31.0	4.7	28.7	32.9	32.4	6.2	28.4
30	42.5	26.1	5.8	25.7	34.1	31.9	5.1	28.9

Table 12 Functional groups from C 1s spectra versus treatment time for amorphous and semicrystalline PET foil.

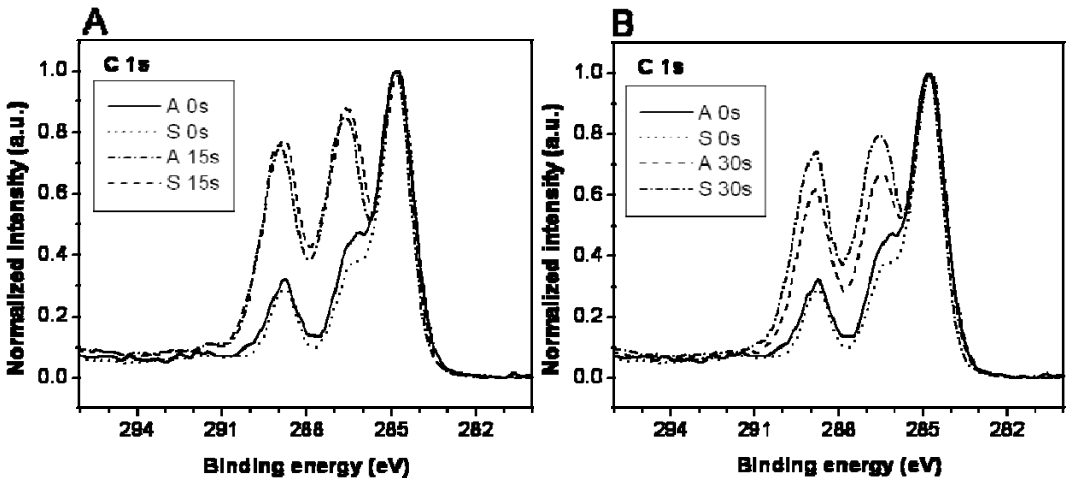

Figure 16 Comparison of high-resolution C 1s peaks of pristine amorphous and semicrystalline PET foil with a.) amorphous and semicrystalline PET foil treated in plasma for 15 s and b.) amorphous and semicrystalline PET foil treated in plasma for 30 s.

4.1.3. Results of XPS analysis on vascular grafts

In order to observe changes in surface modification after oxygen plasma treatment, the chemical composition of vascular grafts was analysed with XPS. Figure 17 shows the XPS spectra of the untreated surface and the surface treated in oxygen plasma for 10 s. Due to the rough surface, the XPS spectra have a low signal with noise, this makes the analysis of fibres with XPS more complex. However, it can be observed even from these spectra, that surface is funcionalized with oxygen functional groups, as an increase in the peak attributed to C-O and the peak attributed to O=C-O can be clearly seen.

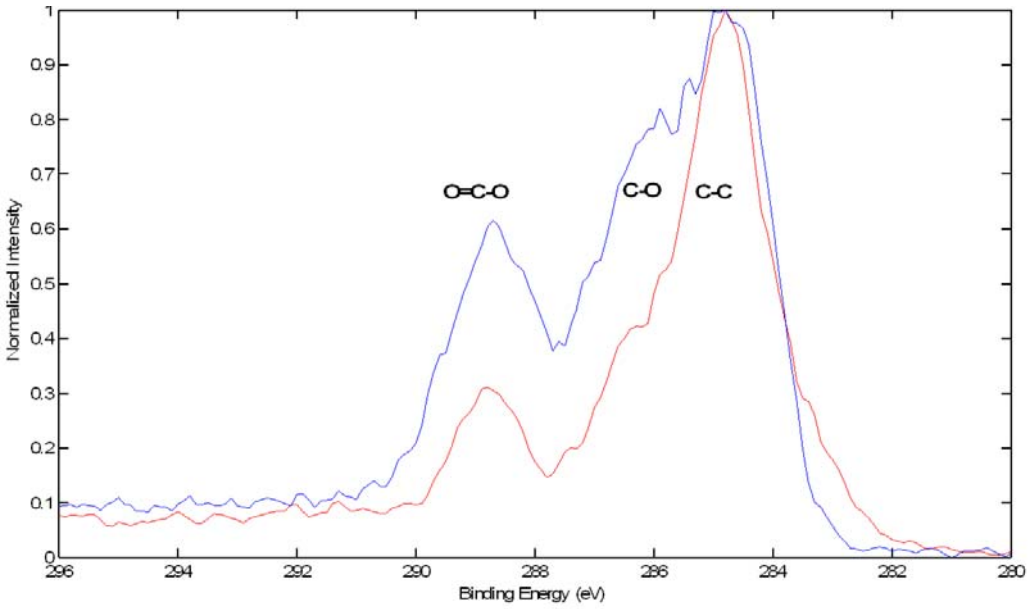

Figure 17 Comparison of high-resolution C 1s peaks of untreated vascular graft (red) and treated vascular graft in oxygen plasma for 30 s (blue).

4.2. Surface morphology

The morphology of untreated and plasma treated surfaces was analysed by atomic force microscopy and scanning electron microscopy. AFM analysis allowed us to obtain 3D images of the surface and measure the average surface roughness; it also allowed us to observe phase images, which show the differences in material properties such as variation of the mechanical (stiffness, friction) and adhesive properties. While the SEM images provided us with a broader view of the surface (by lower magnification - for example 200x or 500x) and so can, if used in conjunction with AFM give a better insight into surface morphology.
The AFM and SEM analysis were done on PET polymers emanating from both manufacturers (Du Pont and Goodfellow) and, as it is shown in the following chapters, surface morphology varies depending on the manufacturer.

4.2.1. Surface morphology of PET foils from Du Pont

The height and phase contrast AFM image of the untreated PET foil (Figure 18 (a)) shows a smooth surface, without any particular features on the surface. While the PET foil treated for only 10 s in oxygen plasma already shows sphere like structures forming on the surface (Figure 18 (c)). However, this is not observed on surfaces treated for 10 s with nitrogen plasma (Figure 18 (b)). The sphere

formation on nitrogen treated surface can be observed only after a longer treatment time of about 30 s (Figure 18 (d)). The topography of oxygen plasma treated surface for 30 s (Figure 18 (e)) is similar to the nitrogen treated surface (Figure 18 (d)), only with higher sphere features. After an even longer treatment time (60 and 90 s) the PET foil treated in oxygen and in nitrogen plasma shows a highly oriented structure (Figures 18 (f) – (i)). The difference between the samples treated with oxygen and nitrogen plasma is noticeable: the samples treated by oxygen plasma for 60 s have structures which are higher and further apart, than those treated with nitrogen plasma. This becomes even more pronounced after 90 s of oxygen plasma treatment, where oxygen plasma treated surfaces have structures measuring approximately 35 nm in height (Figure 18 (h)), while the height of nitrogen treated surfaces structures measures approximately 12 nm (Figure 18 (i)). It can be seen from phase contrast AFM images, that on 60 s and 90 s oxygen plasma treated surfaces the sphere like structures are elongated and further apart (Figures 18 (g) and (i)), while sphere like structures on nitrogen plasma treated surface are closer together, especially on surfaces treated for 60 s (Figure 18 (f)).

Height **Phase**

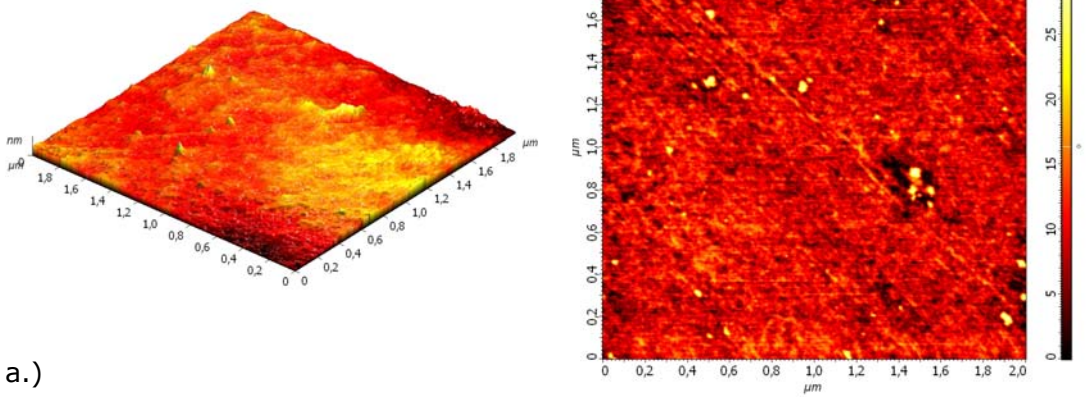

a.)

Height **Phase**

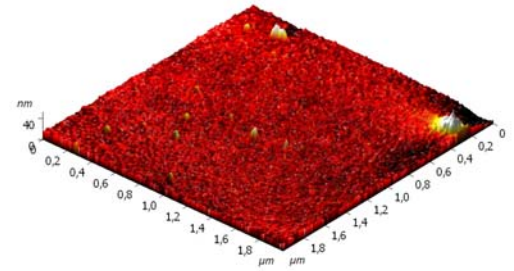

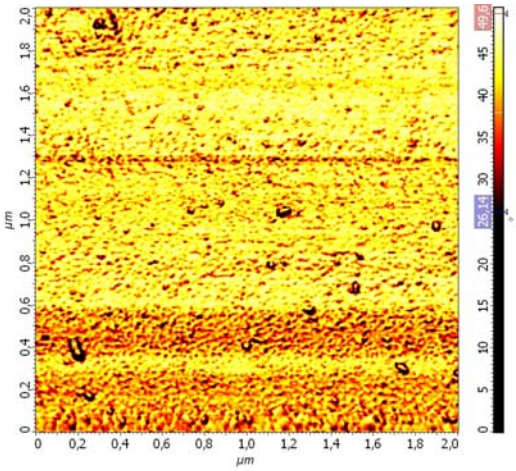

b.)

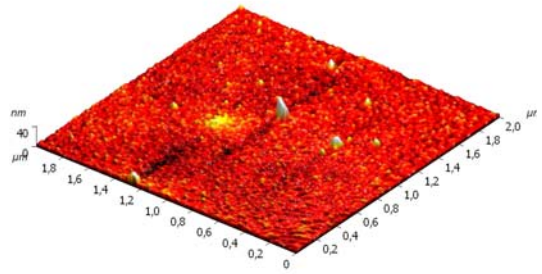

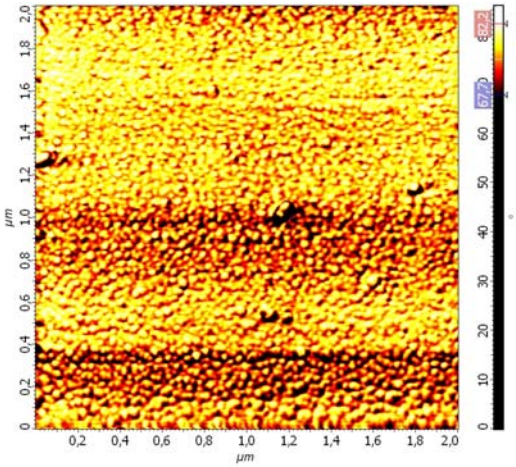

c.)

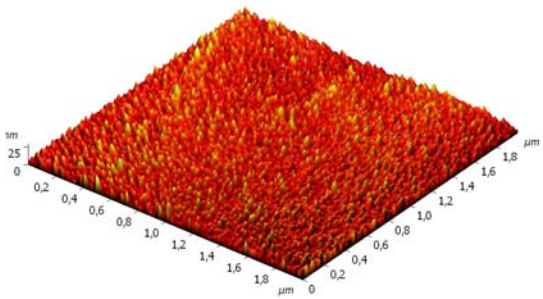

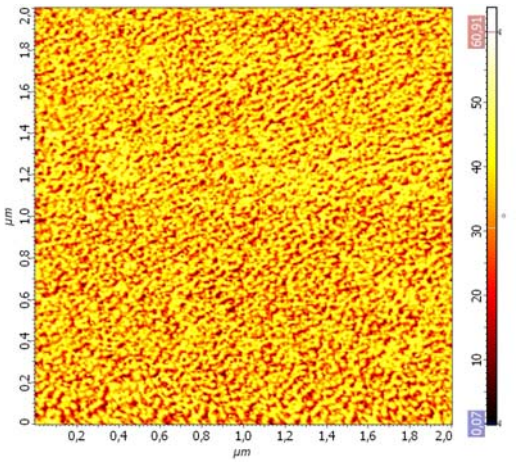

d.)

Height **Phase**

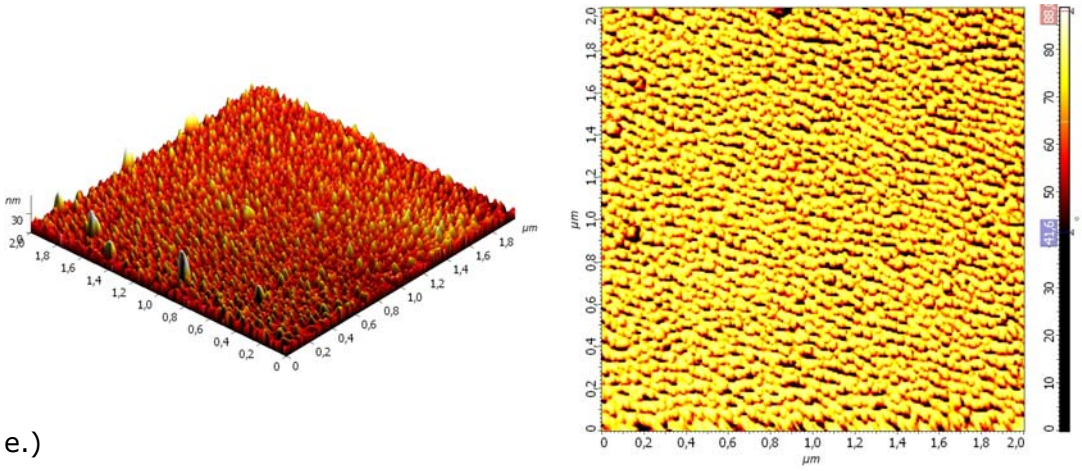

e.)

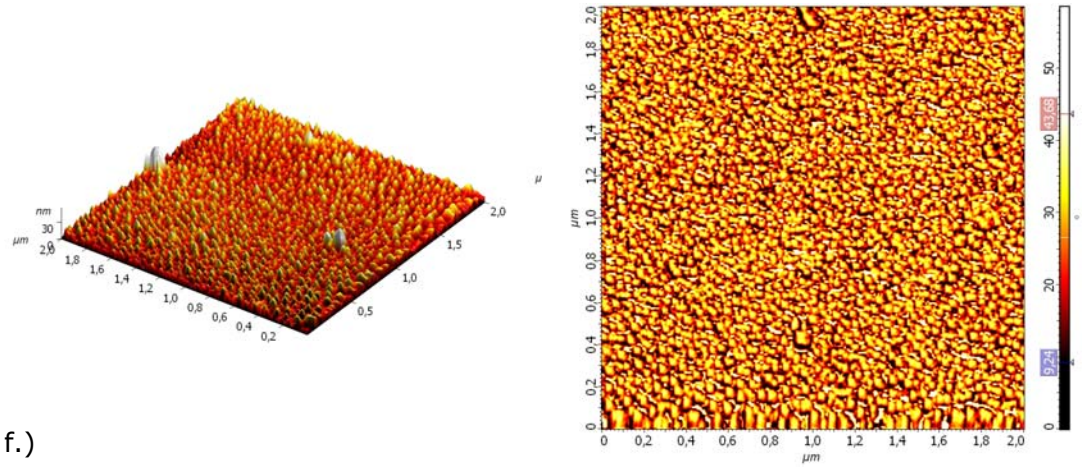

f.)

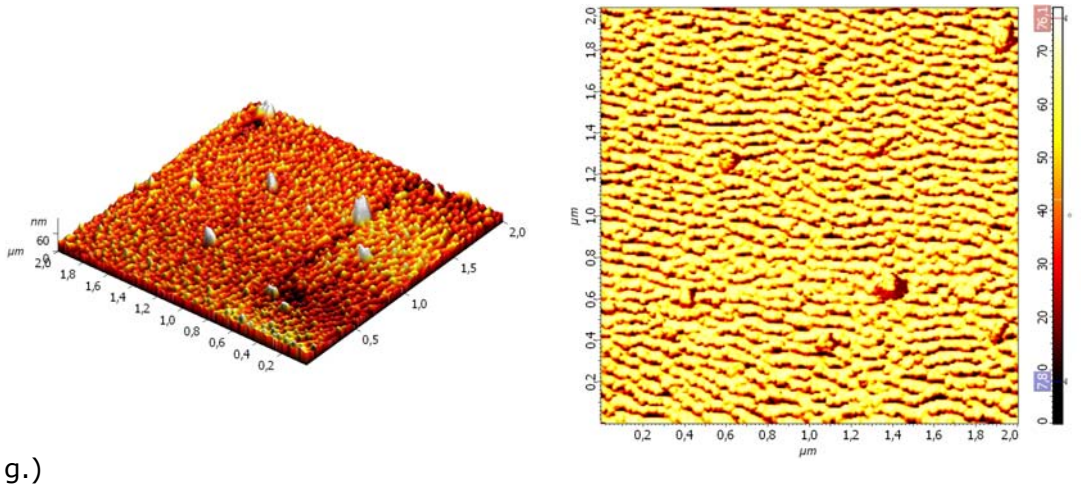

g.)

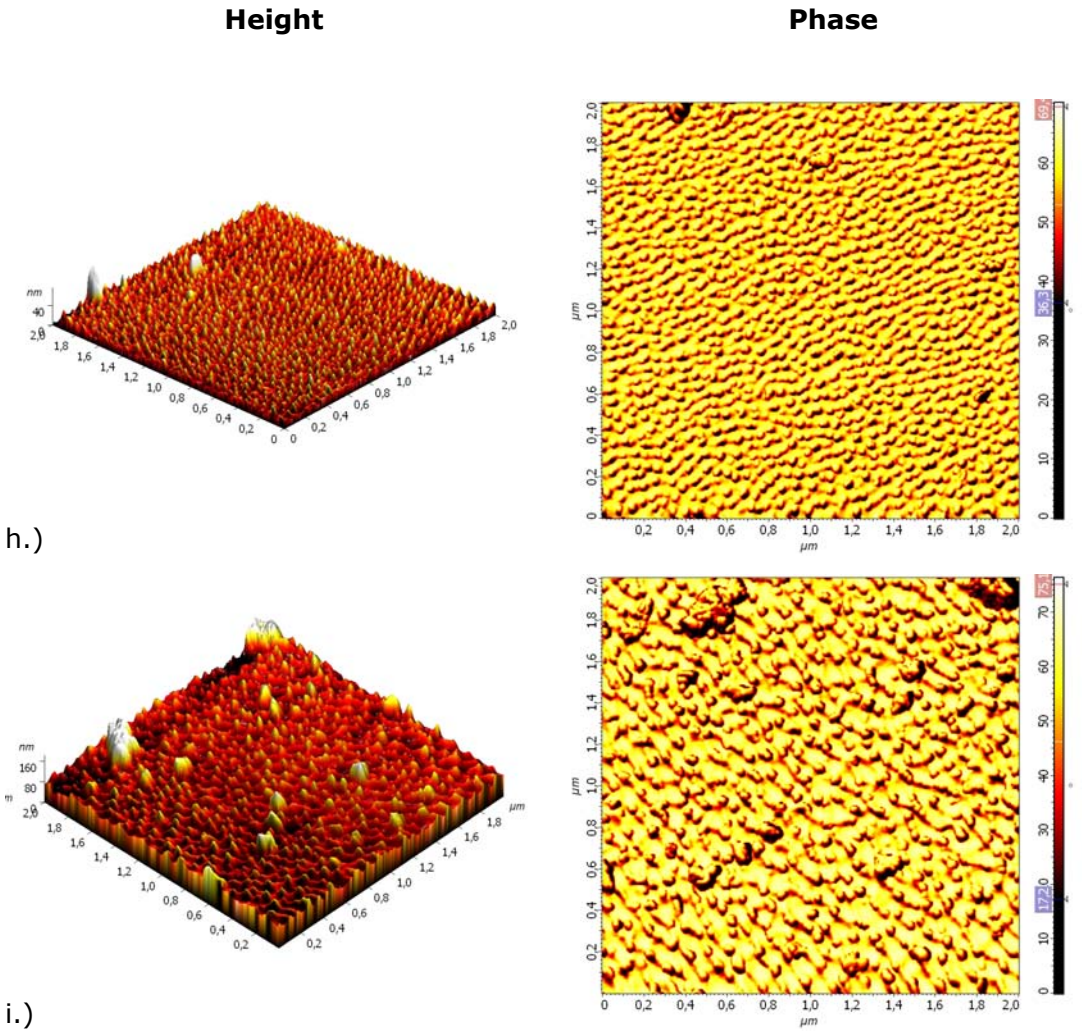

Figure 18 Height and phase contrast AFM images of PET foil: (a) untreated (b) treated for 10 s in nitrogen plasma, (c) treated for 10 s in oxygen plasma, (d) treated for 30 s in nitrogen plasma, (e) treated for 30 s in oxygen plasma, (f) treated for 60 s in nitrogen plasma, (g) treated for 60 s in oxygen plasma, (h) treated for 90 s in nitrogen plasma and (i) treated for 90 s in oxygen plasma.

Small oriented sphere like structures can also be seen from SEM images, their orderly structure is more or less pronounced, depending on treatment time (Figure 19). After 60 s of oxygen plasma treatment, sphere like formation on the surfaces becomes more pronounced (Figures 19 (d) and (e)). It should be noted that the SEM images do not only show small oriented sphere like structures; after longer treatment time the surface is also covered with lager sphere aggregates, which can be attributed to low molecular weight degradation products (Figure 19 (e)). The number and height of these products increases with plasma treatment time. However, after a certain point, the morphology of polymer surfaces become flat and without any special features (Figure 19 (f)). This is due to temperature effects and melting of the polymer due to longer plasma treatment.

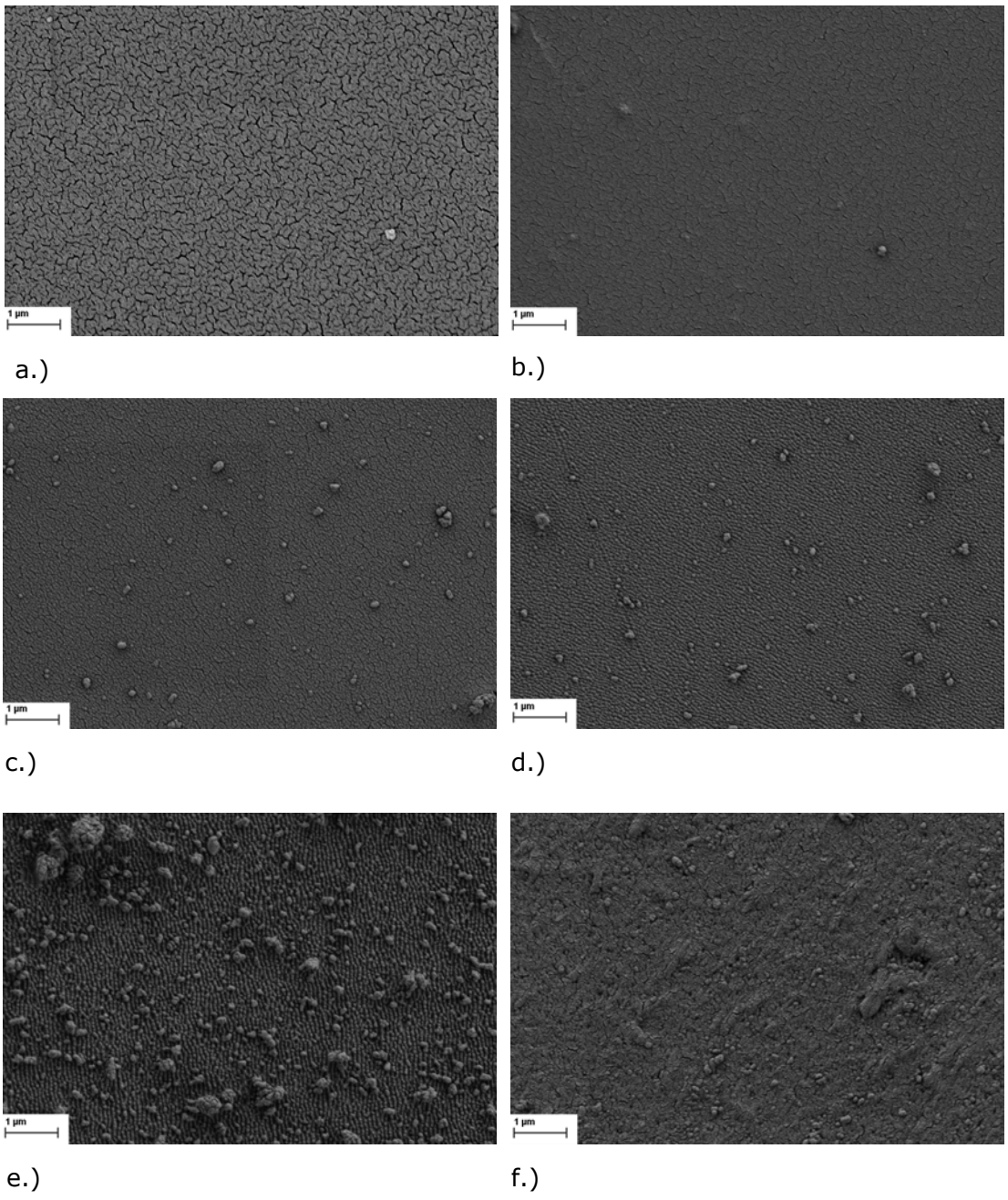

Figure 19 SEM image of PET foil (a) untreated, (b) oxygen plasma treated for 3 s, (c) oxygen plasma treated for 30 s, (d) oxygen plasma treated for 90 s, (e) oxygen plasma treated for 3 min, (f) oxygen plasma treated for 4 min.

The changes in surface topography after plasma treatment are mostly caused by the chemical erosion by atoms and physical erosion by ions in plasma. Thus, the surface is slowly eroded with time. Since the amorphous polymer is removed many times faster than its crystalline counterpart, a surface topography can be generated, with the amorphous zones appearing as valleys (Strobel et al., 1994). It can thus be seen that plasma treatment can provide surfaces with higher crystallinity, because of the preferential etching of the softer amorphous parts of the polymer in plasma (Krump et al., 2006, Morent et al., 2008). This was in fact confirmed by DSC (differential scanning calorimetry) on very thin PET foils (see Chapter 4.4.), where an increase in crystalline fraction was observed after longer plasma treatment time.

The roughness analysis carried out on 2 x 2 μm^2 AFM images shows that the average roughness (Ra) increases with plasma exposure time (Figure 20).

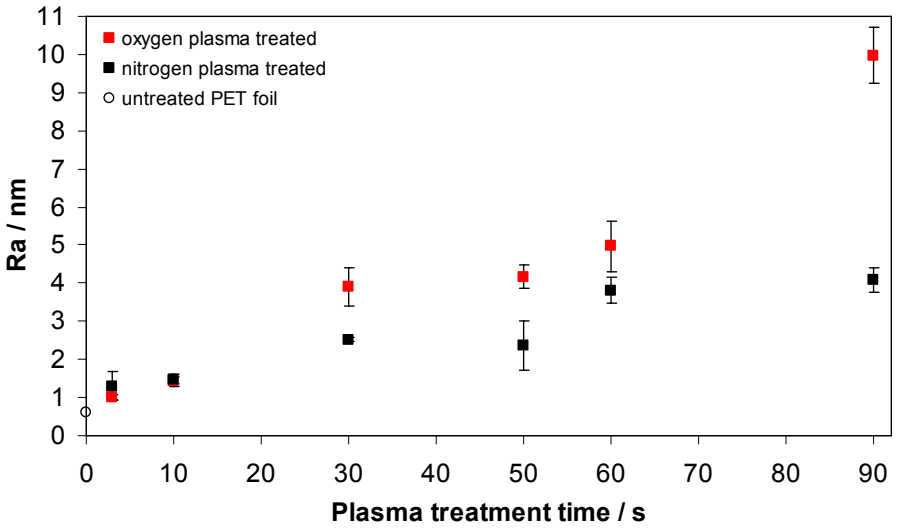

Figure 20 Average roughness (Ra) measured from 2 x2 μm^2 AFM images as a function of treatment time and plasma gas, (■) oxygen plasma treatment, (■) nitrogen plasma treatment.

Treatment with oxygen plasma shows higher roughness values for the same treatment time and conditions. The most significant change occurs after one minute of plasma treatment time, as the surface roughness is still increasing on the oxygen treated samples, while this is not the case for the nitrogen plasma treated samples. Nitrogen plasma does not have such an effect on surface roughening, probably due to a lower etching rate (see Chapter 4.4).

4.2.2. Surface morphology of PET foils from Goodfellow

Figure 21 shows the differences in surface morphology observed by AFM on amorphous and semicrystalline PET polymer after different exposure times to oxygen plasma.

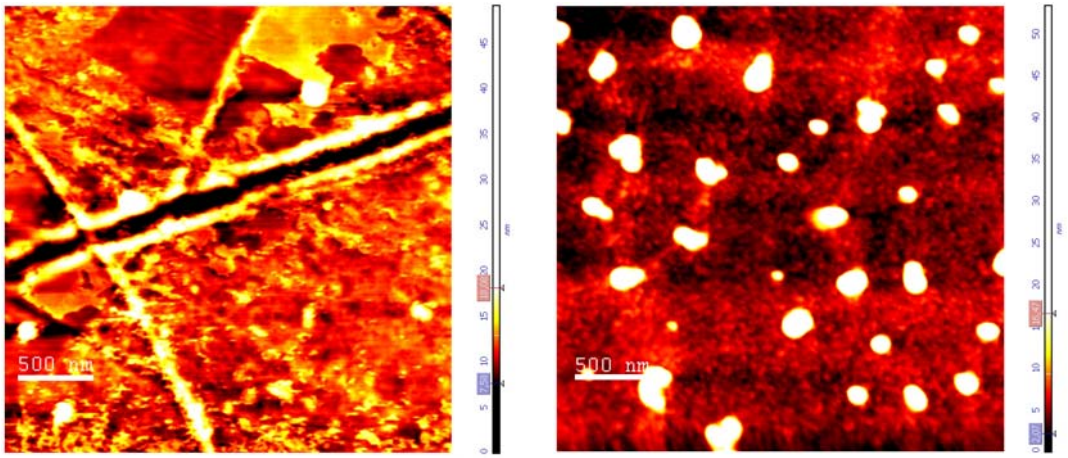

a.) b.)

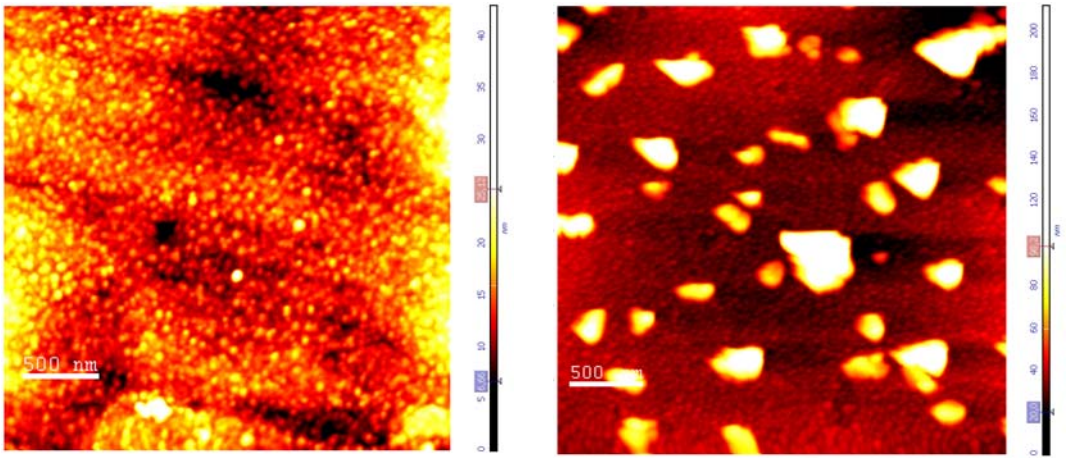

c.) d.)

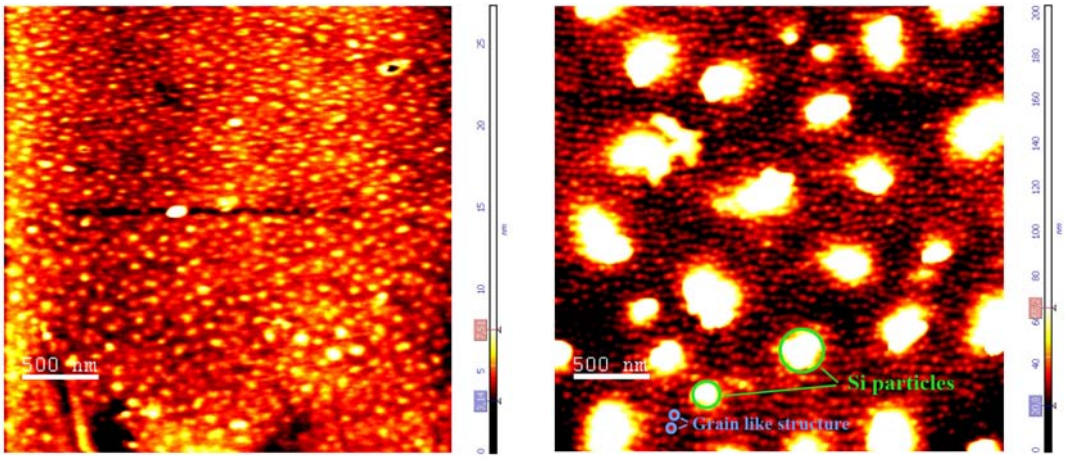

e.) f.)

Figure 21 AFM images of PET foil: pristine (a) amorphous and (b) semicrystalline; (c) amorphous and (d) semicrystalline plasma treated for 30 s; (e) amorphous plasma treated for 60 s; (f) semicrystalline plasma treated for 90 s.

The pristine semicrystalline PET polymer exhibits a surface with embedded silica additives, which have an average height of 40-50 nm. The amorphous PET polymer did not exhibit any special topography on the surface; only a few scratches were observed and these were probably caused by the manufacturing process (Figure 21 (a)). The average surface roughness measured over 9 μm^2 surface area was 1.7±0.2 nm and 2.8±0.1 nm for pristine amorphous and semicrystalline PET, respectively (Figure 22). After treatment with oxygen plasma the amorphous polymer exhibited morphological changes, which were more pronounced after longer plasma treatment times (Figures 21 (a), (c), (e)). Already after 3 s of treatment grain like structures were observed on the surface of the amorphous polymer (in the text referred to as polymer grain structure; see Figure 21 (h)). The height of these polymer grains increased with plasma treatment time from 2 nm after 3 s of plasma treatment to 6 nm after 30 s of treatment. However, with longer plasma treatment time (more than 30 s) the height of polymer grains did not seem to increase any more, in fact even a decrease in their height was observed (the observed height was approximately 3 nm). This decrease may occur due to temperature effects and melting of the amorphous fraction of polymer matrix in plasma (Figure 21 (e)). It is also important to note, that longer treatment times (i.e., longer than 30 s) already caused the burning of the amorphous foil, while this was not the case for the semicrystalline polymer. An AFM analysis on these samples was also conducted to observe how this affects surface morphology. It seems that treatment of amorphous polymers which is longer than 30 s, causes polymer degradation as the surface features are lost (Figure 21 (e)). A similar

process was noticed for semicrystalline PET foils from Du Pont treated for more than 4 min in oxygen plasma.

If surface morphology of semicrystalline polymer is examined on the lower scale, we can observe very similar polymer grain like structures as the ones seen on the amorphous polymer (Figures 21 (a)-(f)). The grains on the semicrystalline polymer become even more pronounced with longer treatment time; after 90 s of treatment their height reaches a value of 18 nm. Therefore, longer treatment manifests well-defined polymer grain like structures which are evenly distributed throughout the sample surface; this was confirmed with AFM images (Figure 21 (f)) as well as by SEM (Figure 19). Even after 180 s of plasma treatment we do not observe melting of this sample; this is due to higher crystallinity. However, the most noticeable morphological changes on semicrystalline polymer after plasma treatment are the increased height of silica particles on the surface (Figures 21 (b), (d), (f)). After 30 s of plasma treatment the height of silica particles increased from 40 nm for pristine polymer to about 200 nm.

The increase of surface roughness (Figure 22) is observed on semicrystalline polymers, predominantly due to the increased height of silica particles and the formation of orderly polymer grain like structure. This effect is not seen on amorphous polymers (Figures 21 (a), (c), (e)). The surface of the amorphous polymer sample only exhibits a higher surface roughness due to the manufacturing scratches, which disappear after plasma treatment. It should also be noted, that the polymer grain structure formed after plasma treatment on amorphous polymer is not as pronounced as in the case of semicrystalline polymer. This is mostly due to homogeneous etching of the amorphous polymer, which initially has practically no crystalline phase (crystalline fraction calculated from DSC measurement was about 4. 4 %), nor silica particles and thus, the change in surface roughness is almost negligible. On the other hand, the DSC thermogram for semicrystalline polymer initially shows about 30.6 % of crystalline fraction, which seems to remain practically the same, even after annealing (the second heating – see Chapter 4.3.). In this case we observed non uniform etching; as amorphous parts were preferentially degraded then the crystalline parts followed, while the silica particles were left intact.

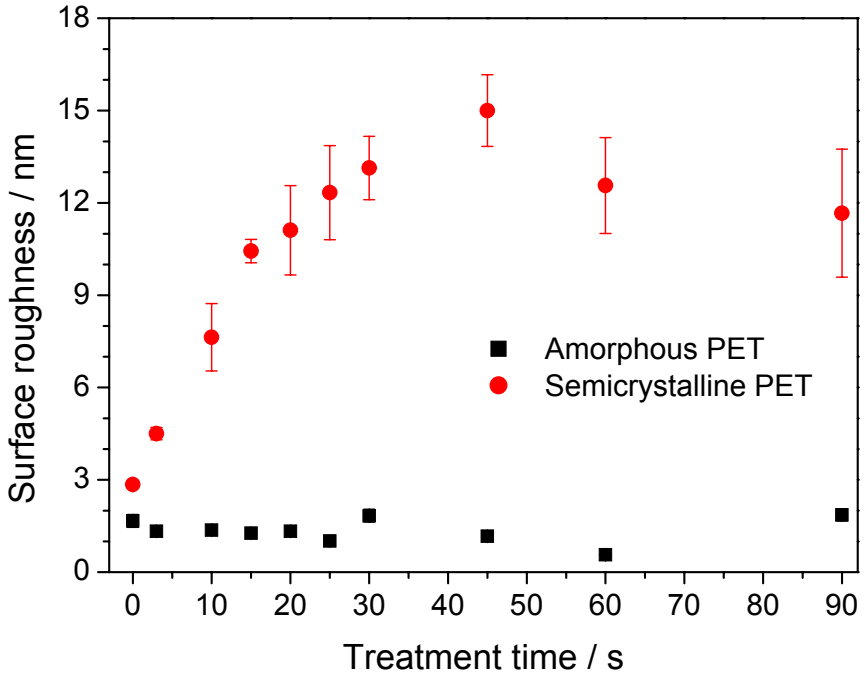

Figure 22 Average roughness (Ra) measured from 3 x 3 μm^2 AFM images as a function of treatment time on (●) semicrystalline PET foil and (■) amorphous PET foil.

The highest surface roughness on semicrystalline polymer was observed after 30 s of treatment, as, by that time, the height of silica particles had reached its maximum (Figure 22). The surface roughness did not change much after that, because the highest silica particles were removed from the surface due to etching of the polymer matrix in which they were embedded. This was further confirmed by measuring the difference in height ($h=h_{max}-h_0$, where h_{max} is the maximum height of silica particles after plasma treatment and h_0 is the initial height of silica particles on the pristine polymer surface) measured from AFM images (Figure 23), and presuming that silica particles are not etched by plasma. Figure 23 also presents the calculated height of removed material from the amorphous and semicrystalline polymer surface, measured from weight loss experiments. Thwerefore results presented in Figure 23 are obtained from weight loss experiments and from the AFM analysis of semicrystalline polymer. From this Figure it can be observed that as long as the silica particles are still embedded in the polymer matrix (up to 30 s of treatment), the height of the removed material determined from AFM analysis (blue dots) matches with the height determined by weight loss experiments (red dots) After that, the change in height of silica particles can no longer be correlated with the actual height of removed material. The height of removed material could not be calculated from AFM for amorphous

polymer, as the etching was homogenous and the surface did not exhibit any embedded silica particles.

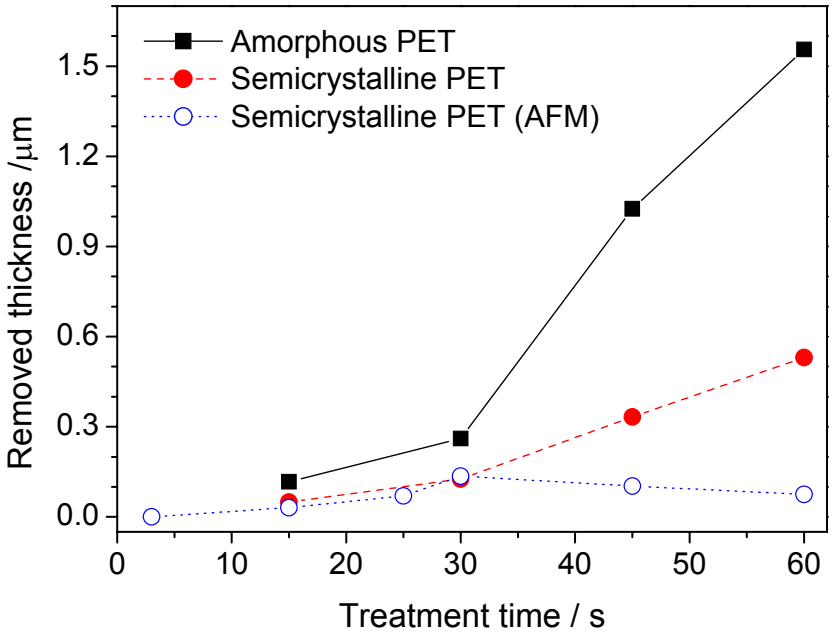

Figure 23 Thickness of removed material measured by gravimetry for (●) semicrystalline and (■) amorphous PET foil, and (○) the difference in height of silica particles on semicrystalline PET foil.

4.2.3. Surface morphology of Dacron vascular grafts

Similar changes in surface morphology after plasma treatment were also observed on PET fibres employed for vascular grafts. The surface of an untreated PET fibre is rather smooth, with no special topography (Figure 24 (a)), while, after short plasma treatment in oxygen plasma (20 s of treatment), the surface exhibits an orderly structure (Figure 24 (b)), similar to the one observed on plasma treated PET foils (grain like structures - or the formation of elongated spheres).

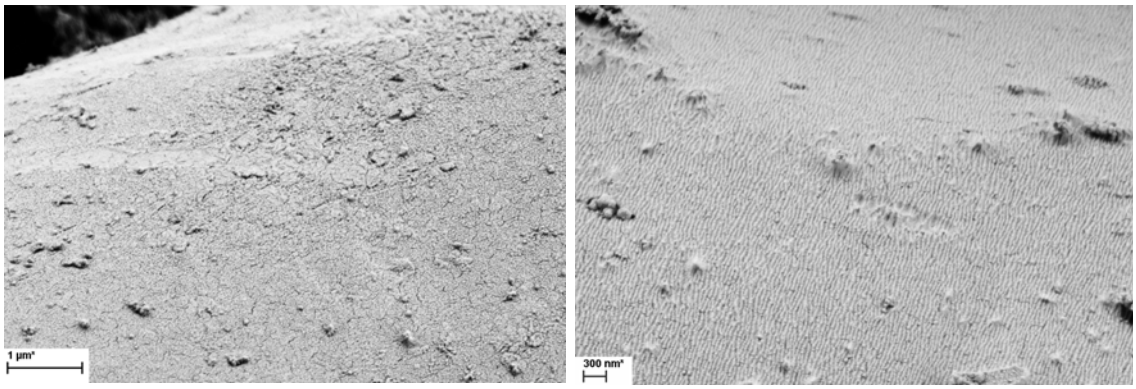

a.) b.)

Figure 24 Surface morphology of PET fibres: (a) untreated and (b) 20 s oxygen plasma treated.

This observation is confirmed through AFM analysis, as the change in surface morphology can be observed from height and phase images (Figure 25). The AFM phase images also provide further interesting information about surface properties. The untreated surface exhibits dark and bright regions (Figure 25 (b)) corresponding to different mechanical properties of the surface and can be attributed to the processing of fibres and the change in surface crystallinity. The phase image, after plasma treatment (Figure 25 (d)), shows the combination of the two parts, which are alternating; the bright regions can be attributed to the parts between the orderly grain-like structures. Presumably these parts have different mechanical properties and could be correlated to amorphous and crystalline regions, as surface crystallinity increases with plasma treatment time. It is also important to note that the morphology of PET fibres was altered after plasma treatment in a similar manner as on PET foils. This confirms that PET foils are an appropriate model material for studying the effects of plasma treatment and that the results obtained on PET foils can be employed for plasma treatment of PET fibres.

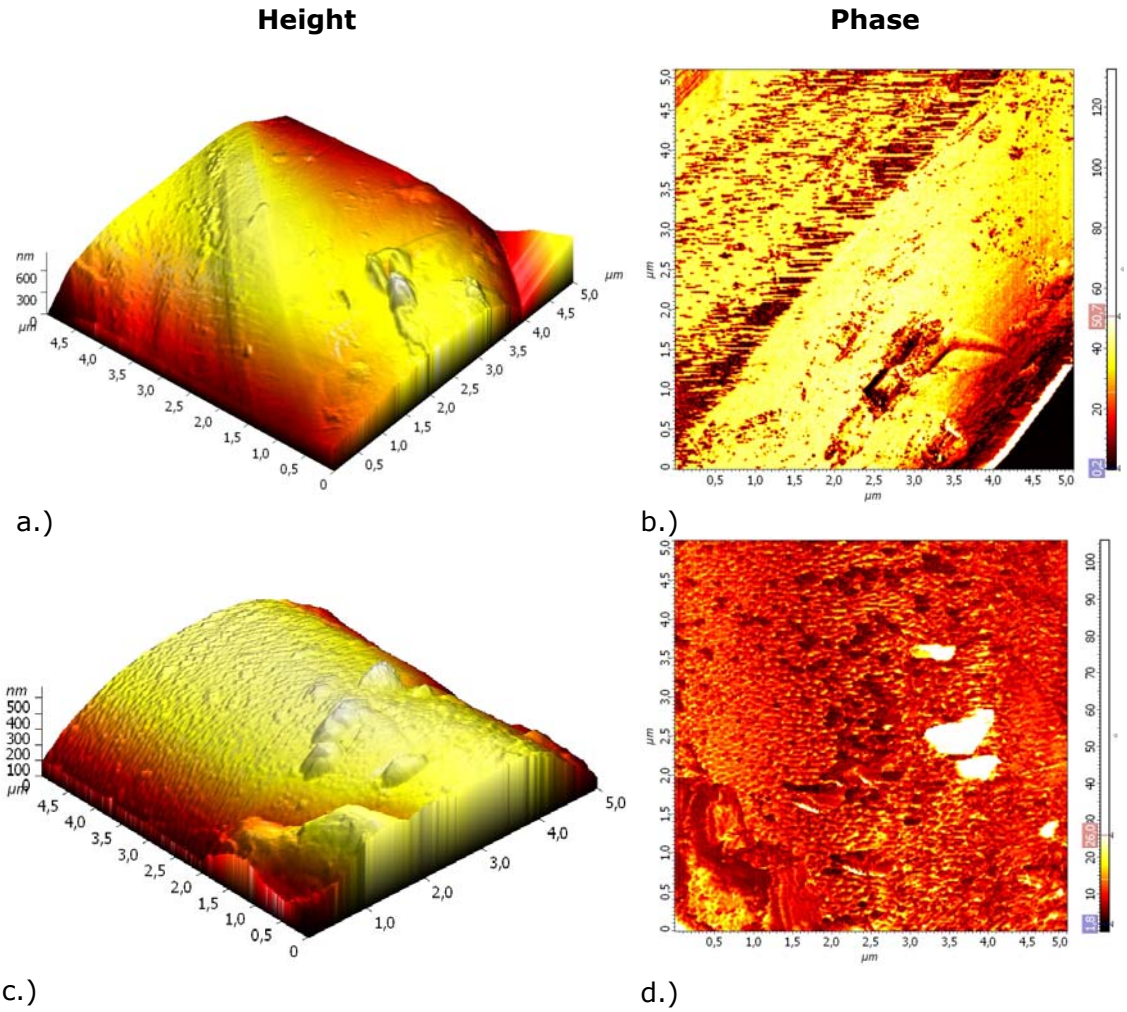

Figure 25 Height and phase contrast image of PET fibres (a), (b) untreated and (c), (d) 20 s oxygen plasma treated surface.

4.3. Wettability

Wettability measurements were performed for PET foils from Du Pont and for amorphous and semicrystalline foils from Goodfellow. As the amorphous foils from Goodfellow could only be treated in plasma for shorter treatment times due to temperature effects, the wettability measured on these foils was done only till 30 s of plasma treatment.

4.3.1. WCA on PET foil from Du Pont

Contact angle measurements show a decrease in contact angles after oxygen and nitrogen plasma treatment (Figure 26), corresponding to a higher hydrophilicity of the polymer surface. The oxygen plasma treated samples exhibit lower values of

contact angles, and thus demonstrating that this treatment provides a higher hydrophilic character. Even after short exposure times the surfaces show an increased hydrophilicity, regardless of the type of gas used. The treatment with nitrogen plasma, however, seems to be less efficient in reaching high hydrophilicity. The surface ceases to change its hydrophilicity from 60 s of treatment with nitrogen plasma. Hydrophilicity remains roughly the same even at longer treatment times (90 s). The results obtained by oxygen plasma treatment are different, especially with high treatment time. Namely, the surface hydrophilicity changes significantly even after 60 s of treatment. The contact angle measured from 90 s of treatment time in oxygen plasma is so low, that it is below the detection limit of our method. Therefore, the contact angle measured on this sample has been given the value of 1 degree and corresponds to a very small contact angle and high hydrophilicity of the sample. The high hydrophilycity of oxygen plasma treated surfaces could also be attributed to degradation products, that are formed on the surface after longer treatment times and could cause a lower contact angle, due to surface roughening.

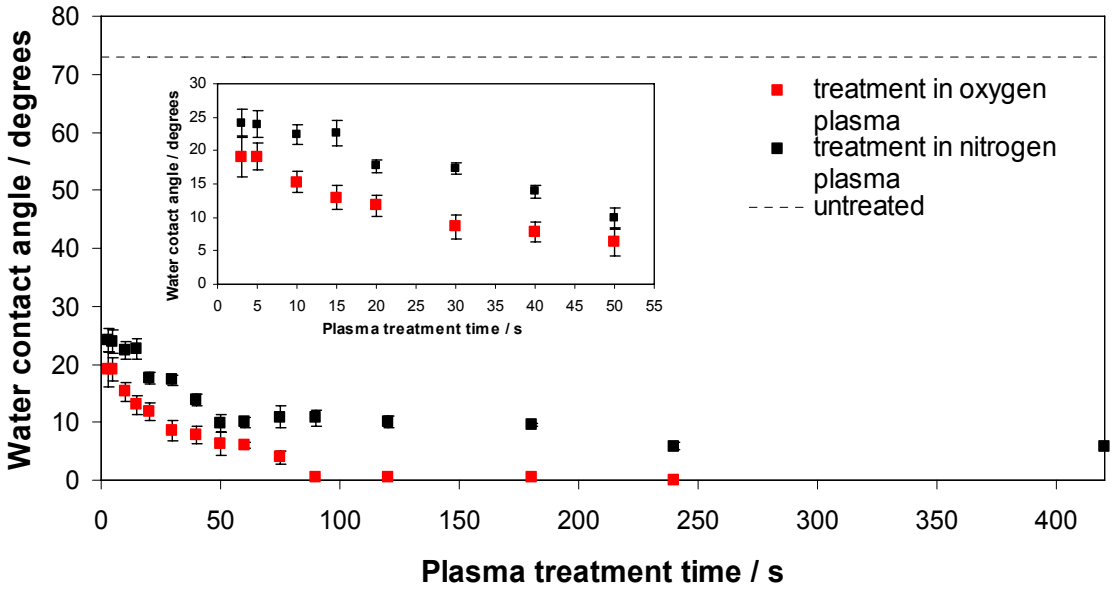

Figure 26 Water contact angle measured on the PET foil as a function of treatment time and plasma gas, (■) oxygen plasma treatment, (■) nitrogen plasma treatment.

Oxygen plasma treatment seems to produces more hydrophilic surfaces; this is probably due to high oxygen incorporation and to lower saturation time with these functional groups, as was observed from the XPS analysis. The XPS analysis shows that the atomic concentration of C on the nitrogen plasma treated surface

decreases to about 60.2 at. % after 30 s of treatment, a similar decrease is achieved with oxygen plasma treatment already after 3 s (C concentration is about 60.8 at. %). In comparison to the measured contact angle it can also be seen that the contact angle after 30 s of nitrogen plasma treatment is very similar to the contact angle measured on surface treated for only 3 s in oxygen plasma. To study how the incorporation of oxygen and nitrogen functionalities affect the surface hydrophilicity a comparison of water contact angle (WCA) with the ratio of O/C and N/C was made. Figures 27 (a) and (b) show the correlation between WCA and the ratio of O/C or N/C for oxygen and nitrogen plasma treatment respectively.

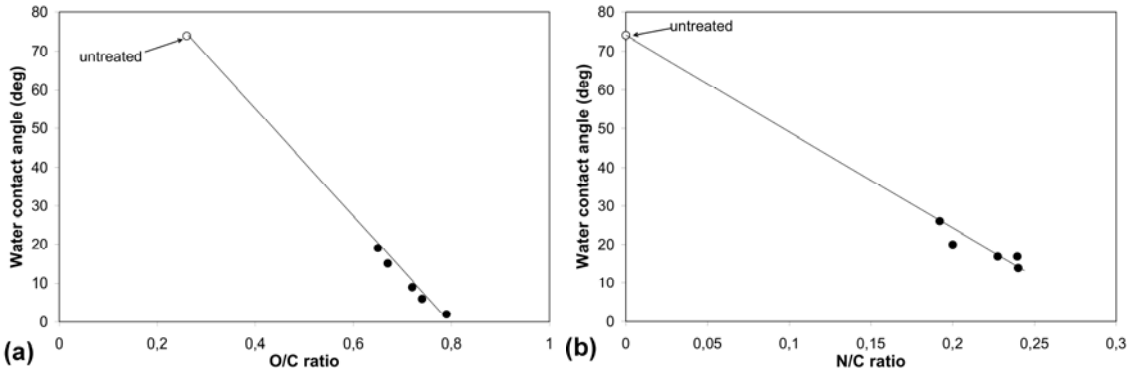

Figure 27 Correlation between water contact angle and (a) O/C ration for oxygen plasma treatment and (b) N/C ratio for nitrogen plasma treatment.

Since almost linear correlation was observed, it can be assumed that the contact angles were greatly reduced due to incorporation of oxygen and nitrogen functionalities into the PET surfaces. However, the difference in wettability could also be attributed to different functional groups which are formed on the surface - as not all of them have a high hydrophilic character. For example, functional groups like carbonyl, hydroxyl, aldehyde/ ketone and amine (-COOH, -OH, -CO, -NH_2) are hydrophilic, while amides and esters are regarded as compounds with lower water solubility (more hydrophobic), but they still have more pronounced hydrophilic characteristics than hydrocarbons. In view of this, higher wettability after longer treatment times in oxygen plasma, could be assigned to an increase in C=O functional groups, which were in fact observed from XPS analysis. Interestingly, longer treatment times in oxygen plasma produce surfaces with almost super hydrophilic properties, as the water droplet completely spread on the surface and the contact angle was impossible to measure. As can be seen from AFM, plasma treatment modifies surface roughness and, according to Wenzel equation, this could also influence the measured contact angle (Sprang et al., 1995, Wolansky and Marmur, 1999, Brandon et al., 2003). According this equation,

surfaces having a contact angle, which is lower than 90°; this is the case with PET polymer, the increase in surface roughness decreases the contact angle. In the present case, surface roughness measured by AFM on virgin and plasma treated PET surfaces showed that the surface roughness Ra is 10 nm or less, and this could therefore contribute to some extent to a lower contact angle. However, according to Busscher et al. (Busscher et al., 1984), roughness bellow 100 nm should not have any influence on the contact angle measurement. Therefore, it can be presumed that, at least for short plasma treatment times, the influence of roughening is negligible. It should also be noted that longer treatment times (90 s and above) produce degradation products on the surface, which are well seen also from SEM images (Figure 19), these products could cause capillary effects resulting in high wetting properties of the material.

- **Ageing effects**

XPS and contact angle measurements were carried out continuously for several days, in order to determine the rate of ageing of the PET surface treated in nitrogen and oxygen plasma.

Figure 28 shows how different plasma treatment times affect the ageing of PET surfaces, as determined from the water contact angle. These results show that the length of plasma treatment has an influence on ageing of the PET surface. Interestingly, in spite of the high trend of ageing observed by XPS (Chapter 4.1.), the contact angle measurements in Figure 28 show less ageing effects for oxygen plasma treatment than in the case of nitrogen plasma, where the XPS analysis showed only a slight trend of ageing.

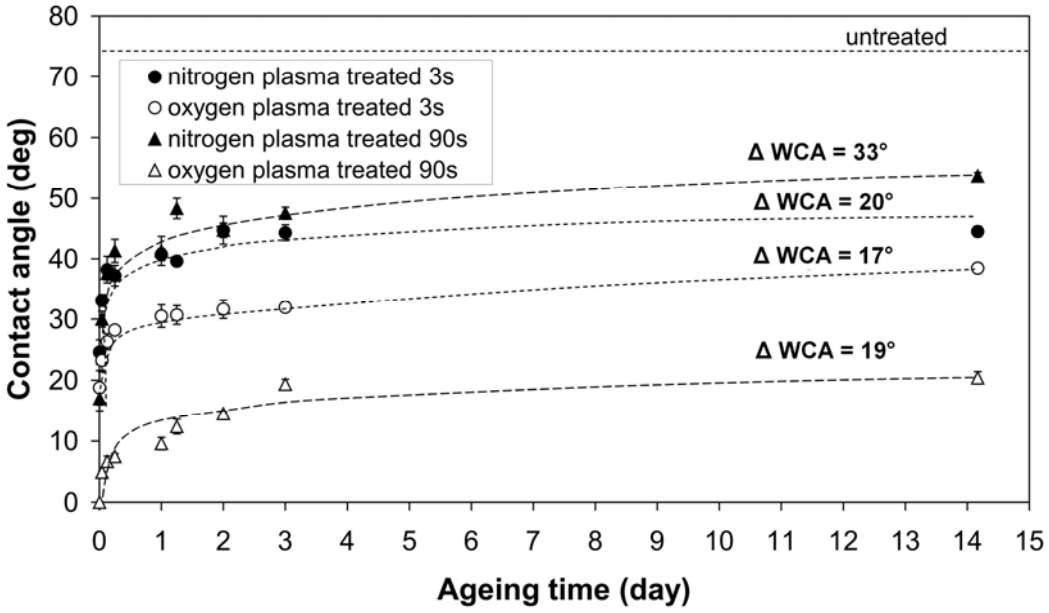

Figure 28 Contact angle measurements, which show the ageing of a PET foil treated for 3 s and 90 s in nitrogen and oxygen plasma.

After 14 days of ageing, the nitrogen plasma treated surface exhibited a contact angle of about 45°, while the oxygen plasma treated surface exhibited a contact angle of just 35°. In both cases surface hydrophilicity was stabilized after 3 days, as by that time the water contact angle reached a constant value.

These unusual phenomena where the XPS measurements of nitrogen plasma treated PET showed slight changes after ageing and the oxygen plasma treated a high ageing rate, while the opposite was observed for ageing measured by water contact angle, can be explained by the difference in the measuring techniques. At this point it should be noted that the contact angles are controlled by the few outermost angstroms of polymer materials and are thus strongly affected by the reorientation of functionalities present on the surface (Jannasch, 1998, Larrieu et al., 2005b, Morent et al., 2007, Riccardi et al., 2003). The analysing depth for C1s photoelectrons in XPS analysis is estimated at about 8.5 nm ($3\lambda \sin 45° = 8.5$ nm at $\lambda = 4$ nm (Inagaki et al., 2004). Thus, the observed discrepancy can be due to the combination of two processes – the first is the reorientation of the polar groups into the bulk polymer and the second is the mobility of the small polymer chain segments into the matrix, both leading to different free surface energy. In the case of oxygen plasma treatment, where high etching rates and big changes in surface topography were observed, thus it can expected to have more polymer chain scission and the appearance of small fragments which are either desorbed from the surface or moved into the bulk. This is reflected in the XPS results. Therefore, it

can be concluded, that oxygen plasma treatment produces more pronounced chain mobility; while nitrogen plasma treated surfaces probably exhibit a surface reorientation. It should also be noted that there were no observable changes in surface topography and roughness during the ageing study.

It is also interesting to view the comparison of ageing of the samples treated for a shorter (3 s) and longer time (90 s), as seen in Figure 28. In the literature different treatment times used for surface modification of polymers ranging from milliseconds to several minutes are reported. At milliseconds of treatment, it is difficult to talk about surface functionalization, since the first thing that occurs at the polymer surface is the removal of contaminants, which may also lead to improved wettability. With further treatment time, insertion of oxygen/nitrogen atoms at active sites on the polymer surface occurs, leading to the formation of various functional groups, which change surface wettability. With prolonged treatment time, excessive chain scission may appear, leading to a layer of low-molecular-weight fragments on the surface. Such a surface will have a greater tendency for ageing due to the migration of small fragments to the bulk. It was also reported that chain mobility mainly occurs in the amorphous region, while the mobility in the crystalline region is fairly limited, because of an orderly packed structure. Therefore, polymers with higher degree of crystalline fraction exhibit lower hydrophobic recovery with ageing time. This is why some authors observed slow ageing of polymers treated for longer times (Strobel et al., 1994, Morent et al., 2007, Borcia et al., 2003). However, the ageing studies ($\Delta WCA = WCA_{14days} - WCA_{0day}$) of the PET samples treated for longer time (90 s) showed that the ageing is faster than for those treated just for 3 s (Figure 28). Nevertheless, in all cases, a constant water contact angle (WCA) was reached after 3 days. Interestingly, the constant value of WCA on 90 s oxygen plasma treated surfaces was lower than the one measured on surfaces treated for 3 s. More specifically the constant value of WCA on 90 s oxygen plasma treated surfaces was about 25 degrees, while for the 3 s treated surface the WCA was about 32 degrees. The opposite was observed for nitrogen plasma treated surfaces; the constant value of WCA on the surface treated for 90 s was about 49 degrees and 40 degrees on the surface treated for 3 s. This may be due to increased surface roughness, mostly because of degradation products, which could result in lower WCA. As it can be seen from the SEM images (Figure 19), the surfaces treated for longer treatment times are already overtreated, having a layer of low-molecular-weight fragments on the surface, which could cause the capillary phenomena. Such a surface is unsuitable for

applicability due to the fast ageing process, this is despite the best wettability measured immediately after the treatment on this kind of surface.

4.3.2. WCA on PET foil from Goodfellow

The wettability measurements were performed on amorphous and semicrystalline polymers less than 30 s after plasma treatment. The results indicate that already after 3 s of oxygen plasma treatment, the surface becomes hydrophilic, as the contact angle decreases from 72 degrees to about 20 degrees, independent of polymer crystallinity. Longer plasma treatment produces even more hydrophilic surfaces. However, differences in wettability between amorphous and semicrystalline polymer can be observed, as longer treatment times produce lower contact angles on the semicrystalline polymer. Thus, the semicrystalline polymer obtains a contact angle of about 8 degrees after 20 s of treatment, while the contact angle of the amorphous polymer is about 16 degrees. This can be seen in Figure 29.

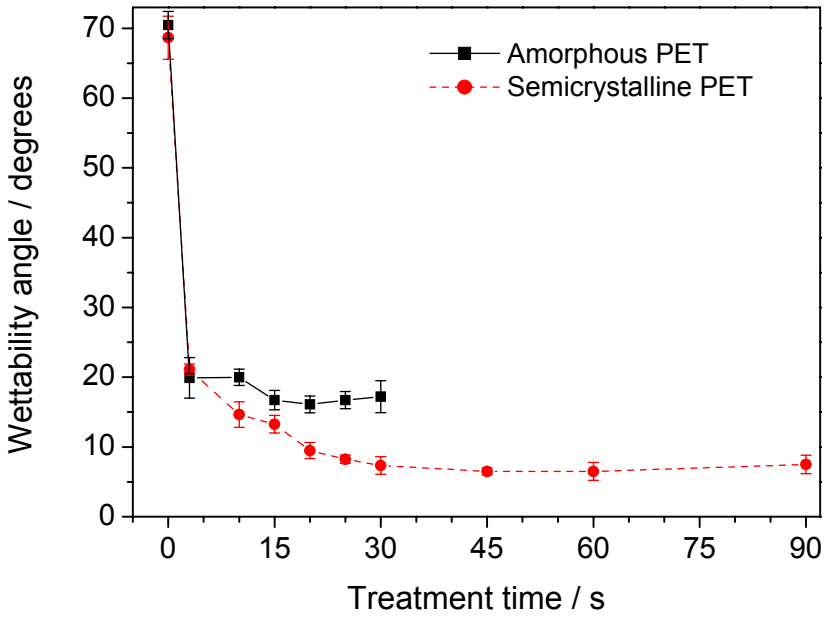

Figure 29 Wettability angle measured on PET foil as a function of treatment time on (●) semicrystalline and (■) amorphous PET.

Longer treatment times produce even more hydrophilic surfaces; similar observations were also obtained for PET foil from Du Pont (see Chapter 4.3.1). It has been established that newly incorporated oxygen functionalities (Cui and Brown, 2002) and increased surface roughness (Pandiyaraj et al., 2008) play a major role in wettability. Since longer treatment times on semicrystalline polymers

produce higher surface roughness (Figure 22) and an increased oxygen concentration (Figure 16), it can be presumed that such surfaces would have better wettability. These effects were indeed observed on semicrystalline polymers, where wettability increased with treatment time (Figure 29), the same was also observed on semicrystalline PET foils from Du Pont (see Chapter 4.3.1). However, the wettability of amorphous polymers was not lowered, even after longer treatment times, mostly due to unchanged surface roughness, lower oxygen incorporation and the degradation of polymer (after 30 s of treatment).
Therefore, the main differences in surface wettability between semicystalline and amorphous polymers can be attributed to the incorporation of oxygen functional groups and the change in surface morphology, as plasma treatment of semicrystalline polymers produces high silica particles which could cause capillary phenomena.

- Ageing effects

Ageing of amorphous and semicrystalline polymers was most pronounced in the first few hours after plasma treatment. From Figure 30 that the ageing of the amorphous polymer is higher; after 16 days the WCA on this surface was about 42 degrees, while for semicrystalline it was about 36 degrees.

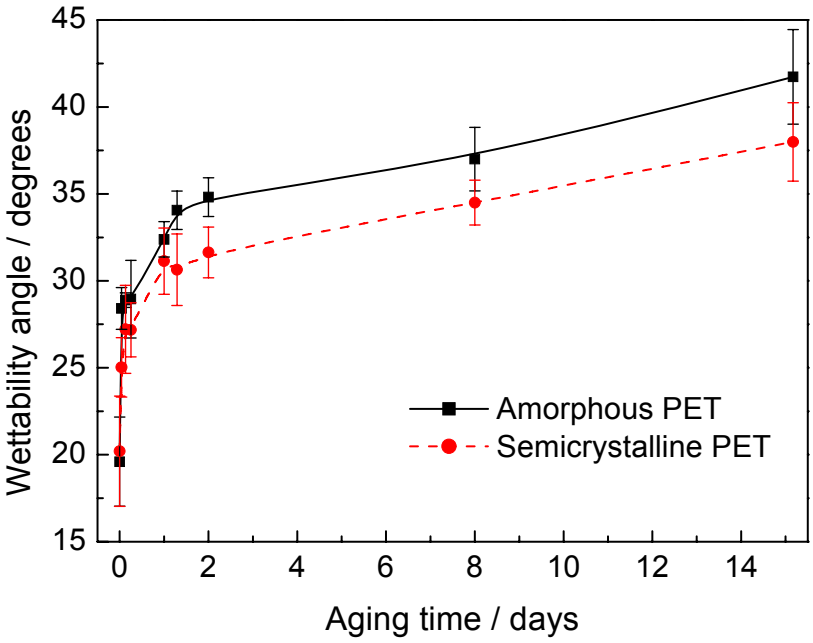

Figure 30 Ageing of (●) semicrystalline and (■) amorphous PET foil treated in plasma for 3 s.

Faster ageing of amorphous PET foil, especially in the first hours after treatment, is also in accordance with results published by Kim et al. for high and low density polyethylene (Kim et al., 2003). The main driving force of ageing after plasma treatment is the reorientation of newly formed functional groups. As the polymer chains are mobile, especially in the amorphous parts of polymer, they can respond to interfacial forces and thus minimize the interfacial free energy between the polymer surface and the environment (Cui and Brown, 2002). Ageing of the sample is most evident in the first few hours after plasma treatment and it reaches a constant value after a few days. However even after a few days, the aged plasma treated samples offer improved wettability, as the contact angle of pristine surface is 72 degrees and after 16 days of ageing reaches about 36 degrees for the semicrystalline polymer and 42 degrees for the amorphous polymer.

However, both ageing curves follow a logarithmic-like trend, typical for the decay of functional groups after plasma treatment. Results show that better wettability is obtained after ageing, compared to pristine (untreated) samples. Interestingly, similar results were obtained after ageing of PET film (Goodfellow Ltd.) treated in air plasma by DBD discharge (Morent et al., 2007). Accordingly in the present case the improved wettability, even after ageing, can be attributed to incorporation of polar groups, rather than to increased surface roughness, because the change in surface roughness after 3 s of treatment is almost negligible for both samples.

4.3. Thermal analysis

DSC thermograms were obtained, in order to determine the degree of crystallinity (x_{DSC}), glass temperature (T_g), crystallization temperature (T_c) and melting temperature (T_m) of PET foils from Du Pont, and Goodfellow and also the PET fibres from vascular grafts, (Figure 31). The results from DSC indicate, that vascular grafts made from PET fibres have the highest degree of crystallinity 40.4 % (Figure 28 (a)), while the semicrystalline foils from Du Pont have 36.5 % (Figure 31 (b)) and the semicrystalline foils from Goodfellow have 30.6 % (Figure 31 (c)). According to the DSC analysis, the amorphous foils from Goodfellow also contain some crystalline fraction, as the calculated crystallinity is about 4.4 % (Figure 31 (d)).

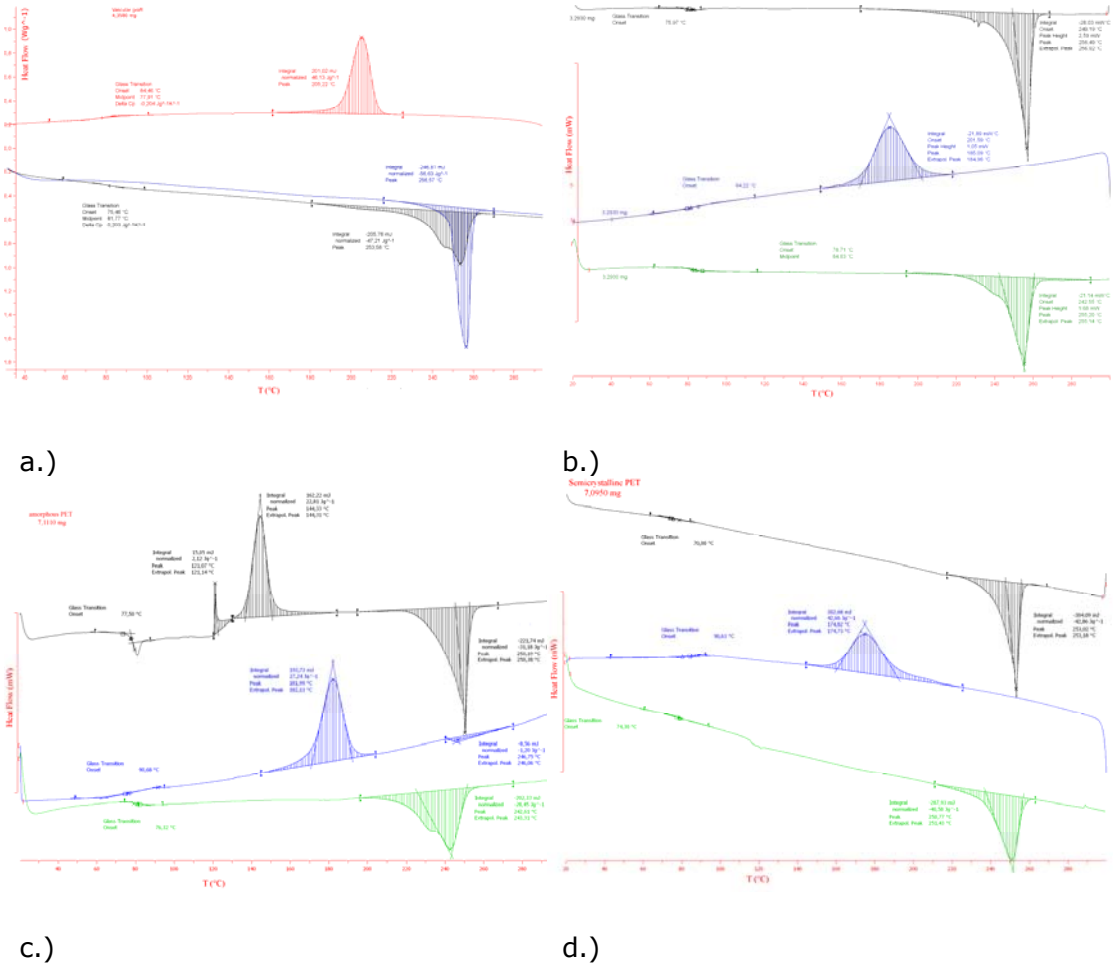

Figure 31 DSC thermogram of (a) PET vascular grafts, (b) semicrystalline PET from Du Pont, (c) amorphous PET from Goodfellow, (d) semicrystalline PET from Goodfellow.

The comparison of melting peaks obtained from fibres (Figure 31 (a)) and semicrystalline PET foils (from Du Pont and Goodfellow from Figures 31 (b) and (c)) shows, that fibres have a much narrower melting peak, which can be attributed to a more uniform size of crystallites in fibres. Table 13 shows the comparison of glass temperatures, crystalline temperatures and melting temperatures together with calculated crystalline fraction.

PET polymer	T_g [°C]	T_c [°C]	T_m [°C]	x_{DSC} [%]
Semicrystalline (Du Pont – 125 um)	75.9	201.6	249.2	36.5
Semicrystalline (Goodfellow – 250 um)	70.1	191.8	247.7	30.6
Amorphous (Goodfellow – 250 um)	77.5	191.7	245.4	4.4
Vascular graft	74.3	205.2	256.6	40.4

Table 13 Results of DSC analysis for untreated PET foils.

Foils from Du Pont exhibit the glass transition at about 75.9 °C, which is similar to T_g measured for fibres (T_g = 74.3 °C). While the T_g of foils from Goodfellow is at 77.5 °C and at 70.1 °C for amorphous and semicrystalline PET respectively.

DSC was also used in order to study effects of plasma treatment on the crystallinity of polymers. First 125 μm thick foils from Du Pont were used to calculate the change in crystalline fraction between untreated and oxygen plasma treated surfaces (Figures 32 and 33). As DSC analysis is not a surface technique, thinner foils with the thickness of 8 μm from Du Pont were also employed, in order to lower the contribution of bulk crystallinity. The DSC thermograms are presented in Figure 33, together with a DSC termogram for 125 μm thick foils treated in oxygen plasma.

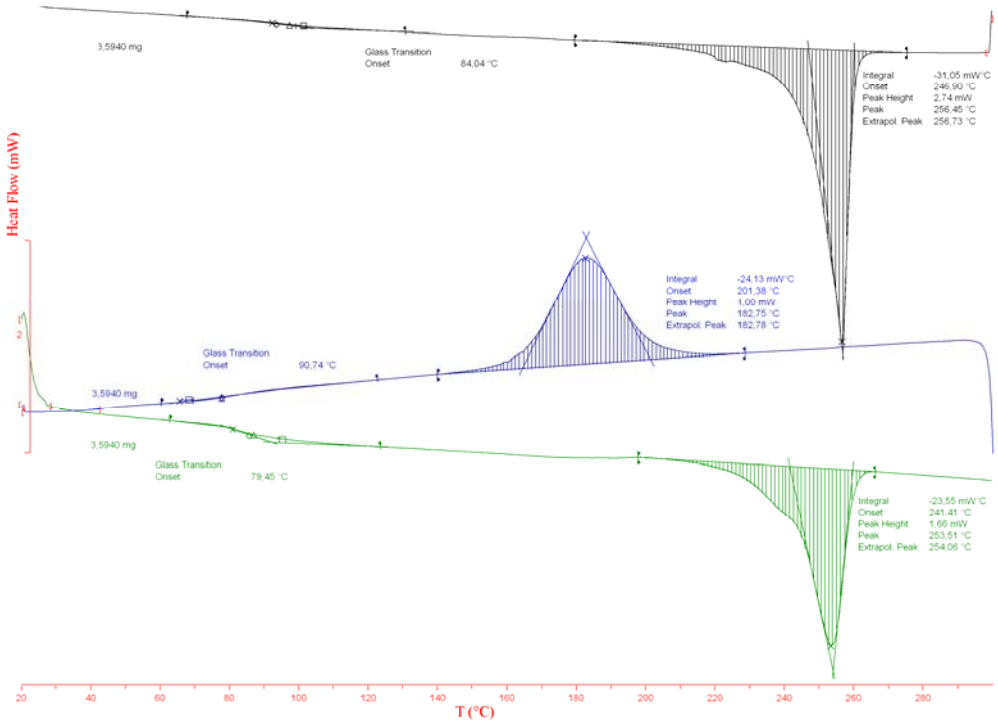

Figure 32 DSC thermogram of PET foil (Du Pont, 125 μm thick) treated in oxygen plasma for 90 s.

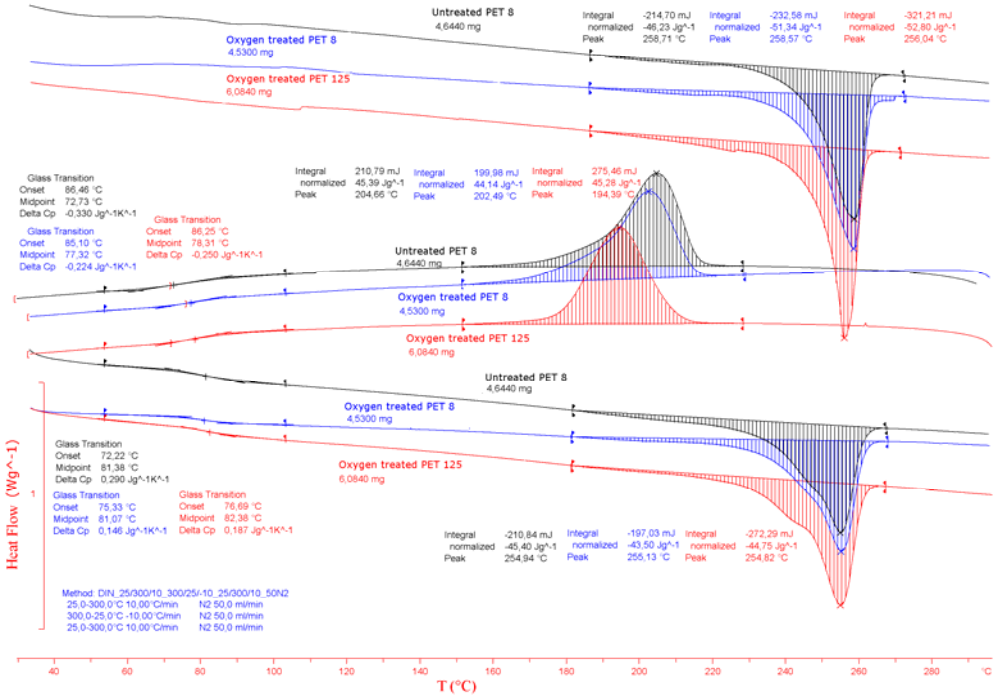

Figure 33 DSC thermogram of; untreated PET foil (Du Pont, 8 μm thick) - black line, PET foil (Du Pont, 8 μm thick) treated in oxygen plasma for 20 s - blue line and PET foil (Du Pont, 125 μm thick) treated in oxygen plasma for 90 s – red line.

The difference in crystalline fraction might not be seen from the melting peak, but a small difference can be distinguished from calculating the crystalline fraction, especially for the very thin foils (see Table 14). The thin foils were treated from both sides in oxygen plasma for only 20 s to prevent overheating. The crystallinity of the thin foils increased from the initial 33 % to about 36.6 %. The thicker foils exhibited a less pronounced increase in crystalline fraction (Table 14) and were treated from both sides with oxygen plasma for 90 s.

PET polymer		x_{DSC} [%]
	Untreated	36.5
Du Pont – 125 μm	Treated, 90 s in oxygen	37
Du Pont – 8 μm	Untreated	33
	Treated, 20 s in oxygen	36.6

Table 14 Results from DSC analysis for oxygen plasma treated PET foils.

- **Temperature effects on PET foils treated in oxygen and nitrogen plasma**

The surface temperature of PET foils during plasma treatment was measured by a pyrometer (ε= 0.95). Figure 34 show very small temperature differences between the PET samples treated in oxygen and nitrogen plasma. However, temperature in plasma increased with treatment time, and in the case of oxygen plasma, burning of the foil after 4 min of treatment was observed; this was not the case for the nitrogen plasma treated surface, even at longer treatment times (7 min). This could be explained by the high oxidation nature of oxygen plasma and thus burning of the foil. The change in surface morphology after 4 min of oxygen plasma treatment can be observed also from SEM analysis (see Chapter 4.2.1).

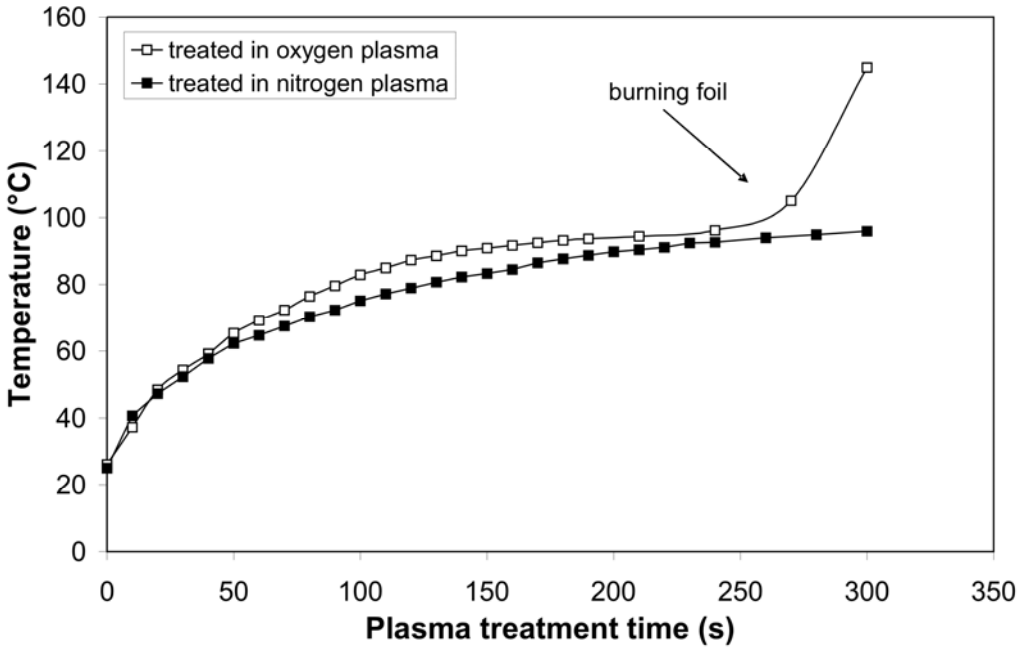

Figure 34 Temperature of the PET foil during treatment in oxygen plasma (□), and nitrogen plasma (■).

To further observe temperature effects on PET foils, the foils were heated in a furnace for 10 min at 150 °C; afterwards the surface was imaged by AFM to observe the structure. Figure 35 (a) shows the morphology of PET foil after heating in a furnace. The morphology changes and surface roughness increases, but the surface does not exhibit small sphere like structures as observed on plasma treated surfaces (Figures 35 (b) and 18). The AFM analysis shows that surface structures are not similar to those observed after plasma treatment and thus cannot be related to temperature effects alone.

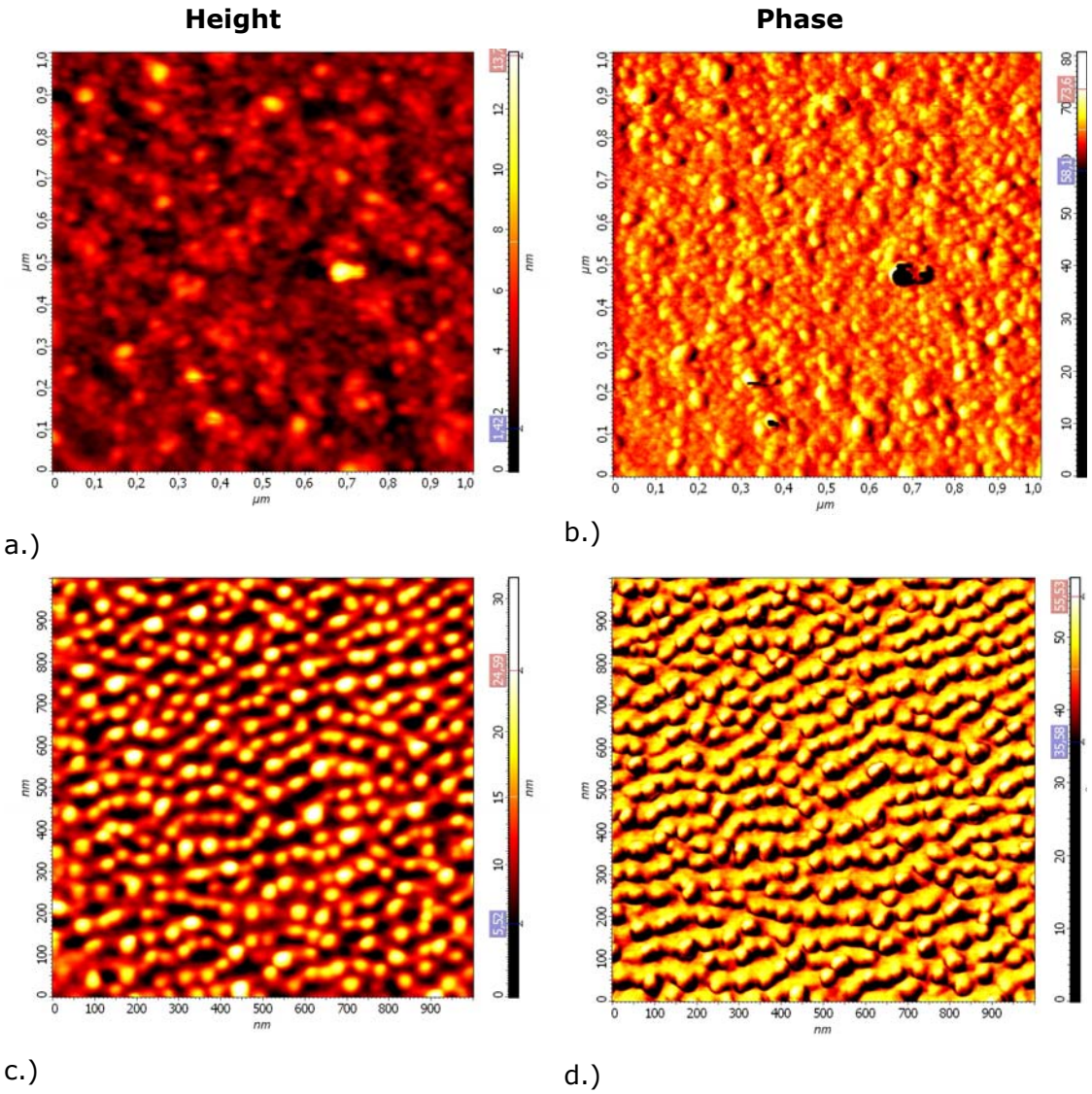

Figure 35 Comparison of surface morphology from height and phase AFM images of PET foils which were (a) heated in a furnace for 10 min at 150°C and (b) treated with nitrogen plasma for 90 s.

- **Temperature effects of oxygen plasma treatment on amorphous and semicrystalline polymers**

The temperature of the surface of amorphous and semicrystalline PET foils from Goodfellow was measured in order to observe the differences in surface heating between these two polymers during oxygen plasma treatment. The heating of the polymer in plasma is predominantly caused by ion bombardment and a recombination of neutral oxygen atoms on the surface. From Figure 36 it can be seen that the temperature on the amorphous polymer increases faster compared to the semicrystalline polymer, which could also lead to different surface reactions of incoming plasma species. The amorphous polymer starts to curl and change colour already after 30 s of plasma treatment, thus the temperature can no longer be measured by the pyrometer.

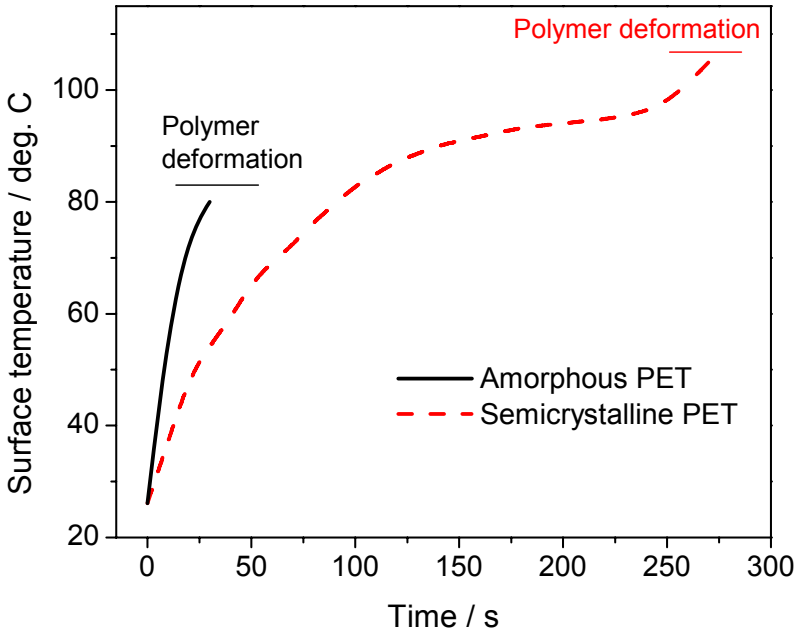

Figure 36 Average surface temperature of (--) semicrystalline and (—) amorphous PET foil during exposure to oxygen plasma measured with an infrared camera.

To only observe the effects of heating on the morphology of amorphous and semicrystalline surfaces, these foils were heated in a furnace at 200 °C for 10 min, after which their morphology was analysed by AFM. It can be observed from AFM images (Figure 37), that surface morphology changes due to heating, as the amorphous parts already starts to melt at about 70 °C or 77 °C for amorphous and

semicrystalline polymer respectively. Images taken by AFM reveal that surface morphology of PET foils heated in a furnace and those treated in oxygen plasma is different.

Height **Phase**

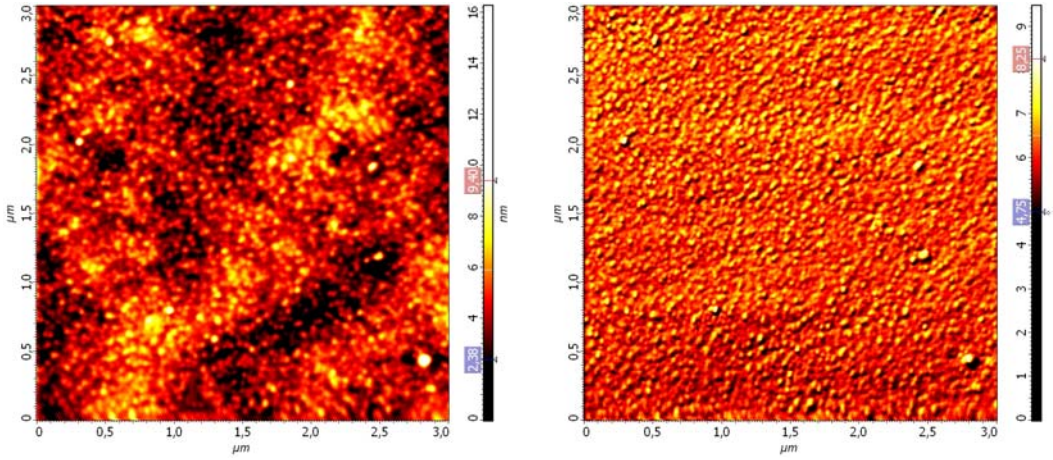

a.)

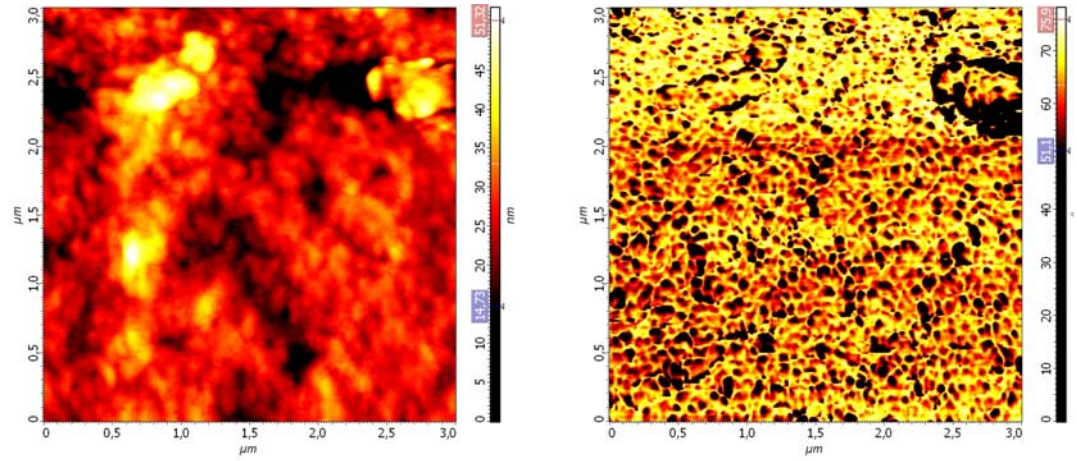

b.)

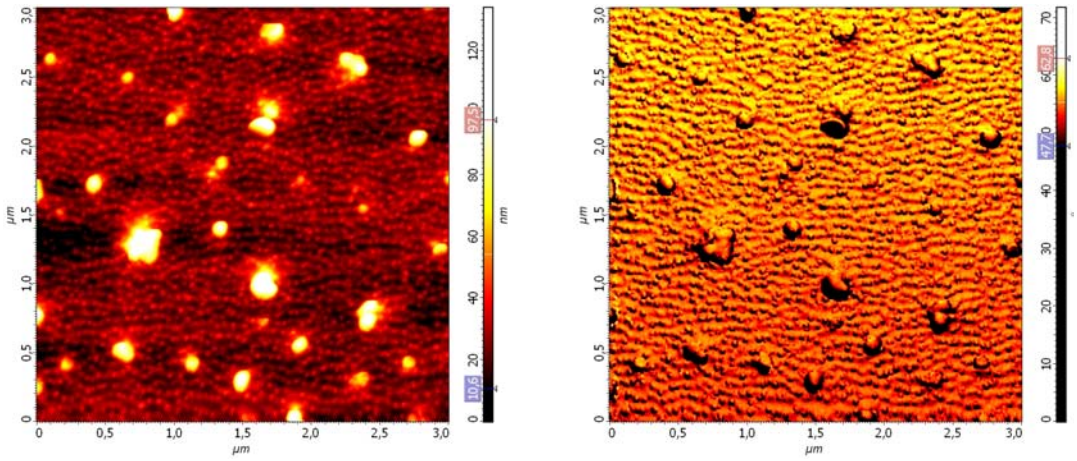

c.)

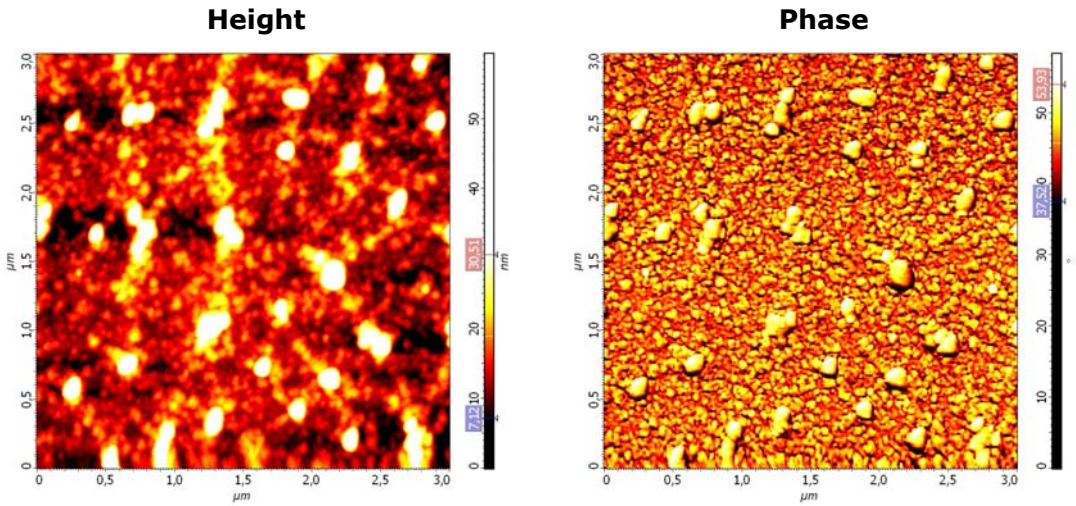

d.)

Figure 37 Comparison of surface morphology from height and phase contrast AFM images on (a-b) semicrystalline PET foil treated in oxygen plasma, (c-d) semicrystalline PET foil heated in a furnace at 200 °C for 10 min, (e-f) amorphous PET foil treated in oxygen plasma and (g-h) amorphous PET foil heated in a furnace for 200 °C for 10 min.

On plasma treated surfaces orderly grain like structure are observed (see Chapter 4.2.2.), while after heating in a furnace, the surface exhibits elongated features, which could be attributed to heat induced crystallisation. It can be seen through roughness analysis (images taken on area of 3x3 μm^2), that roughness after heating in a furnace increases from 1.7 nm to 3.6 nm and from 2.8 nm to 4.6 nm for amorphous and semicrystalline foils, respectively. Higher surface roughness is also observed for amorphous foils heated in a furnace in comparison to foils treated in oxygen plasma. Whereas, these is not noticed for semicrystalline foils, as 90 s of nitrogen plasma treatment produces higher surface roughness than heating in a furnace. Again, it can be confirmed that morphological changes after plasma treatment cannot only be attributed to heating of the foils, as the heating does not produce sphere like structures on the surface. These structures are probably formed due to preferential etching of amorphous parts, which results in higher surface crystallinity after plasma treatment.

4.4. Etching effects

- **Etching of PET Du Pont foils by oxygen and nitrogen plasma**

The etching rate of PET foils treated in oxygen and nitrogen plasma was determined by weight loss measurements, which were carried out before and after plasma treatment. Weight loss vs. treatment time in oxygen and nitrogen plasma is shown in Figure 38. The etching rate was calculated according to these measurements. For oxygen plasma treated samples the etching rate was 12.9 nm/s and for nitrogen plasma treated samples 3.3 nm/s. Much higher etching rates on oxygen plasma treated surfaces can mainly be attributed to the high oxidative nature of oxygen plasma and the formation of volatile compounds that are released from the surface.

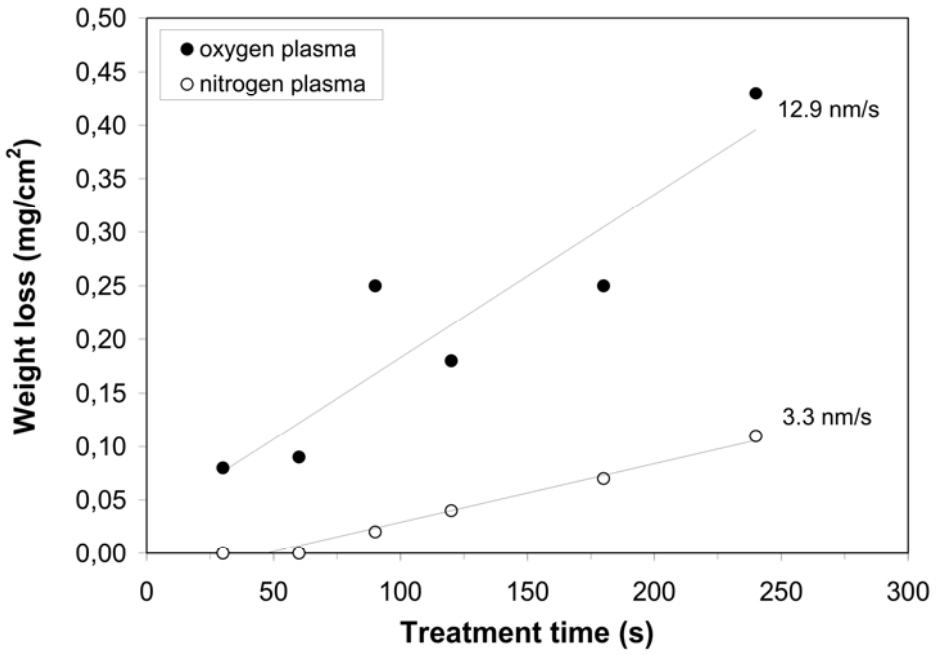

Figure 38 Weight loss of the PET samples during exposure to oxygen and nitrogen plasma.

Nevertheless, the observed difference in time-dependence of the concentration of functional groups between oxygen and nitrogen plasma treatment may be explained by the differences in the probability of oxygen and nitrogen incorporating into the surface. It should also be noted, that this is actually a combination of two effects: sticking of neutral atoms at the surface, and etching by ions, which limits the build-up of polar functionalities. The competition between functionalization by atoms and degradation by ion etching sooner or later balances out. Moreover, the increase of the surface area with treatment time also causes an increase of the area available for chemical interactions of atoms (Strobel et al., 1994). In the present case, the density of ions (n_i = 10^{15} m^{-3}) and their flux j_i = 10^{17} $m^{-2}s^{-1}$ is a few orders smaller than the flux of neutral atoms to the surface and can thus be easily neglected in the calculation above.

- **Etching of amorphous and semicrystalline PET foil with oxygen plasma**

Etching of the amorphous polymer is more pronounced in comparison to the semicrystalline polymer. This can be explained by faster etching of amorphous parts, which are not as densely packed as crystalline parts. After 30 s of plasma treatment the amorphous polymer etches even more rapidly. This is due to higher rise in temperature, which causes even faster degradation of amorphous polymer (Figure 23). This means that optimisation of treatment time on amorphous polymer is restricted and that the changes in morphology on this samples cannot be varied as in the case of the semicrystalline polymer, where an orderly grain like structure was obtained, especially after longer treatment times. Thus, the semicrystalline polymer can be treated in oxygen plasma glow discharge even four times longer than the amorphous polymer.

4.5. Proliferation of fibroblast cells

When assessing the biocompatibility of materials, the proliferation of fibroblast cells on the polymer surface is very important. For this purpose the untreated and oxygen plasma treated polymer surfaces with different degrees of crystallinity were incubated with fibroblast cells. The viability and proliferation of fibroblast cells was analysed by an MTS assay (Figure 39), as well as by counting the number of attached cells from images taken by optical microscopy. The preparation of the samples was done according to the procedure described in the chapter on Method and Materials (Chapter 3.2.4.1.). The proliferation of fibroblast cells seeded directly

onto the PET foils was studied 20 min and 40 min after incubation with 3000 fibroblast cells. The difference between 20 and 40 min of incubation is important to determine cytotoxicity of the surface, as longer incubation of cells with material could reduce their viability and proliferation.

Figure 39 presents the results from MTS assay for different incubation times and different samples. It can be observed that the viability of fibroblast cells was higher after plasma treatment compared to untreated surfaces. Longer incubation times resulted in lower viability on all samples, however only slight changes in viability of cells were observed on the amorphous surface treated in oxygen plasma. Thus, it can be presumed that plasma treatment improves cell proliferation and is not cytotoxic.

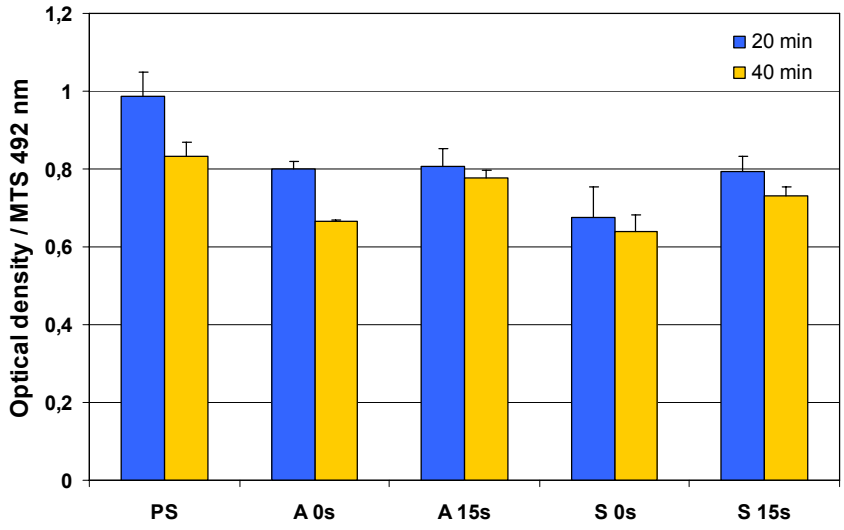

Figure 39 Viability and proliferation of fibroblast cells on virgin and oxygen plasma treated amorphous (A) and semicrystalline (S) PET polymer by MTS assay, where PS – control, A 0s – untreated amorphous, A 15s - oxygen plasma treated amorphous, S 0s – untreated semicrystalline, S 15s – oxygen plasma treated semicrystalline.

The number of fibroblast cells attached to the polymer surface was then analysed by optical microscope. Figure 40 shows the number of fibroblast cells per unit surface. On all samples, except the untreated ones, the number of attached cells increased with incubation time, In the case of the untreated semicrystalline sample (S 0s), the number of cells decreased with longer incubation time, and a similar observation was also made for the untreated amorphous sample (A 0s). These results also confirm that oxygen plasma treatment is not cytotoxic, and it even promotes cell proliferation.

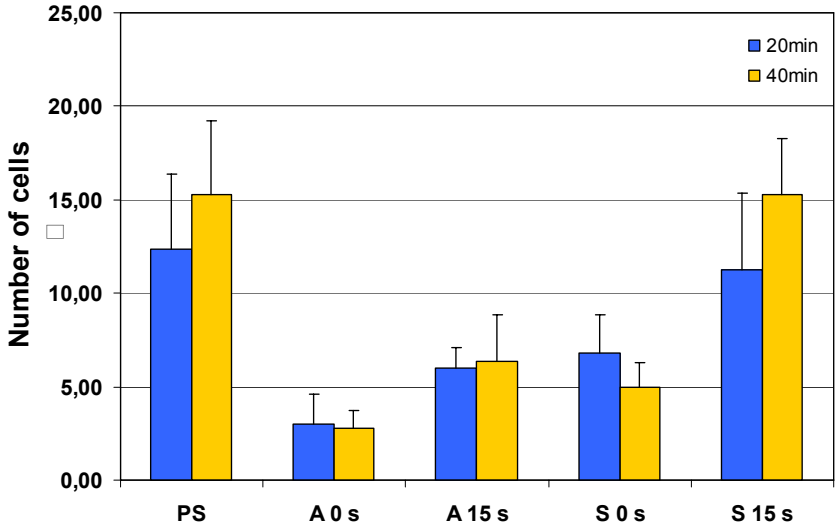

Figure 40 Number of adherent fibroblast cells on virgin and oxygen plasma treated amorphous (A) and semicrystalline (S) PET polymers per unit surface, where PS – polystyrene (control), A 0s – untreated amorphous, A 15s - oxygen plasma treated amorphous, S 0s – untreated semicrystalline, S 15s – oxygen plasma treated semicrystalline sample.

As can be seen in Figure 41, fibroblast cells seem to be well proliferated on plasma treated surfaces. Furthermore, it can be observed that cells are more evenly spread on plasma treated semicrystalline samples (S 15s, Figure 41 (b)) compared to plasma treated amorphous samples (A 15s, Figure 41 (a)). Thus, semicrystalline surfaces seem to be more appropriate for proliferation of fibroblast cells.

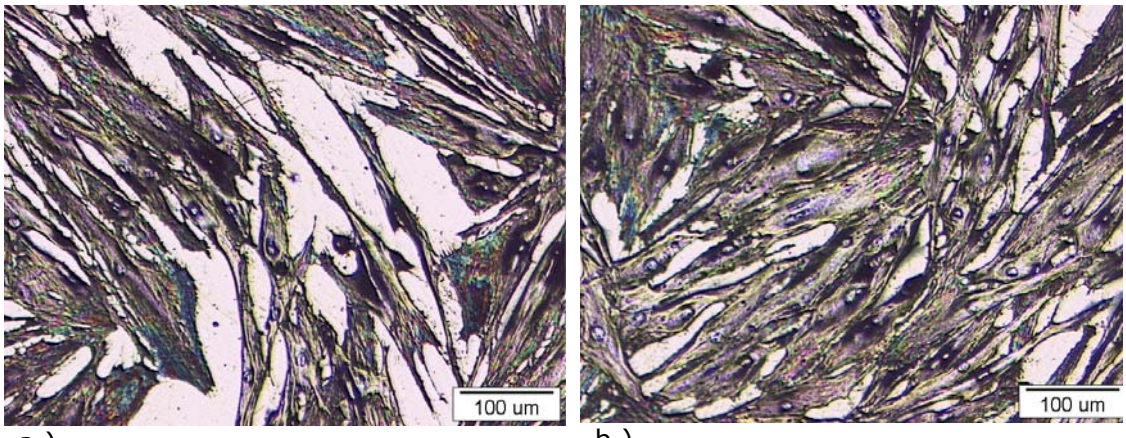

a.) b.)

Figure 41 Image of fibroblasts cultured on oxygen plasma treated PET foil from Goodfellow: (a) amorphous, (b) semicrystalline.

Morphological details of fibroblast cells were further assessed with SEM. All cells showed a high number of oriented filopodia, with orientation mainly towards the nearest cells. It can be observed from Figure 42 (a) and (c), that cells are well

spread, especially on the semicrystalline surface, which was already established from images taken by optical microscopy (Figure 42). By observing the morphology of cells under higher magnification (Figure 43 (b) and (d)) it can bee seen that cells are well spread and flattened in both samples, indicating the formation of stable adhesive contacts.

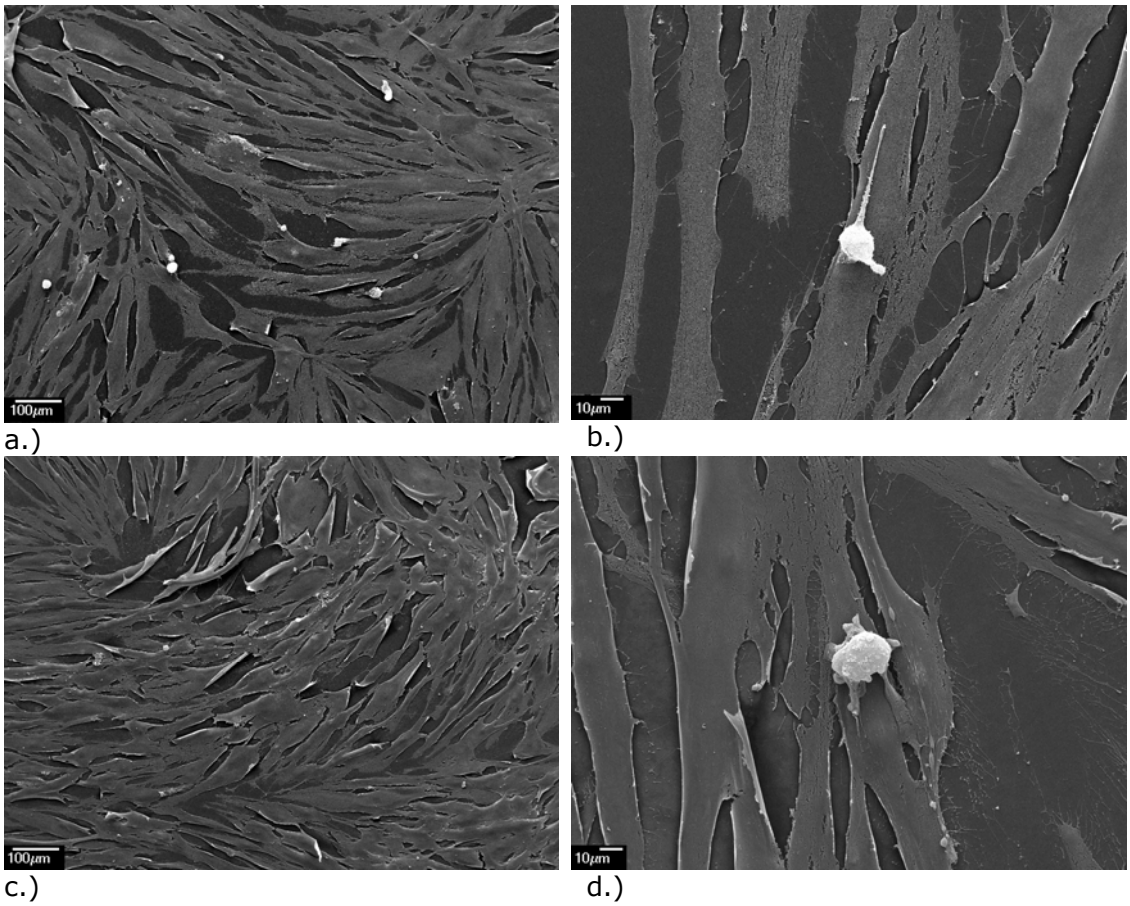

Figure 42 Image of fibroblasts cells cultured on oxygen plasma treated PET foil (a-b) amorphous and (c-d) semicrystalline.

AFM analysis was conducted to observe the morphology of fibroblast cells. The fibroblast cells measure several hundreds of micrometers, exceeding the XY-scan range of the AFM (45 µm x 45 µm), thus only small parts of fibroblast cells could be imaged. No distinctive differences between fibroblast cells cultured on different surfaces were observed. The part of fibroblast cell cultured on oxygen plasma treated semicrystalline polymer is shown in Figure 43. Long stress fibres of a fibroblast cell shown in this figure again confirm good adhesion of cell on oxygen plasma treated surfaces.

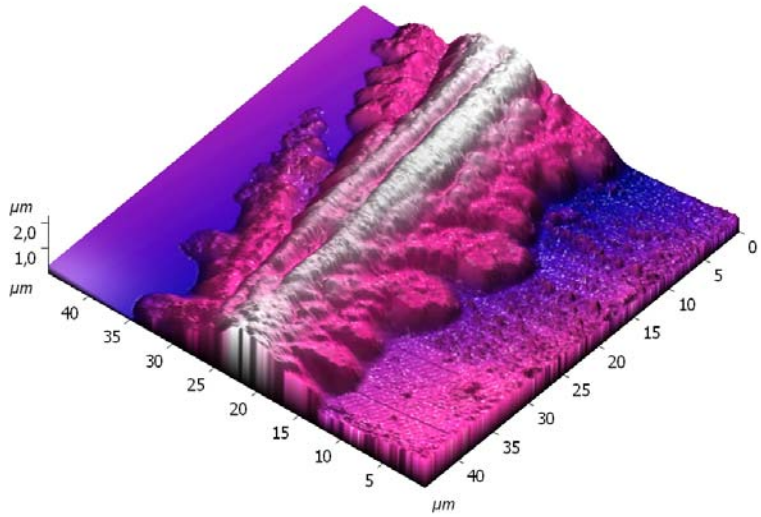

Figure 43 AFM image of fibroblast cell cultured on oxygen plasma treated semicrystalline PET (Goodfellow).

4.6. Proliferation of endothelia cells

Endothelia cell seeding is a common approach to improving hemocompatibility of vascular grafts, as endothelia cells are thought to be an ideal hemocompatible surface. It is known that only poor adhesion of endothelia cells has been achieved for PET and PTFE vascular grafts. Therefore, an improved adhesion and proliferation of endothelia cells on vascular grafts is desired. In order to asses how oxygen and nitrogen plasma treatment affect the adhesion of endothelia cells on a PET polymer, an MTS assay was employed. Figure 44 shows the measured absorbance, which is directly proportional to viability of endothelia cells, cultured on different samples. These results show that proliferation of endothelia cells is improved on all plasma treated surfaces, which is in accordance with the results published in the literature (Chen et al., 2003, Ramires et al., 2000). Improved proliferation of cells can be attributed to newly formed functional groups (oxygen and nitrogen) introduced after short plasma treatment time (3 s), as well as to higher hydrophilicity of the surface, surface morphology etc. It seems that longer treatment time (longer than 30 s) by oxygen plasma is more affective in promoting endothelia cell attachment than nitrogen plasma. However, these differences are not significant and could as well be attributed to an experimental error, thus no correlation with surface properties can be obtained.

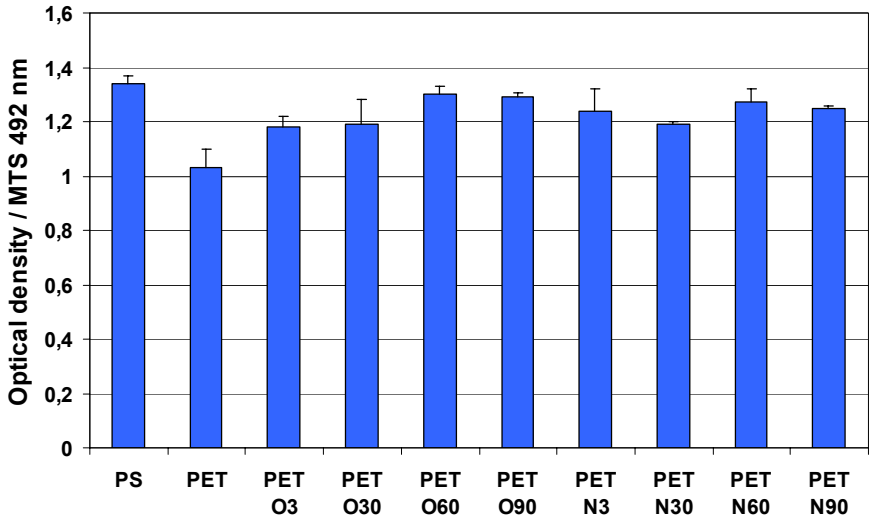

Figure 44 Viability of endothelia cells (HUVEC) cultured on surfaces treated by oxygen and nitrogen plasma for different treatment times.

Interestingly, the results of the MTS assay done on amorphous and semicrystalline PET foils (Figure 45) show more pronounced changes in cell viability, compared to the previous results (Figure 44). After 15 s of oxygen plasma treatment, both amorphous and semicrystalline surfaces exhibited higher viability of endothelia cells. Treatment in nitrogen plasma did not show practically any change compared to the untreated surface; according to the MTS assay there was even a small decrease of viable cells, especially on the amorphous polymer. Of particular interest is also the observation that cells proliferate better on semicrystalline polymers, especially on oxygen plasma treated surfaces, where cell density was even higher than on polystyrene (negative control).

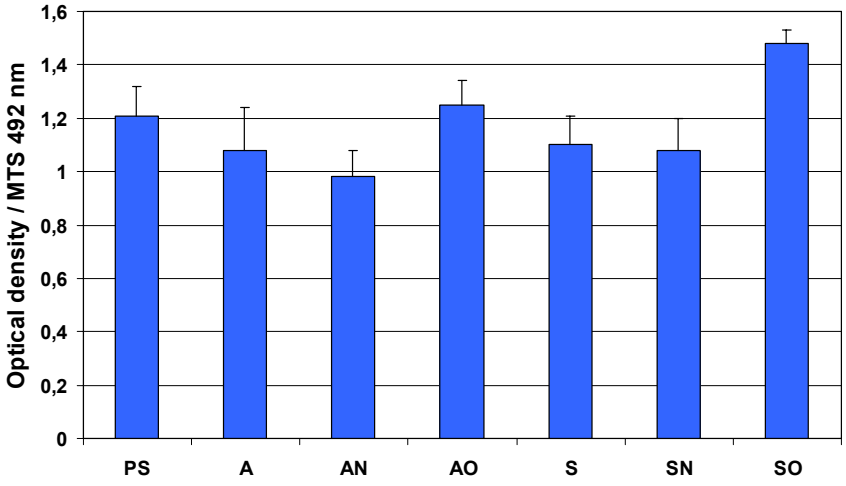

Figure 45 Viability of endothelia cells (HUVEC) cultured on untreated amorphous (A) and semicrystalline (S) surfaces, amorphous (AO) and semicrystalline surfaces treated by oxygen and amorphous (AN) and semicrystalline (SN) surfaces treated by nitrogen plasma for 15 s.

Proliferation of endothelia cells was evaluated also by counting the number of adhered cells per surface area from images taken by optical microscopy (Figure 46). These results show a similar trend was determined by the MTS assay (Figure 45). The number of cells increased on oxygen plasma treated surfaces, while no significant changes were observed on nitrogen plasma treated surfaces. The improved proliferation of endothelia cells on oxygen plasma treated surfaces could be attributed to oxygen incorporated functionalities, which are known to promote cell proliferation (Mooradian et al., 1992).

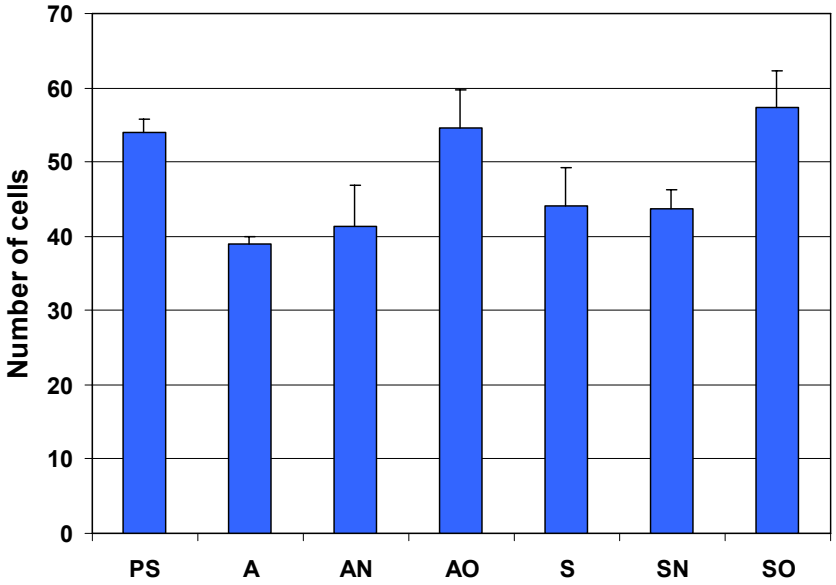

Figure 46 Number of attached endothelia cells (HUVEC) cultured on untreated amorphous (A) and semicrystalline (S) surfaces, amorphous (AO) and semicrystalline surfaces treated by oxygen and amorphous (AN) and semicrystalline (SN) surfaces treated by nitrogen plasma for 15 s.

Thus the higher proliferation on semicrystalline polymers treated in oxygen plasma may to some extent be attributed to higher O/C ratio (O/C ratio was 0.76) in comparison to amorphous polymer (O/C ratio was 0.68) as was observed from XPS analysis (Chapter 4.1.). However, other surface parameters could also affect proliferation, among these is the degree of crystalline fraction, which is much higher for semicrystalline polymers.

The results of endothelia cell proliferation on nitrogen plasma treated surfaces are surprising, as the literature reports that nitrogen functionalities are more effective in promoting cell attachment than oxygen. As this was not observed on amorphous or semicrystalline polymers (Figures 45 and 46) and as it also was not observed on semicrystalline polymers (Du Pont) treated for different exposure times (Figure 44), it could be assumed that newly incorporated functional groups and also other

surface parameters, which are obtained during plasma treatment, could affect cell response.

4.7. Adhesion of platelets

Hemocompatibility of plasma modified surfaces under *in vitro* conditions was assessed by an MTS test and by counting the number of adherent platelets and characterising their morphology. The statistical analysis of platelets interacting with the surface was done from the SEM images, while the morphology of cells was categorised according to Goodman (see Chapter 1.1.2.2.), whereby platelets were put in five groups ranging from lower to higher level of activation. The analysis of platelet morphology was also conducted with AFM to observe the differences between non-activated and activated platelets.

4.7.1. Oxygen and nitrogen plasma treatment

Fresh whole blood (212 $\cdot 10^9$ platelets/ l) was incubated for 1 h with oxygen and nitrogen plasma treated polymers and with untreated polymers. The samples were prepared according to the procedure described in Chapter 3.2.4.3. Observable differences in the number of adherent platelets and their shape can be seen in Figure 47. The number of adherent platelets decreased dramatically on oxygen plasma treated surfaces; as can be seen from Figure 47 (d) after only 3 s of oxygen plasma treatment, a lower number of platelets was observed. After 90 s of oxygen plasma treatment (Figure 47 (e)) virtually no platelets were observed, while those that did adhere seemed to be in a more round form, which is thought to be attributed to low platelet activity. On the contrary there were many aggregated platelets on untreated (Figure 47 (a)) and nitrogen plasma treated surfaces (Figures 47 (b) and (d)). Fibrin formation was also observed on these surfaces, especially on the untreated surface and the surface treated for 90 s in nitrogen plasma. The platelets on the untreated polymer surface are mostly in well spread form and start to aggregate. Nitrogen plasma treatment seems to actually promote platelet activation and spreading; after 3 s of treatment platelets were mostly in fully spread form (Figure 47 (b)), while after 90 s platelets were fully spread and aggregated (Figure 47 (d)).

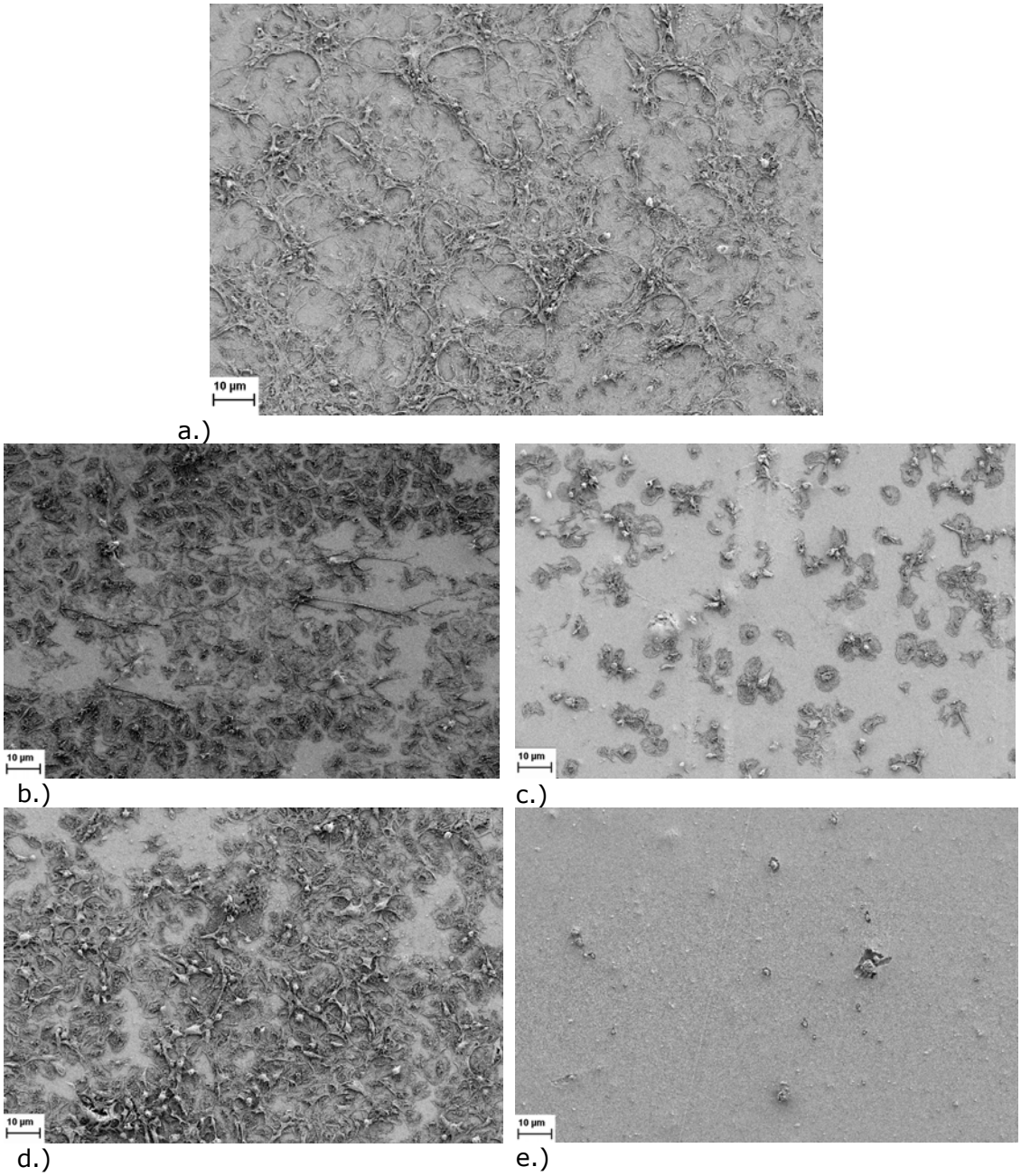

Figure 47 SEM images of platelets interacting with: a.) untreated (PET) b.) 3 s nitrogen plasma treated (PET N3), c.) 3 s oxygen plasma treated (PET O3), d.) 90 s nitrogen plasma treated (PET N90), e.) 90 s oxygen plasma treated (PET O90) surface of PET foils.

The number of adherent platelets was determined from SEM images and is presented in Figure 48. It can be seen that less platelets adhered on oxygen plasma treated surfaces, while no significant changes in the number of platelets were observed on nitrogen plasma treated surfaces. This could be attributed to higher wettability of oxygen plasma treated surfaces as well as to the incorporation of oxygen functional groups. The former might be more important, as the change in wettability between oxygen and nitrogen plasma treated surfaces is not as

significant. However, increased oxygen concentration has been reported to reduce coagulation activation (Grunkemeier et al., 1998, Tyan et al., 2002). Moreover, reduction in platelet adhesion was observed also on -OH terminated SAM surfaces (Tsai et al., 2007, Sperling et al., 2005). Thus incorporation of oxygen functional groups during oxygen plasma treatment could be an important parameter, which influences platelet adhesion on PET polymer surfaces. Nevertheless, other surface parameters probably have an important role in platelet adhesion, as there have been many attempts where radical changes in surface chemistry did not yield any significant differences in platelet adhesion (Sefton et al., 2001).

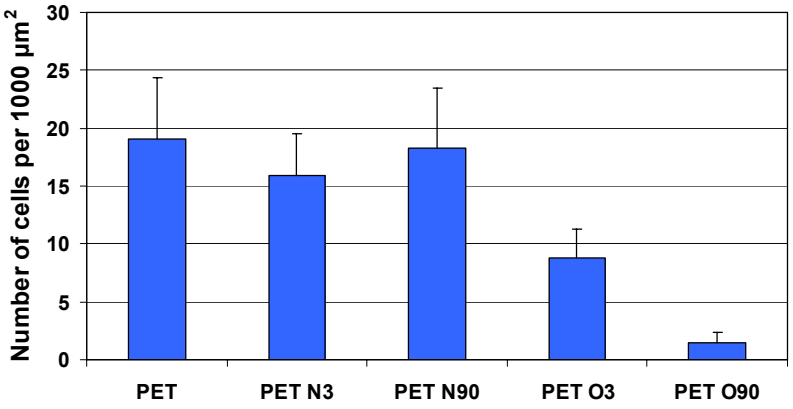

Figure 48 Number of platelets interacting with untreated and plasma treated semicrystalline PET (Du Pont) surfaces.

Similar results were also obtained from the MTS assay, as the number of metabolically active platelets decreased on oxygen plasma treated surfaces (Figure 49). This could be correlated with lower adhesion of platelets onto oxygen plasma treated surfaces. However, these results do not show significant differences from those observed from SEM analysis. The reason for this could be, that the results of the MTS assay also include platelets adhering on the surface of polystyrene wells (used for the MTS assay), as well as other metabolically active cells in blood, like leucocytes and erythrocytes. Thus, only SEM was employed for further analysis to assess the number and activity of platelets.

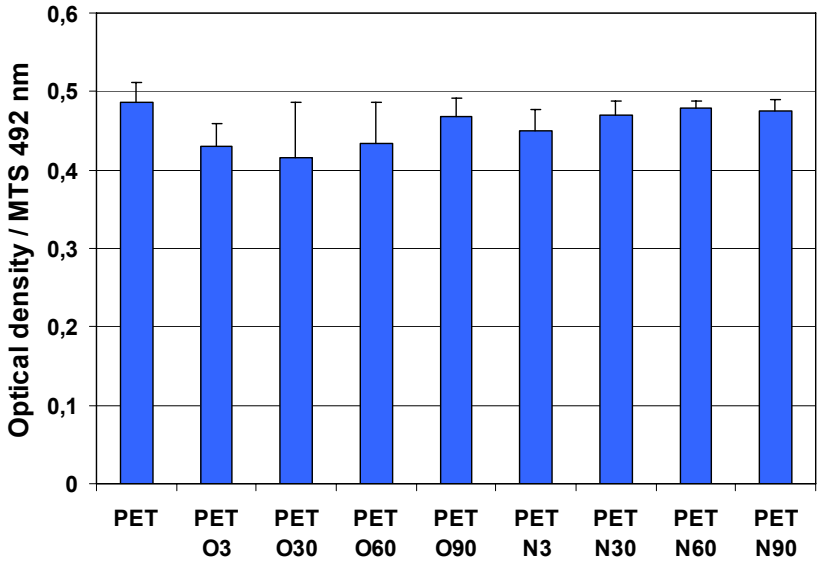

Figure 49 Cell metabolic activity by MTS assay on untreated samples and on samples treated in oxygen and nitrogen plasma.

4.7.2. Amorphous and semicrystalline PET polymers

In order to observe how the degree of crystallinity in PET polymers affects the adhesion of platelets, fresh whole blood (198 $\cdot 10^9$ platelets/l) was incubated with untreated and with 15 s of oxygen plasma treated amorphous and semicrystalline PET polymers (Goodfellow). Unexpectedly, the SEM analysis shows a significant difference in adhesion of platelets between amorphous and semicrystalline surfaces (Figure 50). These differences were already significant on untreated PET surfaces with different degrees of crystalline fraction (Figures 50 (a) and (b)). The amorphous surface seems to promote platelet adhesion, activation, spreading and aggregation; while the semicrystalline surface reduces platelet adhesion. Treatment in nitrogen plasma clearly promotes platelet adhesion, as the number of platelets increased on the nitrogen plasma treated semicrystalline polymer compared to the untreated polymer (Figures 50 (b) and (d)). Although the changes between untreated and nitrogen plasma treated amorphous polymer were not as significant, the morphology of platelets was altered. On the nitrogen plasma treated surface, a higher number of platelets was in a fully spread form, and even some leukocyte adhesion to these surfaces was observed, which may also contribute to the thrombogenicity of the surface. Leucocytes may release tissue factor expression and platelet stimuli as thromboxane and platelet activating factor (Toes et al., 1999), which leads to thrombogenic response.

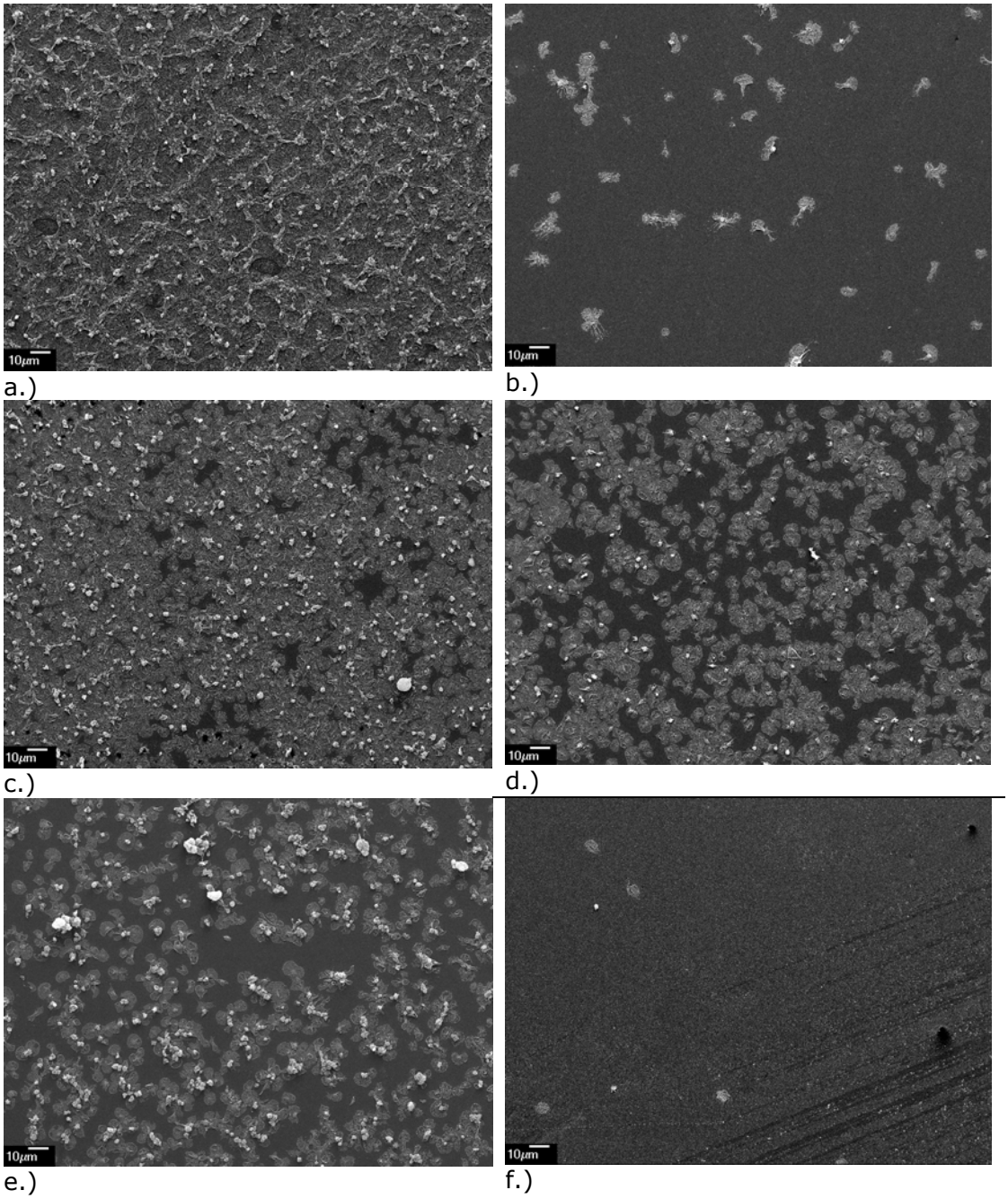

Figure 50 SEM images of platelets interacting with: a.) untreated amorphous (A), b.) untreated semicrystalline (S), c.) nitrogen plasma treated amorphous (AN), d.) nitrogen plasma treated semicrystalline (SN), e.) oxygen plasma treated amorphous (AO) and f.) oxygen plasma treated semicrystalline (SO) PET foils.

Treatment of the amorphous polymer in oxygen plasma reduced the number of platelets, their coverage and aggregation (Figure 50 (e)). It is also important to note, that fibrin formation on these surfaces is practically not observed, while notable fibrin formation is observed on the untreated amorphous polymer. Oxygen treatment of semicrystalline polymer seems to reduce platelet adhesion, as practically no platelets on these surfaces were observed. These results are in

accordance with those done on semicrystalline polymer (Du Pont), where oxygen plasma treatment was found to reduce platelet adhesion (Figure 47).

By analysing the number of adhered platelets from SEM images one can observe (Figure 51) that this number is much lower for oxygen plasma treated surfaces and that significant differences can be noted between amorphous and semicrystalline polymers. Intesting is also the observation that higher platelet adhesion is obtained on semicrystalline surfaces treated in nitrogen plasma than on untreated semicrystalline surfaces. While nitrogen plasma treatment of the amorphous surface seems to reduce platelet adhesion compared to the untreated amorphous sample, although not significantly. Thus, according to these results, the main driving force for platelet adhesion could be attributed to surface crystallinity and surface chemistry.

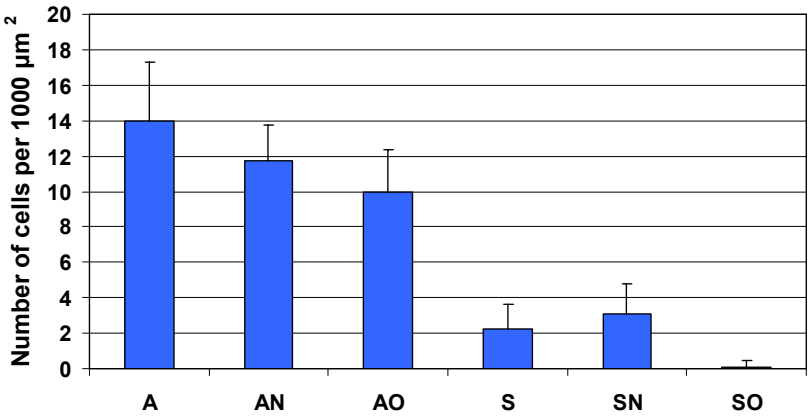

Figure 51 Number of platelets interacting with untreated and plasma treated amorphous and semicrystalline surfaces.

One could argue that lower platelet adhesion to semicrystalline surfaces could be attributed to embedded silica additives in the semicrystalline polymer, which have height of about 50 nm. Although these features could not contribute to higher surface area for platelet adhesion, as the size of platelets is more than 3 µm, these features could have an influence on protein adsorption, their configuration and thus also cell response. However, this still seems to be unlikely, as the semicrystalline polymers from Du Pont showed similar platelet adhesion, while no embedded silica additives were observed on their surface (according to the AFM analysis of PET foils from Du Pont – Chapter 4.2.1.), which would increase its surface area. It is also important to note, that all PET polymers have embedded silica particles, as they are commonly added to increase surface roughness of PET foils.
Surface wettability in this case is also not a decisive factor, as the wettability of the amorphous and semicrystalline polymer is practically the same (WCA is 17 and 13 degrees for amorphous and semicrystalline respectively).

As mentioned above, more importance should be ascribed to the degree of crystalline fraction, as amorphous polymers practically have no crystalline domains (results from DSC analysis – Chapter 4.3.). It could be assumed that a higher degree of crystalline fraction decreases molecular mobility of polymer chains, which could affect the adsorption kinetics of proteins and cells onto the surface. This could also be in agreement with the results obtained from semicrystalline PET foils from Du Pont, where oxygen plasma treatment provides the surfaces with a higher crystalline fraction than nitrogen plasma treatment. This can be further confirmed by the ageing studies; as the surfaces treated in nitrogen plasma age faster than those treated in oxygen plasma. This means that surface molecular mobility on nitrogen plasma treated surfaces is higher due to lower surface crystallinity.

As regards lower platelet adhesion on oxygen plasma treated surfaces, it could be said that oxygen functionalities probably reduce platelet adhesion on PET polymers. However, it should be noted that the decrease in platelet adhesion onto amorphous polymers treated in oxygen plasma was limited; this could be influenced by the degree of surface crystallinity. This could also be one of the reasons why there are so many disputing results regarding different surface parameters and their influence on blood compatibility. The effects of different surface parameters should probably be observed in a wider scope, as their effects could be synergistic.

4.7.3. Different treatment time in oxygen plasma

The samples were treated from 3 to 90 s in oxygen plasma, to further confirm whether different treatment times of semicrystalline polymers (Du Pont) with oxygen plasma affects platelet adhesion. After treatment, the polymers were incubated with platelet rich plasma (PRP), which was diluted to reach $176 \cdot 10^9$ platelets/l (see Chapter 3.2.4.4.). In Figure 52 SEM images of platelets interacting with the surface are presented.

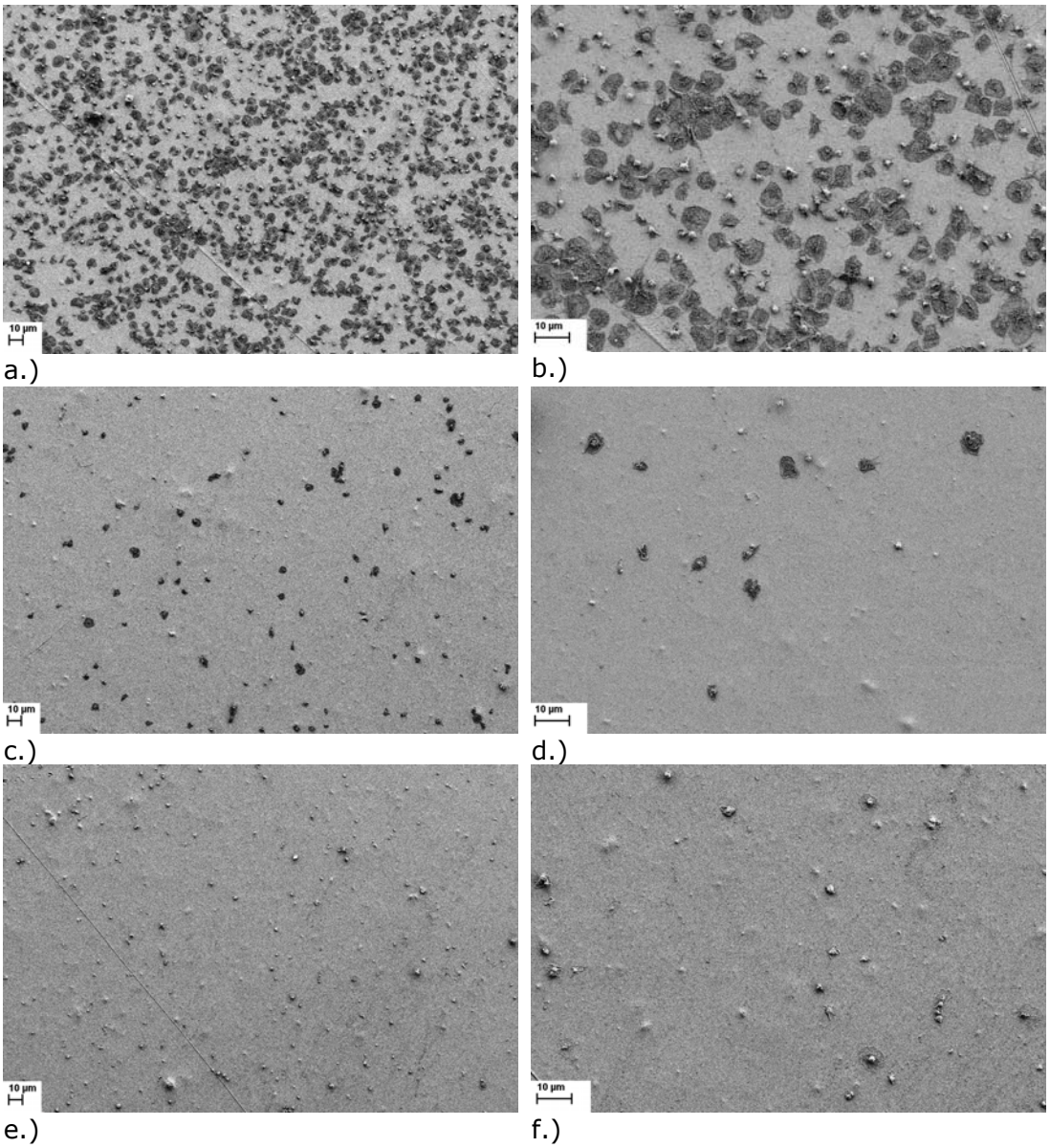

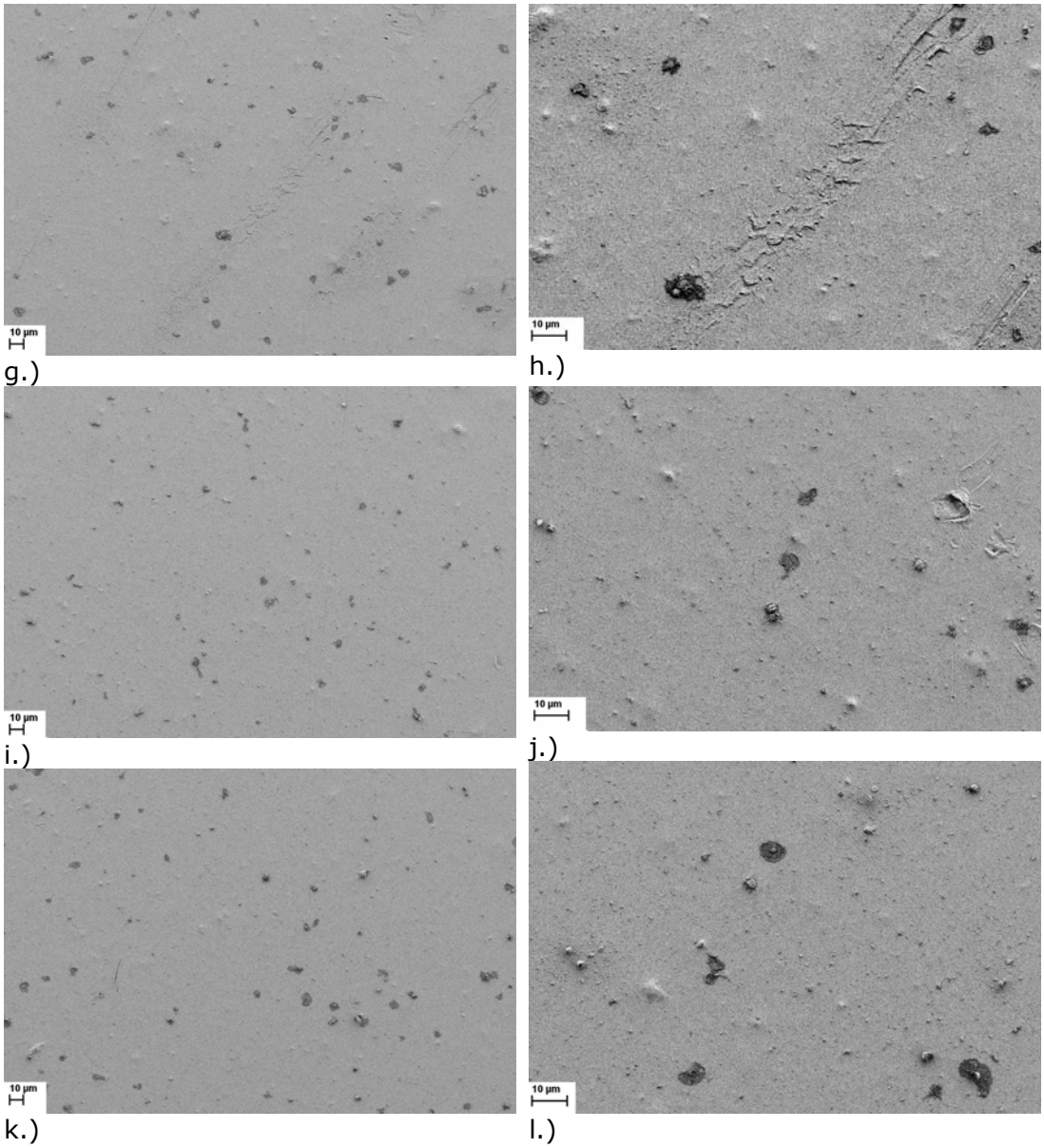

Figure 52 SEM images of platelets interacting with: a.-b.) untreated, c.-d.) 3 s oxygen plasma treated e.-f.) 10 s oxygen plasma treated g.-h.) 30 s oxygen plasma treated, i.-j.) 60 s oxygen plasma treated and k.-l.) 90 s oxygen plasma treated PET foils.

Again, it can be observed that the number of platelets and their activation is highest on the untreated surface (Figures 52 (a) and (b)), as most of platelets were in activated form (spreading or fully spread) and some were aggregating. A significant reduction in the number of adherent platelets was observed even after a short plasma treatment time (3 s). The platelets adhering onto plasma treated surfaces are mostly in a fully spread form, regardless of the treatment time. However, the platelet-platelet interactions (aggregation) on oxygen plasma treated surfaces were not observed, probably due to the low number of adherent platelets. This could mean that although platelets are in fully spread form, the activation of

coagulation would not be initiated. Interestingly, Hunt et al. (Hunt et al., 1997) found that a majority of hydrophobic surfaces cause most activation of platelets yet least activation of coagulation. In the present case, activated platelets were also found on hydrophilic surfaces, but according to Hunt et al., it is not necessary that platelet activation would also lead to coagulation.

In order to observe the difference in morphology between activated and non-activated platelets an AFM analysis was conducted. This method was only employed to distinguish the morphological changes between platelets, as due to the small analysing area of AFM (45 µm x 45 µm), the statistical analysis of activated and non-activated platelets on different surfaces would not be representative. In Figure 53, the difference in platelet morphology can clearly be seen. In Figures 53 a) and b) the height and phase image of round, non-activated platelet can be seen. In this case the platelet is round with no pseudopodia, while the examples of activated platelets can be seen in Figures 53 c) - f). In Figure 53 c) and d) the platelet is in a spread-dendritic form, as the pseudopodia can be clearly seen from both the height and phase image. The next phase of platelate activation can be seen from the height and phase image in Figures 53 e) and f), in these figures the platelate is in a spread form with late pseudopodia and, according to Goodman (Goodman et al.; 2006), this is one of the last phases of platelate activation (the last phase is a fully spread platelate).

Height **Phase**

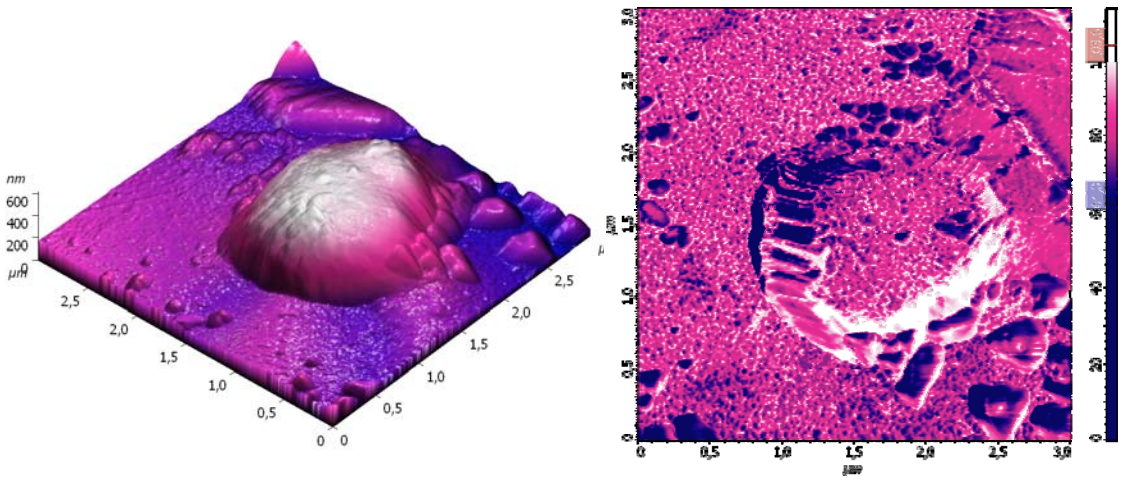

a.) b.)

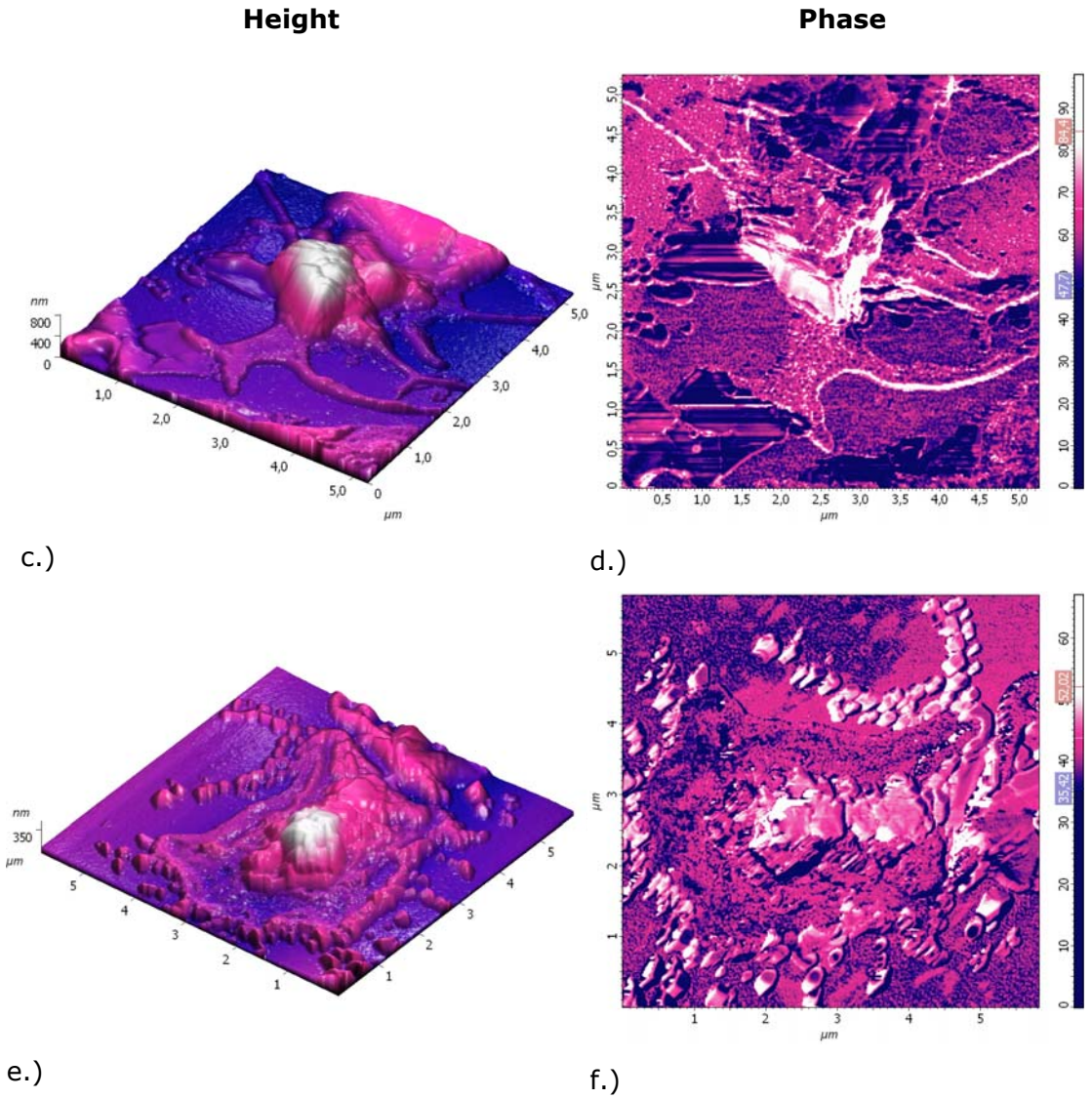

Figure 53 The AFM height and phase image of a.) and b.) non-activated platelet, c.) and d.) dendritic platelate with late pseudopodia, e.) and f.) spread platelate on untreated PET surface (Du Pont) incubated with PRP.

The statistical analysis of platelets adhering onto the surface, obtained from SEM images, is presented in Figure 54. It can be observed that following oxygen plasma treatment, platelet adhesion was significantly reduced on all surfaces, regardless of the treatment time. However, the reduction of platelet adhesion was highest on PET surfaces treated for 30 s and lowest on those treated for 10 s.

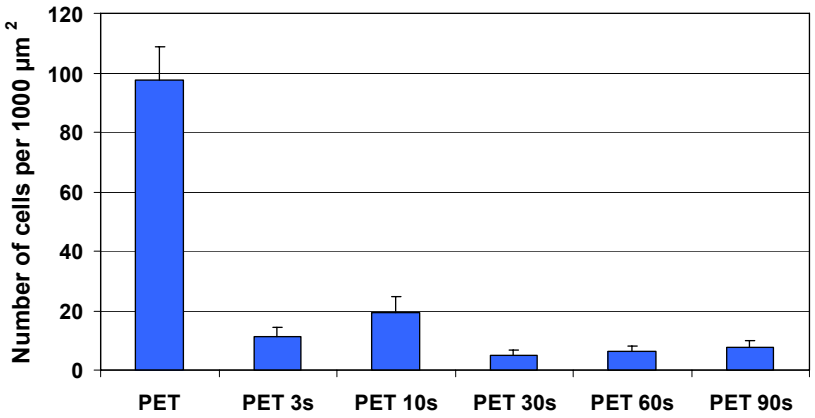

Figure 54 Number of platelets interacting with untreated and oxygen plasma treated surfaces.

These results indicate that even a short exposure of PET polymer to oxygen plasma would reduce platelet adhesion. Again, this could be attributed to the incorporation of oxygen functional groups, which is fairly achieved already after 3 s of treatment (see the XPS results, Chapter 5.1.). If we look at Figure 55 a good correlation between oxygen concentration and the number of adherent platelates can be seen. It seems that a higher O/C ratio would lead to lower platelet adhesion.

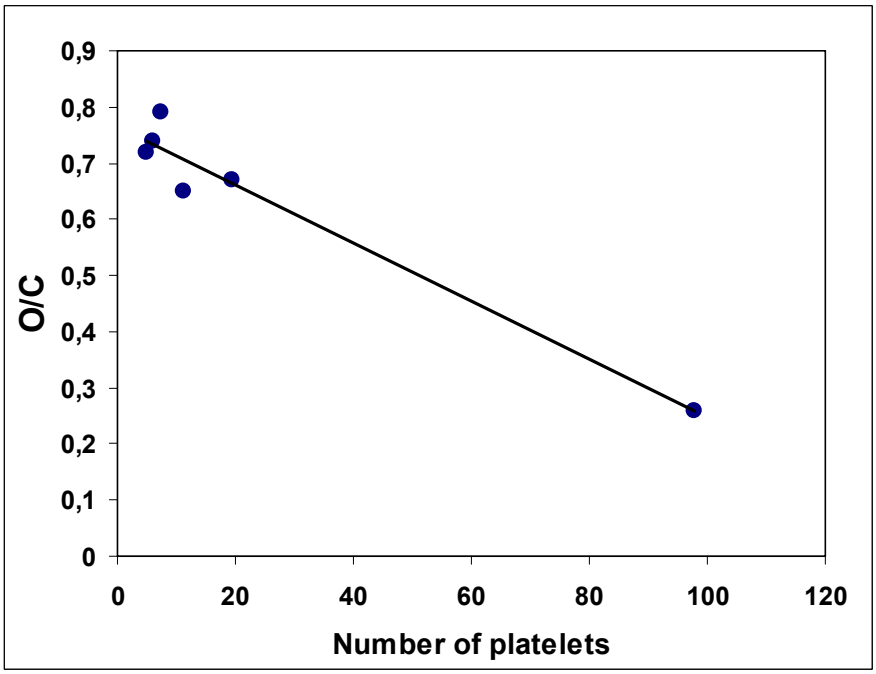

Figure 55 The number of adherent platelets with respect to O/C ratio.

The lowest platelet adhesion was observed on surfaces treated for longer than 30 s, where also a more pronounced increase in O/C ratio was observed. For 3 s and 10 s of treatment time the O/C ratio was 0.65 and 0.67 respectively, while after 30 s the O/C ratio increased to 0.72. Although, this still does not explain the high number of adherent platelets on surfaces treated in plasma for 10 s. Interestingly,

it has been shown by Sperling et al. (Sperling et al., 2005), that different oxygen functionalities have different effects on platelet adhesion. Thus it has been shown that –OH terminated SAM exhibit lower platelet adhesion, while platelet adhesion onto –COOH terminated SAM is not reduced. From the XPS analysis it is possible to determine the concentration of C-O and O-C=O groups, but unfortunately, the concentration of C-O can be attributed to C-OH as well as C-O-C groups, while the concentration of O-C=O groups can be attributed to -COOH as well as O-C=O-C. Thus, it is not possible to propose a correlation between these functional groups and the adhesion of platelets.

The adhesion of platelets could also be linked to surface topography, as noticeable changes in surface morphology were observed after 30 s of oxygen plasma treatment. By this time, the average surface roughness increased from 1.4 nm to about 3.9 nm for 10 s and 30 s treated surfaces respectively. It is also interesting to observe the formation of sphere like particles; at this point their height increased from approximately 3 nm to 13 nm and after 90 s of treatment the spheres had height of about 30 nm. Increased height could be important for protein adsorption and conformation, which would further influence cell response. Moreover, sphere like formation also results in increased surface crystallinity, as it has been established that surface morphology is altered by plasma treatment due to preferential etching of amorphous parts of the polymer. Thus, more pronounced changes in surface topography would result in higher surface crystallinity, which is thought to have an influence on biological response.

4.7.4. Dacron vascular grafts

To observe if platelet adhesion could be reduced with oxygen plasma treatment on commercial vascular grafts, the untreated and oxygen plasma treated vascular grafts were incubated with platelet rich plasma (PRP), which was diluted to reach $176 \cdot 10^9$ platelets/l (see Chapter 3.2.4.4.). Vascular grafts were treated with oxygen plasma for 30 s. It can be seen, from SEM analysis, that platelet adhesion is significantly reduced on oxygen plasma treated surfaces (Figure 56). Many highly activated and aggregated platelets were observed on untreated surfaces Figures 56 (a), (c). Moreover, a high fibrin formation was observed on these surfaces (Figure 56 (e)). On the other hand, oxygen plasma treated surfaces have significantly less adherent platelets, as can be observed form Figures 56 (b) and (d). Platelets on these surfaces are not aggregated and fibrin formation is rare and in small deposition. In Figures 56 (e) and (f) it is possible to see platelet adhering to untreated (e) and oxygen (f) plasma treated surface. It can be seen from these

figures that topography of vascular fibres is altered due to plasma treatment, as small sphere like structures are observed on the surface to which a platelet is adhered. While a very flat surface of an untreated vascular graft can be observed in Figure 56 (e). It cannot be said with certainty whether these structures have an influence on platelet adhesion, but it has been shown that reduced platelet adhesion can be achieved on PET foils as well as Dacron vascular grafts made from PET polymers.

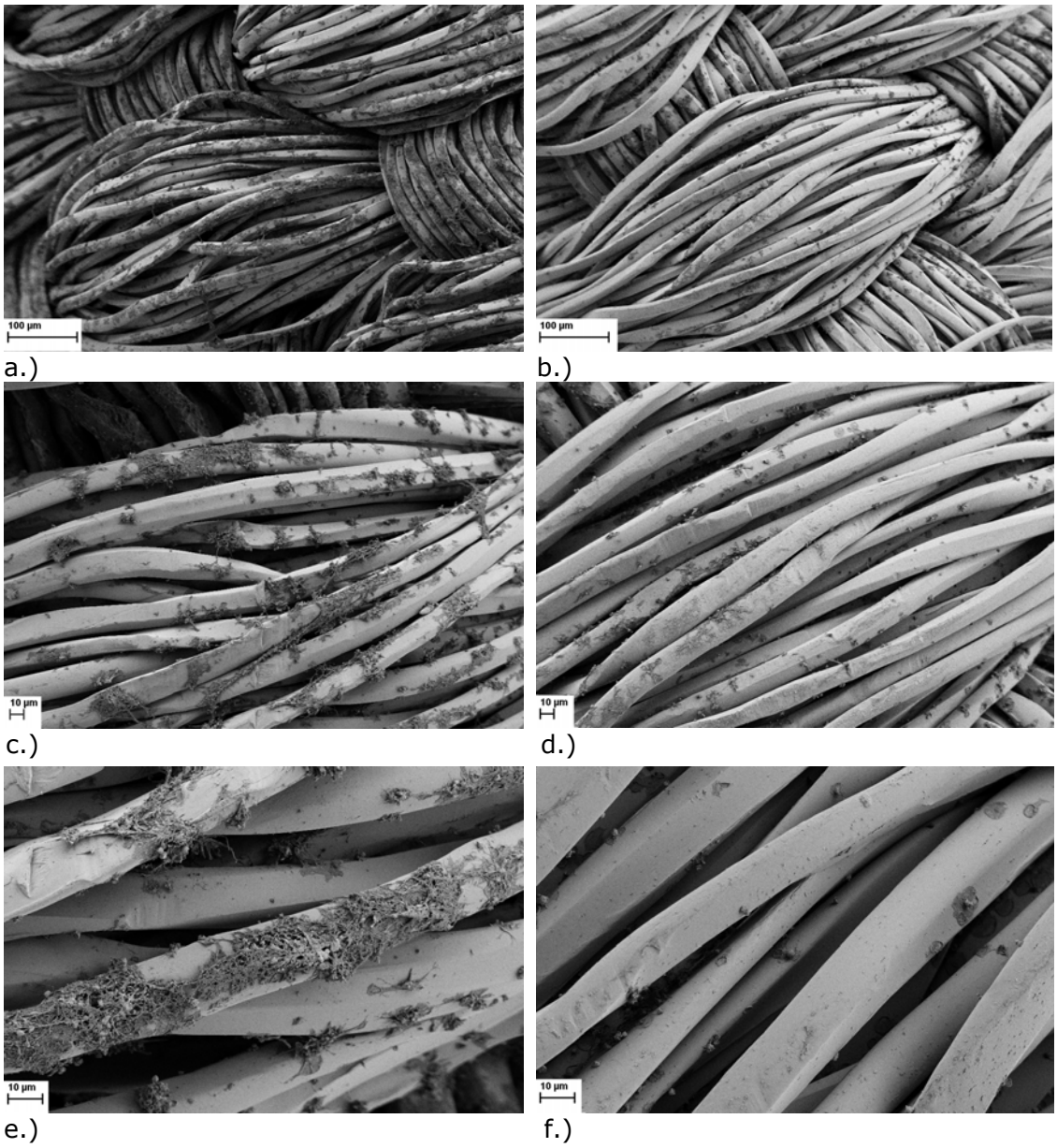

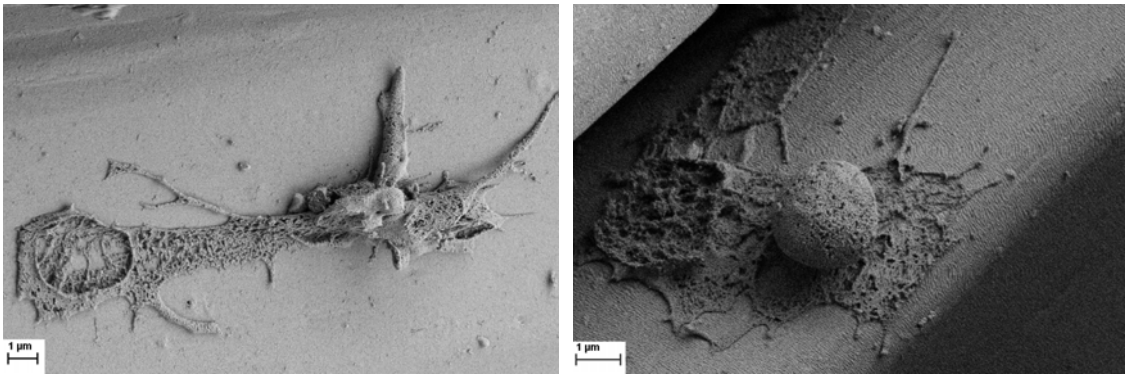

g.) h.)

Figure 56 SEM images of platelets interacting with: untreated (a), (c), (e), (g) and oxygen plasma treated (b), (d), (f), (h) Dacron vascular grafts.

5. Conclusions

The obtained results in this thesis prove that plasma treatment is a promising technique for modification of polymers for biomedical applications. By fine tuning of the discharge and plasma parameters the surface of PET polymer has been modified to such an extent that improved proliferation of endothelia cells and reduced platelet adhesion was achieved.

Most of the hypotheses presented in this work have been confirmed by the experimental results:

1. The first hypothesis regarding the possibility of tailoring surface parameters by optimising plasma treatment, has been confirmed by treating PET foils in oxygen and nitrogen plasma for different times. The surface exhibited changes in morphology, wettability, degrees of crystallinity and functional groups, depending on the employed gas and time of its treatment.

2. The second hypothesis speculating that morphological changes, caused by plasma treatment, may be carried out on a nanometre scale and may have important effects on proliferation and adhesion of cells, mostly due to different adsorption of proteins on such surfaces, has been partially confirmed. It was hard to eliminate other surface parameters which may also bring about a biological response. However, the results in this thesis, proved some connection between surface roughness and adhesion of platelets (Table 15). It seems that surfaces with higher surface roughness are more platelet repellent. However, this observation is not straightforward, mostly due to other surface properties that are altered at the same time. Therefore, further work on this issue should be undertaken.

3. The hypothesis that in plasma treatment the difference in crystalline fraction in polymers could have an influence on the interaction of plasma species with the surface, was also confirmed. The influence of plasma treatment on PET foils emanating from different manufacturers and with different degrees of crystalline fraction was examined. The most pronounced differences occurred between amorphous and semicrystalline polymers. The heating of amorphous polymers in plasma was much faster, due to different interactions of neutral atoms with the surface of amorphous and semicrystalline polymer. We detected differences in surface morphology even before plasma treatment. These differences were primarily due to different manufacturing procedure of PET foils.

4. The last, but not the least important hypothesis, that newly formed functional groups might influence biological response, has been fully confirmed by proving that better proliferation of fibroblast and endothelia cells is obtained on oxygen plasma treated surfaces, which is most probably due to incorporation of oxygen functional groups. Even more pronounced differences between oxygen and nitrogen plasma treatment were revealed from platelet adhesion studies, where a drastic decrease in the number of adhered platelets occurred on the oxygen plasma treated surfaces. This can mainly be attributed to the formation of oxygen functional groups, as other surface parameters were not so drastically altered.

To illustrate the influence of surface parameters and the adhesion of platelets onto such surfaces, the most important surface parameters together with adhesion of platelets are presented in Table 15.

Polymer		Crystallinity X_{DSC} [%]	Chemical composition O/C	N/C	WCA [degrees]	Ra [nm]	Platelet adhesion
untreated	A (Goodfellow)	**4.4**	**0.41**	**0**	**70**	**1.9**	**high**
	S (Goodfellow)	**30.6**	**0.37**	**0**	**69**	**3**	**Low**
	S (Du Pont)	**36.5**	**0.26**	**0**	**72**	**0.9**	**High**
oxygen plasma treated	A, treated 15s (Goodfellow)	/	**0.68**	**0**	**18**	**1.5**	**Low**
	S, treated 15s (Goodfellow)	/	**0.76**	**0**	**14**	**11**	**Very low**
	S, treated 30 s (Du Pont)	**increases**	**0.72**	**0**	**9**	**4.2**	**Very low**
nitrogen plasma treated	S, treated 30 s (Du Pont)	/	**0.43**	**0.23**	**18**	**2.7**	**Medium**

Table 15 The influence of platelet adhesion onto PET surfaces with different surface properties.

The above results indicate that surfaces with a high oxygen ratio (where O/C is more then 70%) are platelet repellent, as almost no platelets were observed on such surfaces. However, it can also be seen that the initial surface properties of the polymer, play an important role. It seems that the degree of crystalline fraction is also a decisive factor in provoking biological response.

Unpredictably high differences in platelet adhesion between amorphous and semicrystalline PET foils from Goodfellow have been detected. Namely, a substantially lower number of platelets adhered on semicrystalline polymers. This effect could also be important for plasma treatment of polymers, as the degree of crystalline fraction actually increases after oxygen plasma treatment. It could be suggested that surfaces with higher degrees of surface crystallinity have a reduced

mobility of functional groups, thus their surface configuration in not likely to undergo any significant changes when such surfaces come into contact with blood plasma. Therefore, the stability of the surface may also have an important impact on the extent of the initial adsorption of plasma proteins and their conformational changes influencing cellular interactions.

The stability of oxygen plasma treated surfaces was examined by the ageing experiments, as the ageing effects were not so pronounced as in nitrogen plasma treated surfaces. Furthermore, the differences between ageing of amorphous and semicrystalline surface were examined; the ageing of oxygen plasma treated semicrystalline PET foil was less pronounced than that of amorphous PET foil. The crystalline fraction in polymers and their influence on adhesion of platelets was one of the parameters, which we did not focus on in this work and should be given more attention in the future.

6. References

d'Agostino, R.; Cramarossa F.; and Fracassi, F.; *Plasma Deposition, Treatment and Etching of Polymers* (Academic Press, New York, 1990).

Allender, S.; Scarborough, P.; Peto, V.; Rayner, M., *European heart disease statistics* (British Heart Foundation, London, 2008).

Babic, D.; Poberaj, I.; Mozetic, M.; Fiber optic catalytic probe for weakly ionized oxygen plasma characterization. *Review of Scientific Instruments* **72**, 4110 (2001).

Barral, X.; Gay, J. L.; Favre, J. P.; Gournier, J. P.; Do collagen-impregnated knitted Dacron grafts reduce the need for transfusion in infrarenal aortic reconstruction? *Annals of Vascular Surgery* **9**, 339 (1995).

Beamson, G.; Briggs, D.; (ed). High *Resolution XPS of Organic Polymers – The Scienta ESCA300 Database.* (Wiley, Chichester, 1992).

Björck, C. G.; Bergquist, D.; Glimaker, H.; Hallstensson, S.; Increased thrombogenicity after polymer coating: Experiences with the first version of a new woven Dacron graft for aortic reconstruction. *European Journal of Surgery, Acta Chirurgica* **160**, 9 (1994).

Blajchman, M. A.; Ozge-Anwar, A. H.; The role of the complement system in hemostasis. *Progress in Hematology* **14**, 149 (1986).

Boeuf, J. P.; Pitchford L. C.; Calculated characteristics of an arc plasma display panel cell. *IEEE Transactions on Plasma Science* **24**, 95 (1996).

Borcia, G.; Anderson, C. A.; Brown, N. M. D. C.; Dielectric barrier discharge for surface treatment: Application to selected polymers in film and fibre form. *Plasma Sources Science Technology* **12,** 335 (2003).

Brandon, S.; Haimovich, N.; Yeger, E.; Marmur, A.; Partial wetting of chemically patterned surfaces: The effect of drop size. *Journal of Colloid Interface Scence* **263**, 237 (2003).

Bruck, S. D.; Interactions of synthetic and natural surface with blood in the physiological environment. *Biomedical Materials Research Symposium* **8**, 1 (1977).

Burridge, K.; Chrzanowska-Wodnicka, M.; Focal adhesions, contractility, and signaling. *Annual Review of Cell and Developmental Biology* **12**, 3745 (1996).

Busscher, H. J.; van Pelt, A. W. J.; de Boer, P.; de Jang, H. P.; Arends, J.; The effect of surface roughening of polymers on measured contact angles of liquids. *Journal of Colloid Surface* **9**, 319 (1984).

Buttiglione, M.; Vitiello, F.; Sardella, E.; Petrone, L.; Nardulli, M.; Favia, P.; d'Agostino, R.; Gristina, R.; Behaviour of SH-SY5Y neuroblastoma cell line grown in different media and on different chemically modified substrates. *Biomaterials* **28**, 2932 (2007).

Callow, A. D.; Problems in the construction of a small diameter graft. *International Angiology* **7**, 246 (1988).

Chan, C. M.; Ko, T. M.; Hiraoka, H.; Polymer surface modification by plasmas and photons. *Surface Science Reports* **24**, 1 (1996).

Chandy, T.; Das, G. S.; Wilson, R. F.; Rao, G. H. R.; Use of plasma glow for surface-engineering biomolecules to enhance bloodcompatibility of Dacron and PTFE vascular prosthesis. *Biomaterials* **21**, 699 (2000).

Charpentier, P. A.; Maguire, A.; Wan, W. K.; Surface modification of polyester to produce a bacterial cellulose-based vascular prosthetic device. *Applied Surface Science* **252**, 6360 (2006).

Chen, M.; Zamora, P. O.; Som, P.; Pena, L. A.; Osaki, S.; Cell attachment and biocompatibility of polytetrafluoroethylene (PTFE) treated with glow-discharge plasma of mixed ammonia and oxygen. *Journal of Biomaterial Science Polymer Edition 14* **9**, 917 (2003).

Chevallier, P:, Castonguay, M.; Turgeon, S.; Dubrulle, N.; Mantovani, D.; McBreen, P. H.; Wittmann, J. C.; Laroche, G.; Ammonia RF - Plasma on PTFE surfaces: Chemical characterization of the species created on the surface by vapor - Phase chemical derivatization. *Journal of Physical Chemistry B* **105**, 12490 (2001).

Li, C. I.; Tu, C. Y.; Huang, J. S.; Liu, Y. L.; Lee, K. R.; Ali, J. Y.; Surface modification and adhesion improvement of expanded poly(tetrafluoroethylene) films by plasma graft polymerization. *Surface and coatings Technology* **201**, 63 (2006).

Choee, J. H.; Lee, S. J.; Rhee, Y. M.; Lee, H. B.; Khang, G.; Proliferation rate of fibroblast cells on polyethylene surfaces with wettability gradient. *Journal of Applied Polymer Science* **92**, 599 (2004).

Chu, P. K.; Chen, J. Y.; Wang, L. P.; Huang, N.; Plasma- surface modification of biomaterials. *Material Science Engineering R* **36**, 143 (2002).

Coen, M. C.; Lehmann, R.; Groening, P.; Schlapbach, L.; Modification of the micro- and nanotopography of several polymers by plasma treatments. *Applied Surface Science* **207**, 276 (2003).

Cook, J. G.; (ed). *Handbook of textile fibres, Man made fibres.* (Woodhead Publishing Limited, Cambridge, 2009)

Cui, N. Y.; Brown, N. M. D.; Modification of the surface properties of a polypropylene (PP) film using an air dielectric barrier discharge plasma *Applied Surface Science* **189**, 31 (2002).

Curtis, A.; Wilkinson, C.; New depths in cell behaviour: reactions of cells to nanotopography. *Biochemical Society Symposia* **65**, 15 (1999).

Curtis, A.; Wilkinson, C.; Topographical control of cells. *Trends in Biotechnology* **19**, 97 (2001).

Dalby, M. J.; Riehle, M. O.; Johnstone, H.; Affrossman, S.; Curtis, A. S. G.; In Vitro Reaction of Endothelial Cells To Polymer Demixed Nanotopography. *Biomaterials* **23**, 2945 (2002).

Dalby, M. J.; Riehle, M. O.; Yarwood, S. J.; Wilkinson, C. D. W.; Curtis, A. S. G.; Nucleus alignment and cell signaling in fibroblasts: Response to a micro-grooved topography. *Experimental Cell Research* **284**, 274 (2003).

Dardik, I.; Dardik, H.; Vascular heterograft: human umbilical cord vein as an aortic substitute in baboon. A preliminary report. *Journal of Medical Primatology* **2**, 296 (1973).

De Geyter, N.; Morent, R.; Leys, C.; Penetration of a dielectric barrier discharge plasma into textile structures at medium pressure. *Plasma Sources Science and Technology* **15**, 78 (2006).

Dee, K. C.; Puelo, D. A.; Bizius, R.; *An introduction to tissue-biomaterial interactions* (Hoboken, John Wiley & Sons, New Jersey, 2002).

Deslandes, Y.; Pleizier, G.; Poiré, E.; Sapieha, S.; Wertheimer, M. R.; Sacher, E.; The surface modification of pure cellulose paper induced by low-pressure nitrogen plasma treatment. *Plasmas and Polymers* **3**, 61 (1998).

Domurado, D.; Thomas, D.; Brown. G.; *A new method for producing proteic coatings*. Journal of Biomedical Material Research **9**, 109 (1975).

Donovan, T. J.; Zimmerman B.; *The effect of artificial surfaces on blood coagulability, with special reference to polyethylene.* Blood **4**, 1310 (1949).

Drury, J. K.; Ashton, T. R.; Cunningham, J. D.; Maini, R.; Pollock, J. G.; Experimental and clinical experience with a gelatin impregnated Dacron prosthesis. *Annals of vascular surgery* **5,** 542 (1987).

Eyble, E.; Griesmacher, A.; Grimm, M.; Wolner, E.; Toxic effects of aldehydes released from fixed pericardium on bovine aortic endothelial cells. *Journal of Biomedical Materials Research* **23**, 1355 (1989).

Fang, F.; Satulovsky, J.; Szleifer, I.; Kinetics of protein adsorption and desorption on surfaces with grafted polymers. *Biophysics Journal* **89**, 1516 (2005).

Faucheux, N.; Schweiss, R.; Lutzow, K.; Werner, C.; Groth, T.; Selfassembled monolayers with different terminating groups as model substrates for cell adhesion studies. *Biomaterials* **25**, 2721 (2004).

Denes, F. S.; Manolache, S.; Macromolecular plasma-chemistry: An emerging field of polymer science*. Progress in Polymer Science* **29**, 815 (2004).

Florian, A.; Cohn, L. H.; Dammin, G. J.; Collins, J. J.; Small vessel replacement with gore-tex (expanded polytetrafluoroethylene). *Archives of* Surgery **3**, 267 (1976).

Fridman, A.; *Plasma Chemistry* (Cambridge University Press, New York, 2008).

Furie, B; Furie, B. C.; The molecular basis of blood coagulation. *Cell*, **53**, 505 (1988).

Galletti, P.M.; Boretus, J.W.; Report on the consensus development conference on 'Clinical applications of biomaterials'. *Journal of Biomedical Materials Research* **17**, 589 (1983).

Gendler E.; Gendler, S.; Nimni, M. E.; Toxic reactions evoked by glutaraldehyde-fixed pericardium and cardiac valve tissue bioprosthesis. *Journal of Biomedical Materials Research* **18**, 727 (1984).

Goodman, S. L.; Scranton, V. L.; Brendzel, A. M.; Platelet responses to silicon-alloyed pyrolytic carbons. *Journal of Biomedical Materials Research Part A* **83A**, 64 (2006).

Gorbet, M. B.; Sefton, M. V.; Biomaterial-associated thrombosis: Roles of coagulation factors, complement, platelets and leukocytes. *Biomaterials* **25**, 5681 (2004).

Grace, J. M.; Gerenser, L. J.; Plasma treatment of polymers. *Journal of Display Science Technology* **24**, 305 (2003).

Griesser, H. J.; Youxian, D.; Hughes, A. E.; Gengenbach, T. R.; Mau, A. W. H.; Shallow reorientation in the surface dynamics of plasma-treated Fluorinated Ethylene Propylene polymer. *Langmuir* **7**, 2484 (1991).

Grunkemeier, J. M.; Tsai, B. W.; Horbett, T. A.; Hemocomaptibility of treated polystyrene substrates: contact activation, platelet adhesion and proagulant activity of platelets. *Journal of Biomedical Material Research* **41**, 657 (1998).

Guidoin, R.; Suyder, R.; Martin, L.; Albumin coating of a knitted polyester arterial prosthesis: an alternative to preclotting. *The Annals of Thoracic Surgery* **37**, 457 (1984).

Hoffman, G. S.; Weyand, C. M.; (ed). *Inflammatory Diseases of Blood Vessels*. (Mercel Dekker Inc., New York, 2002).

Horbett, T. A.; Principals underlying the role of adsorbed plasma proteins in blood interactions with foreign materials. *Cardiovascular Pathology* **2**, 137 (1993).

Huang-Lee, L. L. H.; Cheung, D. T.; Nimni, M. E.; Biochemical changes and cytotoxicity associated with the degradation of polymeric glutaraldehyde derived crosslinks. *Journal of Biomedical Materials Research* **24**, 1185 (1990).

Humphries, A. W; Hawk, W. A.; Cuthberson, A. M; Arterial prosthesis of collagen-impregnated Dacron tulle. Surgery **50**, 947 (1981).

Hunt, B. J.; Parrat, R.; Cable, M.; Finch, D.; Yacoub, M.; Activation of coagulation and platelets is affected by the hydrophobicity of artificial surface. *Blood Coagulation Fibrin* **8**, 223 (1997).

Hylton, D. M.; Shalaby, S. W.; Latour, R. A.; Direct correlation between adsorption-induced changes in protein structure and platelet adhesion. *Journal of Biomedical Materials Research Part A* **74A**, 722 (2005).

Inagaki, N.; Narushim, K.; Tuchida, N.; Miyazaki, K.; Surface characterization of plasma-modified poly(ethylene terephthalate) film surfaces. *Journal of Polymer Science, Part B: Polymer Physics* **42**, 3727 (2004).

Jannasch, P.; Surface structure and dynamics of block and graft copolymers having fluorinated poly(ethylene oxide) chain ends. *Macromolecules* **31**, 1341 (1998).

Joist, J. H.; Pennington D. C.; Platelet reactions with *artificial* surfaces. *Transactions- American Society* for *Artificial Internal Organs* **33**, 341 (1987).

Kasemo, B.; Biological surface science. *Surface Science* **500**, 656 (2002).

Kempezinski, R. F.; Rosenman, J. E.; Pearce, W. H. ; Roedersheimer, L. R.; Berlatzky, Y.; Ramalanjaona G., Endothelial cell spreading of a new PTFE vascular prosthesis. *Journal of Vascular Surgery* **2**, 424 (1985).

Keselowsky, B. G.; Collard, D. M.; Garcia, A. J.; Surface chemistry modulates fibronectin conformation and directs integrin binding and specificity to control cell adhesion . *Journal of Biomedical Materials Research* **66A**, 247 (2003).

Khang, D.; Kim, S. Y.; Liu-Snyder, P.; Palmore, T. G.; Durbin, S. M.; Webster, T. J.; Enhanced fibronectin adsorption on carbon nanotube/poly(carbonate) urethane: Independent role of surface nano-roughness and associated surface energy. *Biomaterials* **28**, 4756 (2007).

Kim, K. S.; Ryu, C. M.; Park, C. S.; Sur, G. S.; Investigation of crystallinity effects on the surface of oxygen plasma treated low density polyethylene using X-ray photoelectron spectroscopy. *Polymer **44***, 6287 (2003).

Kim, Y. J.; Kang, I.; Huh, M. W.; Yoon, S.; Surface characterization and in vitro blood compatibility of poly(ethylene terephthalate) immobilized with insulin and/or heparin using plasma glow discharge. *Biomaterials* **21**, 121 (2000).

Kito, H.; Matsuda, T. *J.*; Biocompatible coatings for luminal and outer surfaces of small-caliber artificial grafts. *Biomedical Material Research* **30**, 321 (1996).

Kong, Y.; Hay, J. N.; The measurement of the crystallinity of polymers by DSC. *Polymer* **43**, 3873 (2002).

Kongde, A.; Bechtold, T.; Teufel, L.; Modification of cellulose fiber with silk sericin. *Journal Applied Polymer Scienc,* **96**, 1421 (2005).

Kouvroukoglou, S.; Dee, K.; Bizios, R.; McIntire, L.; Zygourakis, K.; Endothelial cell migration on surfaces modified with immobilized adhesive peptides. *Biomaterials* **21**, 1725 (2000).

Krump, H.; Hudec, I.; Jasso, M.; Dayss, E.; Luyt, A. S.; Physical-morphological and chemical changes leading to an increase in adhesion between plasma treated polyester fibres and a rubber matrix. *Applied Surface Science* **252**, 4264 (2006).

Kumar, D. S.; Fujioka, M.; Asano, K.; Shoji, A.; Jayakrishnan, A.; Yoshida, Y.; Surface modification of poly(ethylene terephthalate) by plasma polymerization of poly(ethylene glycol). *Journal of Material Science Materials Medicine* **18**, 1831 (2007).

Larrieu, J.; Clement, F.; Held, B.; Soulem, N.; Luthon, F.; Guimon, C.; Martinez, H.; Analysis of microscopic modifications and macroscopic surface properties of polystyrene thin films treated under d.c. pulsed discharge conditions. *Surf*ace *Interface Analysis* **37**, 544 (2005).

Larrieu, J.; Held, B.; Martinez, H.; Tison, Y.; Ageing of atactic and isotactic polystyrene thin films treated by oxygen DC pulsed plasma. *Surface and Coating Technology* **200**, 2310 (2005).

Lee, J. H.; Khang, G.; Lee, J. W.; Interaction of different types of cells on polymer surfaces with wettability gradient. *Journal of Colloid and Interface Science* **205**, 323 (1998).

Lee, J. H.; Lee, H. B.; Platelet adhesion on to wettability gradient surfaces in the absence and presence of plasma proteins. Journal of Biomedical Material Research **41**, 304 (1998).

Lin, J. C.; Cooper, S. L.; Surface characterization and ex vivo blood compatibility study of plasma modified small diameter tubing: Effect of sulphur dioxide and hexamethyl disiloxane plasma. *Biomaterials* **16**, 1017 (1995).

Lu, A.; Sipehia, R.; Antithrombotic and fibrinolytic system of human endothelial cells seeded on PTFE: The effects of surface modification of PTFE by ammonia plasma treatment and ECM protein coatings. *Biomaterials* **22**, 1439 (2001).

Luk, Y. Y.; Kato, M.; Mrksich, M.; Self-assembled monolayers of alkanethiolates presenting mannitol groups are inert to protein adsorption and cell attachment. *Langmuir* **16**, 9604 (2000).

Meier, M.; von Keudell, A.; Jacob, W.; Temperature dependence of CH3 sticking: consequences for nuclear fusion. *Nuclear Fusion* **43**, 25 (2003).

Michael, K. E.; Vernekar, V. N.; Keselowsky, B. G.; Meredith, J. C.; Latour, R. A.; Garcia, A. J.; Adsorption-induced conformational changes in fibronectin due to interactions with well-defined surface chemistries . *Langmuir* **19**, 8033 (2003).

Montargent B.*;* Letourneur, D.; Toward new biomaterials. *Infection Control and Hospital Epidemiology* **21**, 404 (2000).

Mooradian, D. L.; Trescony, P.; Keeney, K.; Furcht, L. T.; Effect of glow discharge surface modiffcation of plasma TFE vascular graft material on fbronectin and laminin retention and endothelial cell adhesion. *Journal of Surgery Researc*h **53**, 74 (1992).

Morent, R.; De Geyter, N.; Gengembre, L.; Leys, C.; Payen, E.; Van Vlierberghe, S.; Schacht, E.; Surface treatment of a polypropylene film with a nitrogen DBD at medium pressure. *EPJ Applied Physics* **43**, 289 (2008).

Morent, R.; De Geyter, N.; Leys, C.; Gengembre, L.; Payen, E.; Treatment of polymer films with a dielectric barrier discharge in air, helium and argon at medium pressure. *Surface Coating Technoogy* **201**, 7847 (2007).

Morra, M.; Occhielo, E.; Garbassi, F.; *Polymer-Solid Interface* (Galliard Ltd, Great Yarmouth, Norfolk, Great Britan,1991).

Mozetic, M.; Cvelbar, U.; Vesel, A.; Ricard, A.; Babic, D.; Poberaj, I.; A diagnostic method for real-time measurements of the density of nitrogen atoms in the postglow of an Ar/N_2 discharge using a catalytic probe. *Journal of Applied Physics* **97**, 103308 (2005).

Mozetic, M.; Vesel, A.; Cvelbar, U.; Ricard, A.; An iron catalytic probe for determination of the o-atom density in an Ar/O_2 afterglow. *Plasma Chemistry and Plasma Processing* **26**, 103 (2006).

Mustard, J. F.; Packham, M. A.; The role of blood and platelets in atherosclerosis and the complications of atherosclerosis. *Thrombosis et Diathesis Haemorrhagica* **33**, 44 (1975).

Nasser E. *Fundamentals of gaseous ionization and plasma electronics* (Wiley/Interscience, New York:; 1971).

Nunn, D. B.; Freeman, M. N.; Hudgkins, P. C.; Postoperative alterations in size of Dacron aortic grafts. Annals of Surgery **189**, 741 (1979).

Pandiyaraj, K. N.; Selvarajan, V.; Deshmukh, R. R.; Bousmina, M.; The effect of glow discharge plasma on the surface properties of Poly (ethylene terephthalate) (PET) film. *Surface Coating Technology* **202**, 4218 (2008).

Pevec, W. C.; Darling, R. C.; L'Italien, G. J.; Abott, W. M. *J.;* Femoropopliteal reconstruction with knitted, nonvelour Dacron versus expanded polytetrafluoroethylene. *Vascular Surgery* **16,** 60 (1992).

Poberaj, I.; Mozetic, M.; Babic, D.; Comparison of fiber optics and standard nickel catalytic probes for determination of neutral oxygen atoms concentration. *Journal of Vacuum Science and Technology A* **20,** 189 (2002).

Poll, H.U.; Schladitz, U.; Schreiter, S.; Penetration of plasma effects into textile structures. *Surface and Coating Technology* **142-144**, 489 (2001).

Pringle SD, Joss VS, Jones C. Ammonia plasma treatment of PTFE under known plasma conditions. *Surface and Interface Analysis* **24**, 821 (1996).

Quinones-Baldrich, W. J.; Moore, W. S.; Ziomek, S.; Development of a "leak-proof," knitted Dacron vascular prosthesis. *Journal of Vascular Surgery* **3**, 895 (1986).

Ramires, P. A.; Mirenghi, L.; Romano, A. R.; Palumbo, F.; Nicolardi, G.; Plasma-treated PET surfaces improve the biocompatibility of human endothelia cells. *Journal of Biomedical Material Research* **51**, 535 (2000).

Ratner, B. D.; Hoffman, A. S.; Schoen, F. J.; Lemons, J. E.; *Biomaterials Science* (Academic Press, San Diego, 1996).

Reidel, M.; Muller, B.; Wintermantel, E.; Protein adsorption and monocyte activation on germanium nanopyramids. *Biomaterials* **22,** 2307 (2001).

Riccardi, C.; Barni, R.; Selli, E.; Mazzone, G.; Massafra, M. R.; Marcandalli, B.; Poletti, G.; Surface modification of poly(ethylene terephthalate) fibers induced by radio frequency air plasma treatment. *Applied Surface Science* **211**, 386 (2003).

Roach, P.; Farrar, D.; Perry, C. C.; Interpretation of protein adsorption: surface induced conformational changes. *Journal of the American Chemical Society* **127**, 8168 (2005).

Roald, H. E.; Barstad, R. M.; Bakken, I. J.; Roald, B.; Lyberg, T.; Sakariassen, K. S.; Initial interactions of platelets and plasma proteins in flowing non-anticoagulated human blood with the artificial surfaces Dacron and PTFE . *Blood Coagulation and Fibrinolysis* **5**, 355 (1994).

Rodrigues, S. N.; Goncalves, I. C.; Martins, M. C. L.; Barbosa, M. A.; Ratner, B. D.; Fibrinogen adsorption, platelet adhesion and activation on mixes hydroxyl-/methyl-terminated self-assembled monolayers. *Biomaterials* **27**, 5357 (2006).

Rojkjaer R.; Schmaier A. H.; Activation of the plasma kallikrein/kinin system on endothelial cell membranes. *Immunopharmacology* **43**, 109 (1999).

Schröder, K.; Meyer-Plath, A.; Keller, D.; Ohl, A.; On the Applicability of Plasma Assisted Chemical Micropatterning to Different Polymeric Biomaterials. *Plasmas and Polymers* 7, 103 (2002).

Schwarzenbach, W.; Derouard, J.; Sadeghi, N.; Treatment of organic polymer surfaces by CF4 plasmas: Etching by fluorine atoms and influence of vacuum ultraviolet radiation. *Journal of Applied Physics* ***90****, 5491 (*2001).

Sefton, M. V.; Sawyer, A.; Gorbet, M.; Black, J. P.; Cheng E.; Gemmell C. et. al., Does surface chemistry affect thrombogenicity of surface modified polymers? *Journal of Biomedical research* **55**, 447 (2001).

Seifert, B.; Mihanetzis, G.; Groth, T.; Albrecht, W.; Richa. K.; Missirlis, Y.; Paul, D.; Sengbusch, G.; Polyetherimide: A New Membrane-Forming Polymer for Biomedical Applications. *Artificial Organs* **26**, 189 (2002).

Sharma, C. P.; Szycher, M.; (ed), *Blood Compatible Materials and Devices* (Technomic Publishing, Lancaster, 1991).

Shi, D. (ed), Biomaterials and Tissue Engineering (Springer-Verlag, Berlin, 2004).

Sipehia, R.; X-ray photoelectron spectroscopy studies, surface tension measurements, immobilization of human serum albumin, human fibrinogen and human fibronectin onto ammonia plasma treated surfaces of biomaterials useful for cardiovascular implants and artificial cornea implants. *Biomaterials, Artificial Cells, and Immobilization Biotechnology* **21**, 647 (1993).

Sperling, C.; Schweiss, R. B.; Streller, U.; Werner, C.; In vitro hemocompatibility of self-assembled monolayers displaying various functional groups. *Biomaterials* **26**, 6547 (2005).

Sperlinga, C.; Schweiss, R. B.; Streller, U.; Werner, C.; In vitro hemocompatibility of self-assembled monolayers displaying various functional groups. *Biomaterials* **26**, 6547, (2005).

Sprang, N.; Theirich, D.; Engermann, J.; Plasma and ion beam surface treatment of polyethylene. *Surface and Coating Technology* **74-75**, 689 (1995).

Steele, J. G.; Johnson, G.; McFarland, C.; Dalton, B. A.; Gengenbach, T. R.; Chatelier, R. C.; Underwood, R. A.; Griesser, H. J.; Roles of serum vitronectin and fibronectin in initial attachment of human vein endothelial cells and dermal fibroblasts on oxygen- and nitrogen-containing surfaces made by radiofrequency plasmas. *Journal of Biomaterials science. Polymer edition* **6**, 511 (1994).

Strobel, M.; Lyons, C. S.; Mittal, K. L.; *Plasma Surface Modification of Polymers: Relevance to Adhesion* (VSP, Utrecht, 1994).

Tai, H.; Buettner, H.; Neurite Outgrowth and Growth Cone Morphology on Micropatterned Surfaces. *Biotechnology Progress* **14**, 364 (1998).

Tan, J. S.; Martic, P. A.; Protein adsorption and conformational change on small polymer particles. *Journal of Colloidal Interface Science* **136**, 415 (1990).

Tankersley, D. L.; Finlayson, J. S.; Kinetics of activation and autoactivation of human factor XII. *Biochemistry* **23**, 273 (1984).

Tengvall P.; Askendal, A.; Lundstrum, I.; Elwing, H.; Studies of surface activated coagulation: antisera binding onto methyl gradients on silicon incubated in human plasma in vitro. *Biomaterials* **13**, 367 (1992).

Terlingen, J. G.; Brenneisen, L. M.; Super, H. T.; Pijpers, A. P.; Hoffman, A. S.; Feijen, J.; Introduction of amine groups on poly(ethylene) by plasma immobilization of a preadsorbed layer of decylamine hydrochloride. *Journal of biomaterials science. Polymer edition* **3**, 165 (1993).

Toes, G.J.; Dungen, J.; Haan, J.; Hermens, R.; Oeveren, W.; Flurescence labeling to study platelet and leucocyte deposition onto vascular grafts. *Biomaterials* **20**, 1951 (1999).

Tsai, M. Y.; Sun, Y. T.; Lin J. C.; Surface characterization and platelet compatibility evaluation of the binary mixed self-assembled monolayers. *Journal of Colloid and Interface Science* **308**, 474 (2007).

Tu, J. V.; Pashos , C. L.; Naylor, C. D.; Use of cardiac procedures and outcomes in elderly patients with myocardial infarction in the united States and Canada. *New England Journal of Medicine* **366**, 1500 (1997).

Tyan, Y. C.; Liao, J. D.; Klauser, R.; Wu, I. D.; Weng, C. C.; Assessment and activation of degradation effect for the varied degrees of ultra violet radiation onto the collagen-bonded polypropelene non-woven fabric surfaces. *Biomaterials* **23**, 65 (2002).

Tyan, Y. C.; Liao, J. D.; Klauser, R.; Wu, I. D.; Weng, C. C.; Assessment and activation of degradation effect for the varied degrees of ultra violet radiation onto the collagen-bonded polypropelene non-woven fabric surfaces. *Biomaterials* **23**, 65 (2002).

Tzoneva, R.; Seifert, B.; Albrecht, W.; Richau, K.; Groth, T.; Lendlein, A.; Hemocompatibility of poly (ether imide) membranes funcionalised with carboxylic groups. *Journal of Material Science* **19**, 3203 (2008).

Tzoneva-Velinova, R.; *The wettability of biomaterials determines the protein absorption and the cellular responses* (Mathematisch-Naturwissenschaftlichen Fakultät der Universität Potsdam, Teltow, 2003).

Vandencasteele, N.; Reniers, F.; Surface characterization of plasma-treated PTFE surfaces: An OES, XPS and contact angle study, *Surface and Interface Analysis* **36**, 1027 (2004).

Venugopalan, M., *Reaction under cold plasma conditions* (Wiley/Interscience, New York, 1971).

Vertegel, A. A.; Siegel, R. W.; Dordick, J. S.; Silica nanoparticle size influences the structure and enzymatic activity of adsorbed lysozyme. *Langmuir* **20,** 6800 (2004).

Vogler, E. A.; Graper, J. C.; Harper, G. R.; Sugg, H. W.; Lander, L. M.; Brittain, W. J.; Contact activation of the plasma coagulation cascade. I. Procoagulant surface chemistry and energy. *Journal of Biomedical Materials Research* **29**, 1005 (1995).

Vohra, R.; Thomson, G. J. L.; Carr, H. M. H.; Sharma, H.; Walker, M. G.; Comparison of different vascular prostheses and matrices in relation to endothelial seeding. *British Journal of Surgery* **78**, 417 (1991).

Vroman, L.; The life of an artificial device in contact with blood: initial events and their effect on its final state. *Bulletin of the New York Academy of Medicine* ***64***, 352 (1988).

Wang, M. J.; Chang, Y. I.; Poncin-Epaillard, F.; Illustration of the interface between N_2/CO_2 plasmas and polystyrene surface. *Surface Interface Analysis* **37**, 348 (2005).

Weadock, K. S.; Goggins, J. A.; Vascular graft sealants. *Journal of Long-Term Effects* of *Medical Implants* **3**, 207 (1993).

Williams, D. F. *Advances in biomaterials* (Elsevier, Amsterdam, 1988).

Wilson, D. J.; Williams, R. L.; Pond, R. C.; Plasma modification of PTFE surfaces - Part I: Surfaces immediately following plasma treatment. *Surface Interface Analysis* **31**, 385 (2001).

Wissink, M.J.B.; Beernink, R.; Poot, A.A.; Engbers, G.H.M.; Beugeling, T.; van Aken, W.G.; Feijen, J.; Improved endothelialization of vascular grafts by local release of growth factor from heparinized collagen matrices. *Journal of Controlled Release* **64**, 103 (2000).

Wolansky, G.; Marmur, A.; Apparent Contact Angles on Rough Surfaces: the Wenzel Equation Revisited. *Colloids and Surfaces A* **156**, 381 (1999).

Xu, L. C.; Siedlecki, C.; Christopher. A.; Effects of surface wettability and contact time on protein adhesion to biomaterial surfaces. *Biomaterials* 28, 3273 (2007).

Yasuda, H. K.; Yeh Y. S.; Fusselman, S.; A growth mechanism for the vacuum deposition of polymeric materials. *Pure and Applied Chemistry* **63**, 1689 (1990).

Index of figures

Index of tables

Appendix

Publication of the candidate from the dissertation:

Cvelbar, U.; Mozetič, M.; Junkar, I.; Vesel, A.; Kovač, J.; Drenik A.; Vrlinič, T.; Hauptman, N.; , T.; Oxygen plasma functionalization of poly(p-phenilene sulphide). *Applied Surface Scence* **19**, 8669 (2007).

Vesel, A.; Junkar, I.; Cvelbar, U.; Kovač, J.; Mozetič, M.; Surface modification of polyester by oxygen-and nitrogen-plasma treatment. *Surface Interface Analysis* **40**, 1444 (2008).

Junkar, I.; Šuštar, V.; Frank, M.; Janša, V.; Bedina-Zavec, A.; Rozman, B.; Mozetič, M.; Hagerstrand, H.; Kralj-Iglič, V.; Blood and sinovial microparticles as revealed by atomic force and scanning electron microscope. *The Open Autoimmunity Journal* **1**, 50 (2009).

Junkar, I.; Cvelbar, U.; Vesel, A.; Hauptman, N.; Mozetič, M.; The role of crystallinity on polymer interaction with oxygen plasma. *Plasma processes polym. (Print)* **6**, 667 (2009).

Junkar, I.; Vesel, A.; Cvelbar, U.; Mozetič, M.; Strnad, S.; Influence of oxygen and nitrogen plasma treatment on polyethylene terephthalate (PET) polymers. *Vacuum* **84**, 83 (2008).

Patent application:

Junkar, I.; Mozetič, M.; Vesel, A.; Cvelbar, U.; Krašna, M.; Domanovič, D.; Metoda obdelave bio-medicinskih polimernih protez za izboljšanje njihovih antitrombogenih lastnosti : *patentna prijava št. P-200900109*. Ljubljana: Urad RS SLovenije za intelektualno lastnino, 20. 4. 2009.

Patent:

Mozetič, M.; Vesel, A.; Junkar, I.; Cvelbar, U.; Strnad, S.; Metoda in naprava za modifikacijo implantatov in umetnih žil iz PET polimera : *patent SI 22608*. Ljubljana: Urad RS za intelektualno lastnino, 30. 4. 2009.

Acknowladgements

Acknowledgements go to the former head of the Department of Engineering and Optoelectronics **Prof. Dr. Anton Zalar** for giving me the opportunity to work in his department on the Jožef Stefan Institute and to the Slovenian Ministry for Higher Education for their financial support.

I would like to give my special thanks to my supervisor and the present head of Department of Engineering and Optoelectronics **Assist. Prof. Dr. Miran Mozetič** for letting me be a part of his research group and introducing me to the wonderful world of science.

I am also very grateful to my co-supervisor **Assist. Prof. Dr. Uroš Cvelbar** for all the help and guidance throughout my study.

I furthermore extend my thanks to all the co-workers in the Department of Engineering and Optoelectronics for keeping up the pleasant working spirit. Especially I would like to thank to **Dr. Janez Kovač and Dr. Alenka Vesel** for all the discussions and guidance during my work. Also I would like to thank **Janez Trtnik** for the help with plasma reactor and cutting of samples and to **Ruža Bolte, Tatjana Filipič, Dr. Sašo Drenik** and **Kristina Eleršič** for helping me in one way or another during my research.

Such an interdisciplinary work could never be conducted without the experts from other fields. Thus my gratitude goes to **Dr. Dragoslav Domanovič** and **Dr. Metka Krašna** from the Blood Transfusion Centre of Slovenia for many discussions, preparation of *in vitro* biological experiments, help with endothelia cells and platelets and for their great collaboration, hope it will continue.

I would also like to give my sincere gratitude to **Prof. Dr. Kazimir Drašlar** who, without any hesitation, helped me with his knowledge in preparation of biological samples for SEM analysis.

My gratitude for good quality SEM images shown in this work does not only go to Prof. Dr. Kazimir Drašlar for his excellent preparation procedure, but also to the people who helped me with SEM analysis. Thank you **Nina Hauptman, Barbara Šetina** and **Andraž Kocjan**.

I would also like to give my thanks to **Assist. Prof. Dr. Marian Lehocky** from Thomas Bata University in Zlin, Czech Republic, for many fruitful discussions and for enabling me to finish my thesis at his faculty. I would like to thank both Assist. Prof. Dr. Marian Lehocky as well as **Dr. Vladimir Sedlarik** for making my visit in Zlin so pleasant.

Last, but not the least gratitude goes to my family and my boyfriend **Mladen** who all patiently stood by me.